SYNTHESIS AND CHARACTERIZATION OF EPOXIDIZED SOYBEAN OIL / DIISOCYANATE THERMOSET POLYMERS

by

Makbule Gizem KIREVLİYASI

B.S., Chemistry, Bogaziçi University, 2012

Submitted to the Institute for Graduate Studies in
Science and Engineering in partial fulfillment of
the requirements for the degree of
Master of Science

Graduate Program in Chemistry

Boğaziçi University

2015

ACKNOWLEDGEMENTS

First and foremost, I would like to express my sincerest gratitudes for Prof. Selim Küsefoğlu for being the best thesis supervisor already even if he is my first thesis supervisor. His scientific guidance helped to solve many problems but more important than this, his encouragement, tolerance and belief in me supplied the power for completing my thesis in such a short time. It was a great experience for me to work with him.

I wish to express my appreciation to Prof. Viktorya Aviyente for her endless help within the graduation period. I would like to express special thanks to Prof. Duygu Avcı, Prof. Tarık Eren, for their advices and comments on the final manuscripts. I wish to express my appreciation to Prof. Nihan Nugay, Prof. Turgut Nugay for their comments on the study and giving encouragement among the writing process of my thesis. I would like to thank Eliza Kalvo for her moral support, tolerance and help for me to be a better research assistant. Also I would like to thank Aslı Tarkan Kalaycıoğlu for being such a caring person incredibly helped me to move on.

My special thanks go to Merve Seçkin Altuncu, Nur Çiçek Kekeç, Yavuz Öz, Hazal Pekcan, Duygu Tuncel and Tankut Türel for their friendship an their endless support among all of the writing period. I would like to thank Jesmi Çavuşoğlu, Sesil Çınar, Gülşah Çiftçifor their technical support on the instruments, softwares and laboratory work. Additionally I would also thank to our research students, Aslıhan Gölcük, Erhan Sevim, Gökhan Sağlam for helping me with the experiments.

Finally my deepest thanks goes to my family espeacially my father Ahmet Kırevliyası and my mother Hafize Kırevliyası for their morale support. Last but the not least I would like to thank Mustafa Akkaya for his endless support on everything.

ABSTRACT

SYNTHESIS AND CHARACTERIZATION OF EPOXIDIZED SOYBEAN OIL / DIISOCYANATE THERMOSET POLYMERS

In this study, novel vegetable oil based thermoset polymers were synthesized from Epoxidized Soybean Oil (ESO) with several diisocyanates, methylene diphenyl diisocyanate (MDI), toluene diisocyanate (TDI), isophorone diisocyanate (IPDI). The characterization of polymers was done with FTIR spectroscopy. Enhancement of the chemical characterization was done with model compounds synthesized with ESO and phenyl isocyanate by ^{1}H NMR and ^{13}C NMR. Synthesis of polymers and model compounds were conducted in the presence of basic catalyst 1,4diazabicyclo [2.2.2] octane (DABCO) and acidic catalyst Antimony(III) chloride ($SbCl_3$). Results showed that oxazolidone, urethane, isocyanurate, urea, biuret and allophonate groups were obtained varying amounts depending on the reaction conditions. Mechanical properties of polymers were analyzed with TGA (Thermogravimetric Analysis), swelling, compression and surface hardness tests. Thanks to the isocyanurate, biuret and allophonate groups, crosslink density of polymers are high and 5-membered oxazolidone rings gave rigidity to polymers that provide the comparable mechanical properties with commercial polymers. Compression strength 55 MPa for MDI polymers, compression modulus was 308 MPa and surface hardness was 70 shore D units.For one sample, leaching test was done and shows 97 % yield for polymerization was obtained.

ÖZET

EPOKSİDE SOYA YAĞI - DİİZOSİYANAT BAZLI TERMOSET POLİMERLERİN SENTEZİ VE KARAKTERİZASYONU

Bu çalışmada, Epokside Soya Yağı ve çeşitli diizosiyanatlar, metilen difenil diizosiyanat (MDI), toluen diizosiyanat (TDI), izoforon diizosiyanat (IPDI) kullanılarak bitkisel yağ bazlı yeni termoset polimerler sentezlenmiştir. Polimerlerin karakterizasyonu FTIR spektroskopi kullanılarak yapılmıştır. Karakterizasyonu genişletmek için Epokside Soya Yağı ve fenil izosiyanat ile sentezlenen model bileşikler vasıtasıyla 1H NMR ve 13 C NMR kullanılmıştır. Polimerlerin sentezi bazik katalist 1,4 - Diazabisiklo (2,2,2) oktan ve asidik katalist antimon triklorür eşliğinde yapılmıştır. Sonuçlar Epokside Soya Yağı ve diizosiyanat reaksiyonu ortamında elde edilen ürünlerde oksazolidinon, üretan, izosiyanurat, üre, biüret, allofanat gruplarının bulunduğunu göstermiştir. Polimerlerin mekanik özellikleri, termal gravimetrik analiz (TGA), çözücüde şişme, basma-kırılma ve yüzey sertliği yöntemleri ile incelenmiştir. İzosiyanurat, biüret ve allofanat grupları sayesinde çapraz bağ yoğunluğunun artması ve 5 halkalı oksazolidinon gruplarının polimerlere sertlik sağlaması sayesinde, bu projede sentezlenen bitkisel yağ bazlı polimerlerin mekanik özellikleri, ticari polimerlerle kıyaslanabilir hale gelmiştir. Bir örnek için yapılan süzdürme testi ile polimerizasyon veriminin 97 % olduğu anlaşılmıştır.

TABLE OF CONTENTS

LIST OF FIGURES

LIST OF TABLES

LIST OF ACRONYMS / ABBREVIATIONS

ASTM	American Society for Testing and Materials
BMC	Bulk Moulding Compound
BPA	Bisphenol-A
CSO	Carbonated Soybean Oil
DABCO	1,4-diazabicyclo[2.2.2]octane
DBTDL	dibutyltin dilaurate
DGBPA	diglycidyl ether of Bisphenol-A
DMA	Dynamomechanical Analysis
DNA	Deoxyribonucleic acid
EEW	Epoxy Equivalent Weight
EMI	ethyl methyl imidazole
ESO	Epoixidized Soybean Oil
FTIR	Fourier Transform Infrared Spectroscopy
HDI	Hexamethylene diisocyanate
IPDI	Isophorone diisocyanate
MDI	Methylene diphenyl diisocyanate
NDI	Naphthalene diisocyanate
NIOSH	The U.S. National Institute for Occupational Safety and Health
NMR	Nuclear Magnetic Resonance
PVC	Polyvinyl chloride
PPM	Parts Per Million
RIM	Reaction Injection Moulding
SMC	Sheet Moulding Compound
SOMA	Maleinized Soybean Oil
TDI	Toluene diisocyanate
TGA	Thermogravimetric Analysis

1. INTRODUCTION

1.1. Renewable Resources

Approximately 10% of the fossil fuel resources are consumed to produce the vast majority of polymer products and organic chemicals. Price of fossil fuel based polymers, nondegradability, greenhouse gas emission during combustion and dwindling of fossil fuel sources are the reasons of investigating novel biobased polymers. Research efforts are being made for utilizing green polymerization systems which uses renewable materials. Disposal of plastics based of petrochemical sources is another issue. Development of biodegradable or recyclable plastics are encouraged by both legislation and consumer pressure. Biobased polymer may be biodegradable (polylactic acid made from sugar cane, corn starch) or non-biodegradable (biopolyethylene made from sugar cane, wheat grain). Even non-biodegradable biobased polymers are environmentally friendly because when they decompose or burn, the released carbon is less than the carbon consumed by the plant from which the monomer was obtained. Worldwide interest and number of citations in biobased polymers has increased tremendously and at the end of 2015, biobased polymers will be over 1% of the polymer industry [1-3].

1.2. Plant Oils

1.2.1. Physical and Chemical Properties of Plant Oils

Plant oils contain triglycerides which are fatty acid esters of a glycerol. Due to their non-polarity they are water insoluble and are used as energy source in human body. General application areas of fatty acids are shown in Table 1.1.

Table 1.1. General Application Areas of Fatty Acids.

APPLICATON AREAS OF FATTY ACIDS	
Natural Fatty Acids	Food, Food Preservative, Food Packaging, Cosmetics, Detergent, Pharmaceutical, Anti-Static Plastic Additives, Drug delivery, Fire Retardant Hydraulic Fluid
Sulfated Fatty Acids	Cosmetics, Detergent
Hydrogenated Fatty Acids	Detergent
Acrylated Fatty Acids	Cosmetics, Pharmaceuticals, Plastic Additives, Bioplastics
Epoxidized Fatty Acids	Additive for PVC, Bioplastics
Alkyd Resins	Paint, Coatings; Baked finishes for automobiles, refrigerators, stoves; Printing ink, Enamels
Acetylated Fatty Acids	Food Packaging, Wax and plastic additive, Food dye solvent, Cosmetics, Foaming Agent
Polymerized Fatty Acids	Thermoset Polymers for coating, foam, insulation, carpets, adhesives, shoes; Thermoplastic Elastomers

Fatty acid chains can be saturated or unsaturated with mono-,di-, triunsaturation. These double bonds are in the cis geometry in nature and this makes plant oils, liquid at room temperature. Cis bonds prevent the packing of fatty acid chains and disrupts the Van der Waals interactions between the chains which causes to decline in the melting point. Length of hydrocarbon parts of the chains vary between 10 to 30 carbon atoms, most usually 12 to 18. Due to the Van der Waals interaction between fatty acid chains melting point of fats increases with increasing carbon number.

Apart from general triglycerides there are also rare triglycerides with hydroxyl group such as castor and lesquerella oil, epoxy group such as vernonia oil, ketone group in licania oil. General structure of a triglyceride is shown in Figure 1.1.

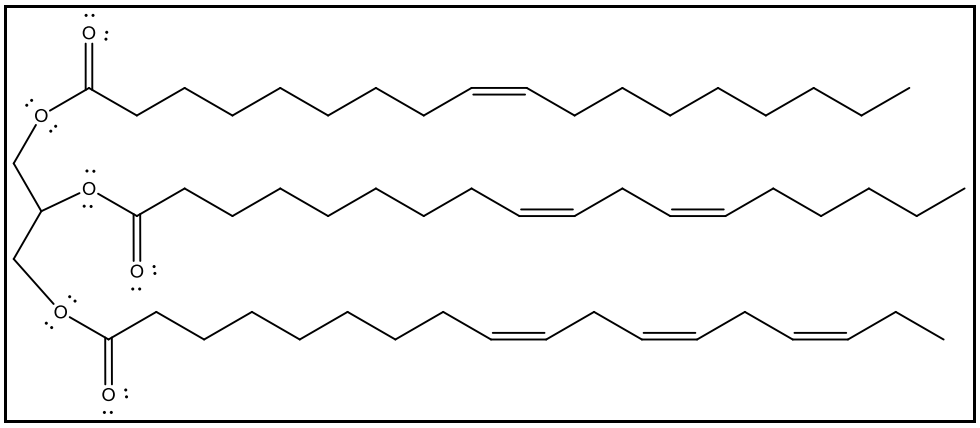

Figure 1.1. General Structure of Vegetable Oils.

1.2.2. Chemical Composition of Vegetable Oils

The ratio between unsaturated fatty acids to saturated fatty acids effects the nutritional value and chemical and physical properties of vegetable oil. Double bonds (unsaturations) could under go oxidative reactions which is the cause of rancidity. To define the position of double bonds Greek Latter ω is used. ω-3 means the position of double bond is between 3rd carbon and 4th carbon. ω-3 and ω-6 double bonds are necessary for human well-being. Knowing the composition of vegetable oils is both important for human life and important for choosing an oil to synthesize a polymer whose mechanical properties is sufficient to be commercialized. In the Table 1.2 there is a list of some common vegetable oils with different kind of fatty acid contents. Moreover at the end of the Table 1.2 there is a ratio of saturation:unsaturation of fatty acids [4,5].

Table 1.2. Fatty Acid Composition in Several Vegetable Oils.

PERCENT BY WEIGHT OF TOTAL FATTY ACIDS IN VEGETABLE OILS						
Name of Oil	Saturated		Mono unsaturated	Polyunsaturated		
	Palmitic Acid	Stearic Acid	Oleic Acid	Linoleic Acid	Linolenic Acid	Unsat:Sat Ratio
	C16:0	C18:0	C18:1	C18:2	C18:3	
Almond	7	2	69	17	-	9.7
Canola	4	2	62	22	10	15.7
Corn	11	2	28	58	1	6.7
Cotton Seed	22	3	19	54	1	2.8
Flax Seed	3	7	21	16	53	9
Grape Seed	8	4	15	73	-	7.3
Olive	13	3	71	10	1	4.6
Palm	45	4	40	10	-	1
Peanut	11	2	48	32	-	4
Safflower	7	2	13	78	-	10.1
Sesame	9	4	41	45	-	6.6
Soybean	11	4	24	54	7	5.7
Sunflower	7	5	19	68	1	7.3
Walnut	11	5	28	51	5	5.3

1.3. Soybean Oil

1.3.1. General Properties and Chemical Composition of Soybean Oil

Soybean oil is a dominating vegetable oil in today's oil market. 80% of soybean oil is used for food products such as margarine, soft spreads, breakfast cereals and snack foods whereas 14% of it is used in chemical industry as soaps, fatty acids, lubricants, coatings,

biodiesel production, inks, paints, varnishes and plastics. The composition of fatty acids in soybean oil is effected by various environmental and geographic conditions but a general composition is showed in Table 1.3.

Table 1.3. Fatty Acid Composition of Soybean Oil.

Type of Fatty Acid	Symbol	Weight Percentage	Structure
Lauric	12:00	4.5	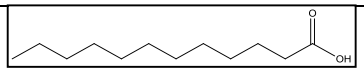
Myristic	14:00	4.5	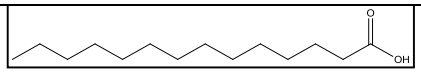
Palmitic	16:00	11.6	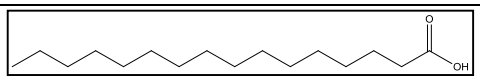
Stearic	18:00	2.5	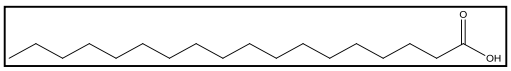
Oleic	18:01	21.1	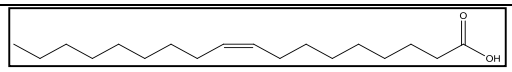
Linoleic	18:02	52.4	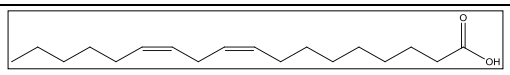
Linolenic	18:03	7.1	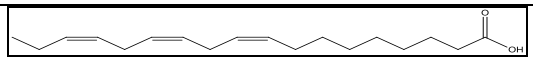

Fatty acid composition of soybean oil has been enhanced by genetic modifications which changes the chemical and physical properties such as melting point, oxidative stability and chemical functionalities. Thanks to genetic engineering, oleic acid percentage was increased to 90% and polyunsaturated fatty acid composition was decreased to 3-5% percentage. This type of soybean oil is rich in ω-3 fatty acid (oleic acid) also it is oxidataviely more stable. At this primitive point of view genetically engineered soybean oil seems suitable for food production although genetically modified organisms are still in debate. Genetic engineering also used for increase the number of double bonds. Normally conventional soybean oil contains about 10% linolenic acid but genetically modified soybean oil contains 50% of linolenic acid. Low price, ready availability and high level of unsaturation makes soybean oil the best candidate for chemical industrial use [6-8].

1.3.2. Chemical Properties of Soybean Oil

Reactive sites of soybean oil has shown in Figure 1.2. Hydrolyzable glycerol unit, ester carbonyl, alpha position of ester group, double bonds, monoallylic position of fatty acid chains and more reactive allylic position (bisallylic position) could be used for further reactions.

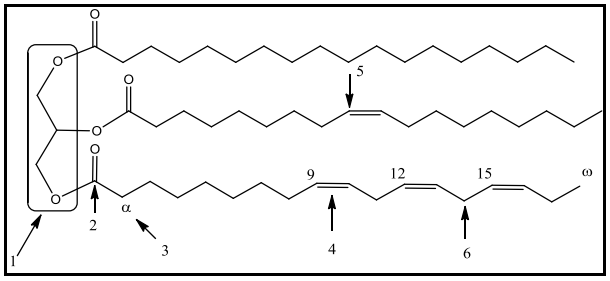

Figure 1.2. A triglyceride molecule contains glycerol linkage (1), ester group (2), α-position of ester group (3), double bonds (4), monoallylic position (5), bisallylic position (6).

Among soybean oil reactions, hydrolysis, epoxidation, acrylation, maleinization are known. Some of the products that could be synthesized from soybean oil which are being used as reactants for polymer industry are shown in Figure 1.3.

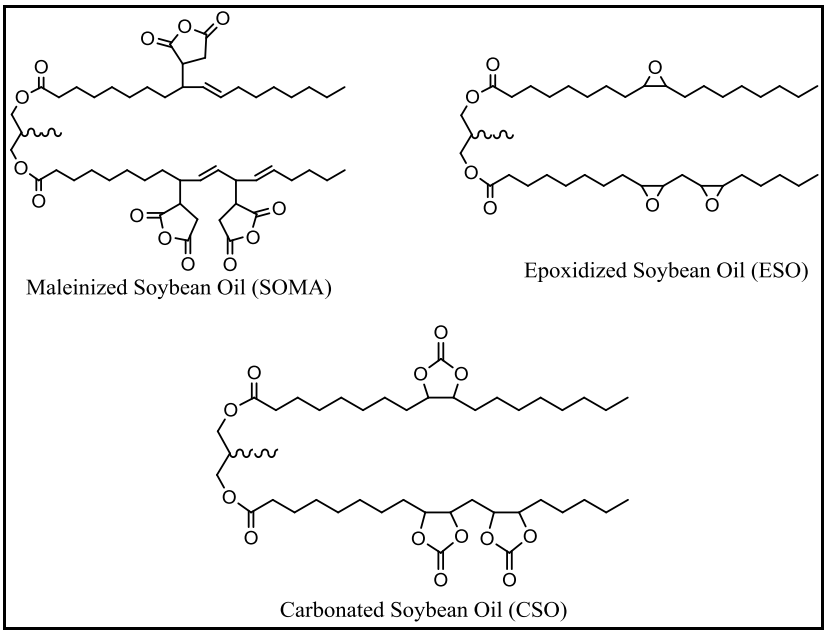

Figure 1.3. Examples of Funcionalized Soybean Oil [9].

1.3.3. Epoxidation of Soybean Oil

Epoxidation introduces a reactive functional group to the triglyceride and makes it suitable for polymerization. Additionally, ESO can be used as a plasticizer in commercial polymers. Long fatty acid chains in vegetable oils provide flexibility and toughness for brittle polymer sistems like epoxy homopolymers, polyurethanes, polyester systems. ESO-containing polyvinyl chloride (PVC) polymers show higher heat and light resistance than normal PVC. Due to lower cost and higher number of unsaturation related with the percentage of linoleic and linolenic acid soybean oil is the advantageous oil for epoxidation.

There are several different methods for epoxidation. Widely used methods are epoxidation with percarboxylic acids, epoxidation by chemoenzymatic process in which lipase enzyme is used, epoxidation using metal catalyst as a homogeneous catalyst system based on tungsten or rhenium compounds or heterogeneous catalyst system based on molybdenum or titanium based systems. These different methods were developed to prevent side reactions of oxirane ring, increase selectivity of epoxidation reactions but

because of financial concerns conventional peracetic or performic acid method is widely used. Figure 1.4 shows general epoxidation reaction, reactivities of different peracids and epoxidation mechanism of double bond [10].

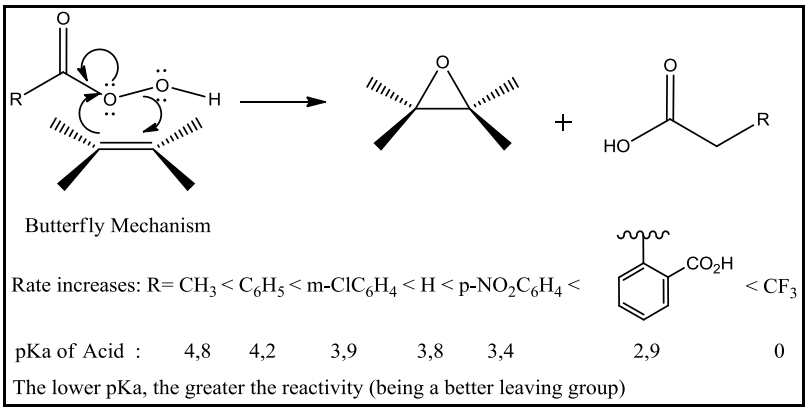

Figure 1.4. Mechanism of epoxidation reaction and effect of pKa on the reaction [11].

ASTM D1652-11$^{\varepsilon 1}$ is a general standard for determination of epoxy equivalent weight (EEW) to determine the epoxidation yield. EEW is weight in grams of resin containing 1 mole equivalent of epoxide (g/mol). Commercial ESO which was used in this work contains 4.1 epoxy groups per triglyceride.

Richard C. Larock et. al. used soybean oil to synthesize polymers with methathesis and comethathesis reactions. As a comonomer divinylbenzene, norbornadiene and dicyclopentadiene were used with $BF_3.OEt_2$ catalyst. Mechanical properties of synthesized polymer were analyzed with DMA and TGA and found to have 10^9 MPa modulus [12].

Selim Kusefoglu et. al. synthesized thermoset polymers from ESO. Process is applicable for RIM, BMC, SMC etc. ESO was polymerized with different monomers such as phthallic anhydride, dicyclohexylamine, Bisphenol-A (BPA) and isophthallic acid [13,14].

James V. Crivello et. al. used epoxidized oil, low molecular weight epoxy resin and cationic photoinitiator for UV-curing coatings. According to the results of the mechanical tests of these polymers shows that they are superior to commercially available coatings due to to their abrasion resistance, adhesion under sterilization conditions and in cure speed [15].

1.4. Isocyanates

1.4.1. Chemical Properties of Isocyanates

Isocyanates are low molecular weight toxic molecules. Their vapor pressures are high which makes them highly hazardous. They are synthesized by the reaction of primary amines with phosgene. A simple isocyanate is shown in Figure 1.5.

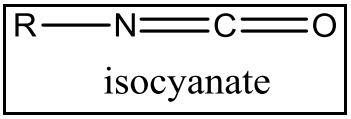

Figure 1.5. General structure of Isocyanates.

The worldwide attention on isocyanates came as a result of an industrial accident in Bhopal, India, in 1984 when 40 tons of methyl isocyanate gas was accidentally released near a populated area. About 18,000 people died and more than 150,000 people were injured. This is the worst single chemical accident in the history of chemistry.

Nowadays isocyanates are the essential raw materials in polyurethane industry which was first discovered by 1930s. Isocyanates can vigorously react with water, primary alcohols and primary amines therefore the storage conditions are important. They can be mono-, di- or polyfunctional. Since at least two functionality is important for polymeric approach in Figure 1.6 some common diisocyanate monomers are shown.

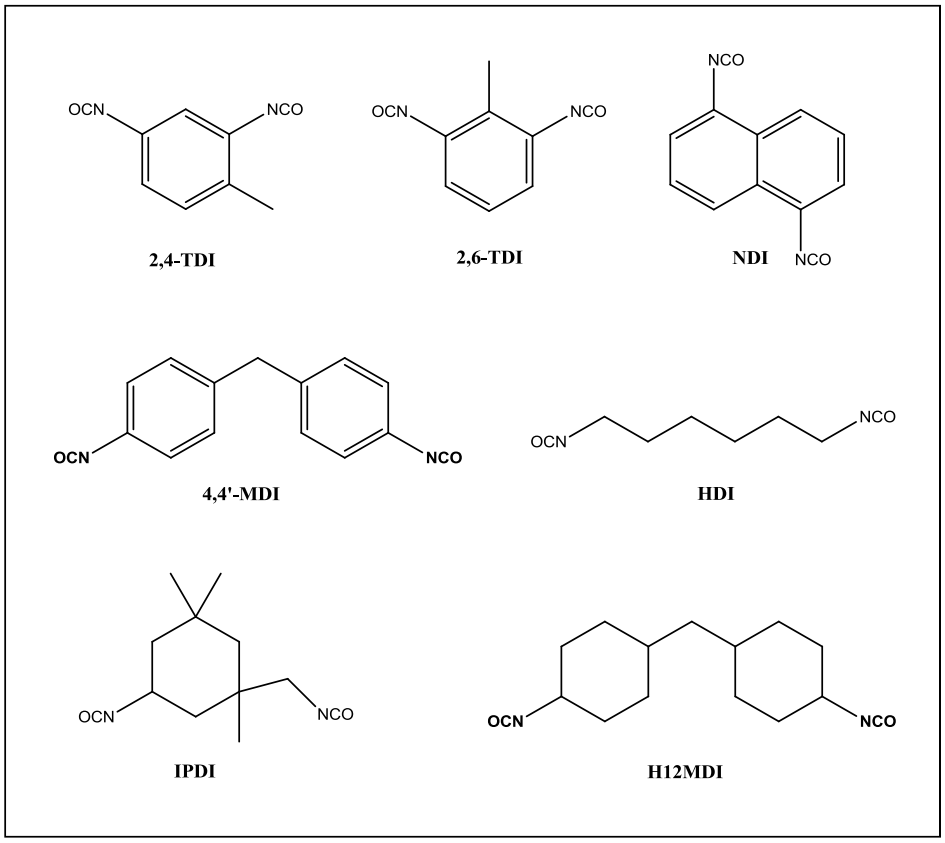

Figure 1.6. Common Isocyanates [16].

Aromatic, aliphatic, cycloaliphatic or polycyclic isocyanates are known. Aromatic isocyanates degrade under UV light. Therefore they are mostly used for indoor applications, such as flexible and rigid foams for the furniture industry. Aliphatic isocyanates however are stable against UV and give transparent polyurethane products. Application areas are coatings, adhesives, sealents and elastomers.

General application areas of isocyanates are indicated below and are generally based on polyurethane products:

- Synthetic rubber
- Synthetic textile fibers
- Glues and adhesives
- Anti-corrosive chemicals

- Wire and cable insulation
- Paints, lacquers, ink and varnishes
- Leather finishes
- Foundry cores (binders)
- Bathtub and sink finishes
- Ornamental plaques and frames
- Packaging materials
- Apply orthopedic casts
- Artificial limbs
- Flexible foam in upholstery
- Flotation materials

1.4.2. Health Effects of Isocyanates

After the Bhopal tragedy, studies about the effect of isocyanate on human health were started to conduct. Although these studies show the effect of methyl isocyanate on humans, the toxicity of all the isocyanates became obvious. Bhopal accident caused severe pulmonary oedema to chronic fibrosis which was proved by amine experiments [17].

N-carbmylation and S-carbamylation of human proteins was also observed. This shows that the isocyanates can react with amino acids. Carbamylation in body can cause atherosclerosis and renal failure. In Figure 1.7, N-carbamylation is shown [18].

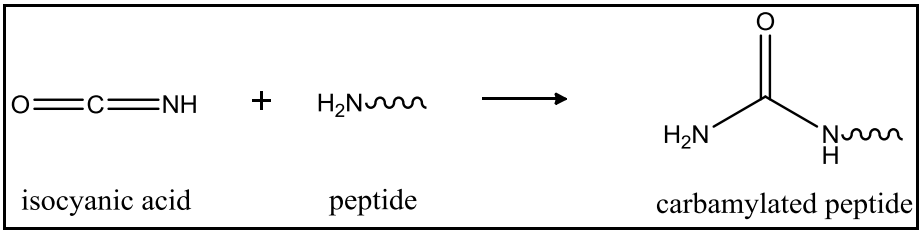

Figure 1.7. Carbamylation Reaction of a Peptide from N-terminus.

Exposure to isocyanates can be acute (single time with high concentration) or chronic (repeated exposure to low concentration). Acute exposure can be with inhalation such as in the Bhopal accident, or skin exposure such as spilling. Chronic exposure can be work-related such as working in polyurethane industry. Acute exposure can cause irritation to mucous membranes (eyes, nose, dry or sore throat), gastrointestinal irritation, nasal congestion, chest tightness, coughing, fever, fatigue, asthma [19].

Chronic exposure symptoms are similar to acute exposure but with the addition of allergies. Occupational asthma, skin irritation (dermatitis) are observed in people who work with isocyanates. Skin exposure can also cause respiratory responses. Symptoms are delayed for 6-10 hours after exposure and cleared in 24 hours which makes them difficult to relate with working conditions. Once a person is sensitized, there is no safe level of exposure to work with isocyanates. Skin sensitization is not permanent and heals after isocyanate exposure stops, however lung damages are permanent. Aerosol applications makes isocyanate vapors more dangerous because air-borne particles are smaller than 1 μm and can penetrate alveoli. Genotoxicity studies of isocyanates shows that isocyanates can alter the DNA in vitro which is a remark for carcinogenity. Commercial grade of TDI has an effect of making tumorigenic responses in rats and mice and cause the formation of brain tumors. TDI is a potential carcinogen for humans [20].

To decrease the vapor pressure of isocyanates, prepolymers of isocyanates and blocked isocyanates were developed to decrease their reactivity and vapor pressure at room temperature. Table 1.4, shows the vapor pressures of both monomeric and polymeric isocyanates and Figure 1.8, shows the prepolymer and blocked types of isocyanates.

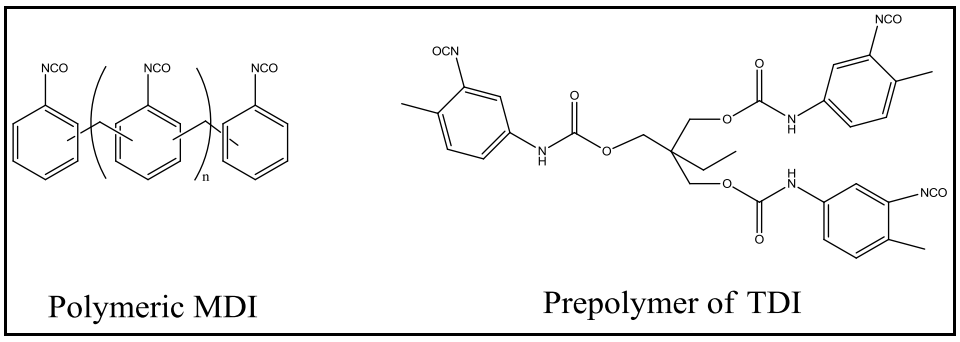

Figure 1.8. Polymeric MDI and Prepolymer of TDI.

Table 1.4. Physical and Chemical Properties of Common Isocyanates.

PHYSICAL AND CHEMICAL PROPERTIES OF ISOCYANATES			
Name of Isocyanate	CAS Number	Vapor Pressure (mm Hg at 20 ºC)	Saturation Concentration in Air (ppm)
Methyl Isocyanate	624-83-9	390	510000
Butyl Isocyanate	111-36-4	16	21000
Phenyl Isocyanate	103-71-9	2	2600
Hexamethylene Disocyanate (HDI monomer)	822-06-0	0.025	33
Hexamethylene Disocyanate (HDI polyisomer)	28679-16-5	0.000075	0.099
Toluene-2,4 Diisocyanate	584-84-9	0.02	33
Toluene Diisocyanate (80:20 mix of isomers)	26471-62-5	0.02	33
Isophorone Diisocyanate	4098-71-9	0.0005	0.66
Diphenylmethane-4,4' diisocyanate	101-68-8	< 0.00001	< 0.013
Prepolymer diphenylmethane-4,4' diisocyanate	9016-87-9	< 0.00001	< 0.013
Dicyclohexylmethane diisocyanate-4,4'	5124-30-1	0.00001	0.013

The U.S. National Institute for Occupational Safety and Health (NIOSH) and Occupational Safety and Health Administration declared exposure limits and periods of isocyanates. Obeying these rules, ventilation of work place, wearing full face supplied air

respiratiors especially for spraying activities, using nitrile, butyl or vinyl gloves instead of latex, using disposable coveralls are required [21-23].

1.4.3. Chemical Reactions of Isocyanates

Reactivity of isocyanates is related with the positive character of carbon atom in isocyanate group. If the alkyl group attached to isocyanate is aromatic, negative charge can be delocalized on the alkyl group which increases the positive character of carbon atom. Therefore aromatic isocyanates are more electrophilic and reactive than aliphatic isocyanates. But the reactivity is also effected with substituents on the aromatic alkyl group and steric hindrance. For instance, in the case of diisocyanates, electron attraction of second isocyanate group increases the reactivity of first isocyanate group. Para-substituted diisocyanates are more reactive than ortho-substituted diisocyanates because of the steric reasons. Isocyanates give reaction with nucheophilic compunds. According to compounds nucleophilicity such as with amines reaction could take place even at room temperature which is one of the reasons that isocyanates are toxic for living things.

The order of reactivity of nucleophiles with isocyanates in uncatalyzed conditions is indicated below:

Aliphatic amines > aromatic amines > primary alcohols > water >secondary alcohol > tertiary alcohol > phenol > carboxylic acid > ureas > amides > urethanes

Resonance structure of isocyanate group is also effects the isocyanate reactivity. Figure 1.9, shows the resonance forms of isocyanate group.

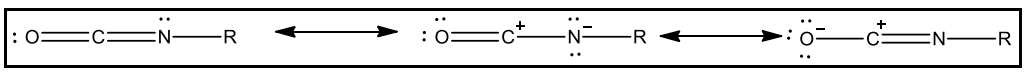

Figure 1.9. Resonance Forms of Isocyanate.

As well as nucleophilic substances, isocyanates give many self-reaction products. Considering the isocyanate self reactions is crucial for understanding the reaction products. Isocyanurate is the most important side products. General reaction pathways of isocyanates is shown in Figure 1.10 [24,25].

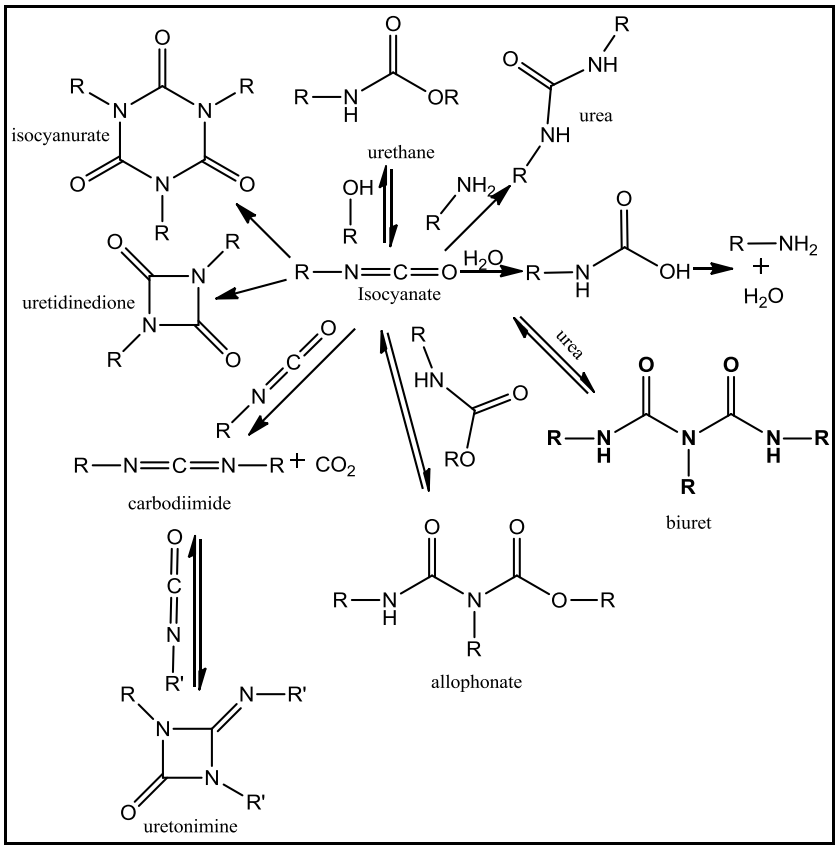

Figure 1.10. Schematic illustration of over all primary and secondary reactions that may occur during polyurethane synthesis.

1.5. Catalysts for Isocyanate Reactions

1.5.1. Commercial Properties of Catalysts

Commercial products of isocyanates are generaly generated with catalytic reactions. Catalyst choice is industrially important because physical properties of the polymeric products depend on the catalyst used. Five types of catalysts are available: Gelling

catalysts, blowing catalysts, delayed action catalysts, surface cure catalysts, reactive catalysts.

Gelling catalysts favor the isocyanate-active hydrogen compound reaction while blow catalysts increase the rate of isocyanate-water reaction. Some catalysts such as ***1***,***4***-diazabicyclo[2.2.2]octane (DABCO) shows both gelling and foaming behaviour. Reaction of isocyanate with water produces an amine and CO_2 which acts as a foaming agent and this has become a very convenient method for producing polyurethane foams.

Surface cure catalysts are tertiary amines that have high vapor pressure. In the mold, while they vaporize on the heated mold surface, they catalyze the reaction on the surface. This improves the surface properties and decreases surface tackyness of the product. Triethylamine (TEA) and morpholine containing compounds are the examples of surface cure catalysts. Industrially these catalysts are known as “skin forming” catalysts.

Delayed action catalysts help the adjustment of gellation time. They are amine catalysts blocked with carboxylic acids, can be deblocked with an exothermic reversible reaction. In the mold, while unreacted monomers are being heated, amine catalysts are released by deblocking and catalyze urethane formation.

Reactive catalyts remain bonded to polymer products and they cause degradation and yellowing in the product [26].

The catalysts could increase the rate of either the self-reactions of isocyanates or the reactions of the isocyanate with active hydrogen compounds. Tertiary amines and metal compounds as Lewis acids are generally used in the literature. Generally used catalysts for different isocyanate reactions are shown in Table 1.5.

Table 1.5. Main types of catalysts commercially used in Polyurethane Industry.

CATALYSTS USED IN POLYURETHANE INDUSTRY	
Reaction	Catalysts
Isocyanurate Formation	Strong bases (potassium octoate), quaternary ammonium salts, phosphines
Uretidinedione Formation	Phosphorous compounds
Isocyanate Homopolymerization	Alkaline metal hydroxides
Isocyanate - Alcohol Reaction	Tertiary amines, organometals, metallic soaps
Isocyanate-Water Reaction	Tertiary amines
Urethane Formation	Metallic soaps
Urea Formation	Tin and Zinc Soaps

1.5.1.1. Trimerization/dimerization/carbodiimide Catalysts. Dimerization of isocyanates gives uretidinedione which may reaarange further to a carbodiimide while releasing carbondioxide. Dimerization is a reversible reaction. Dimerization is generally catalyzed by trialkylphosphines and some tertiary amines such as pyridine. Trimerization catalysts are similar to carbodiimide catalysts and they are alkali metal carboxylates, quaternary ammonium carboxylates, and some tertiary amines. Reactions are shown in Figure 1.11 [27].

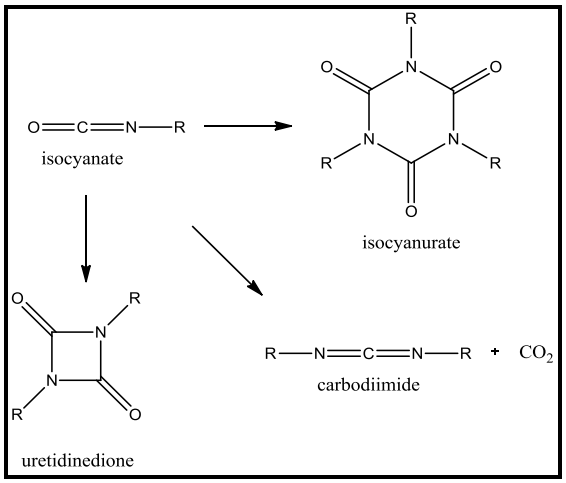

Figure 1.11. Trimerization, Dimerization, Carbodiimide Formation.

1.5.1.2. Isocyanate Alcohol Reaction Catalysts. Polyurethane industry is based on isocyanate-alcohol reaction. Succesful catalyts for the reaction are tertiary amines and organometallic catalysts. Catalytic activity of tertiary amines depends either their basicity or steric hindrance on the nitrogen atom. Lack of steric hindrence on the nitrogen atom makes DABCO a very reactive tertiary amine catalyst for polyurethane industry.

Organometallic compounds are the second type of catalysts that are more selective towards isocyanate-hydoxyl reaction. Most common organometallic catalysts for urethane reactions are Sn based catalysts such as dibutyltin dilaurate (DBTDL) and stannous octoate. Apart from Tin; Bismuth, Iron, Nickel, Cobalt compounds could be used as catalysts. Nowadays banning tin catalysts due to their aquatic toxicity is in question. Fortunately novel catalysts based on Zirconium were found such as Tetrakis-(2,4-pentanedionato) zirconium, which provide better properties than DBTDL with longer shelf-life, less gassing and higher glossing properties to the polymers. Figure 1.12 shows the isocyanate–alcohol reaction [28,29].

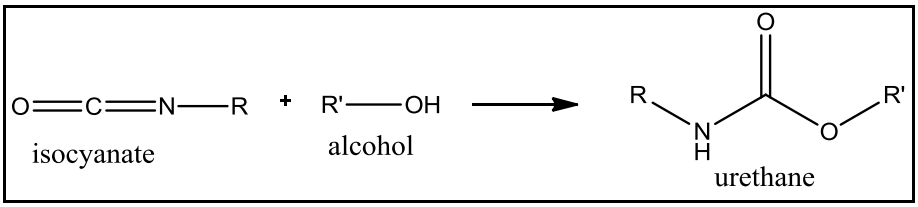

Figure 1.12. Isocyanate–alcohol reaction.

1.5.1.3. Isocyanate-Water Reaction Catalysts. Reaction product of an isocyanate with water is carbamic acid further degrades which rearranges into carbondioxide and amine. Since carbondioxide is in gaseous state, product turns into foam-like matter. Therefore catalysts that fasten this reaction, are called blowing agents. One of which is Bis[2-(N,N-dimethylamino)ethyl] ether (BDMAEE). Figure 1.13 shows the isocyanate-water reaction [30].

Table 1.6. Examples of isocyanate-water reaction catalysts and relative catalysis rate.

Relative Reactivity of Catalysts in Isocyanate-Water Reactions	
Catalyst	Order of Activity
Stannous Octoate	1
N-Ethyl Morpholine	1.1
Dibutyltin dilaurate	1.3
Triethylamine	1.5
DABCO	2.7

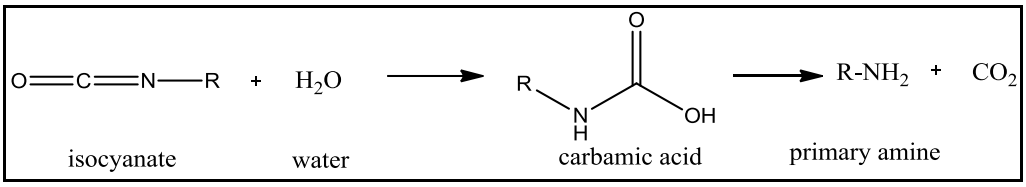

Figure 1.13. Isocyanate–water reaction.

1.5.1.4. Isocyanate-Epoxy Reaction Catalysts. Reaction between isocyanate and epoxy is an uncommon reaction and gives a 5-membered ring known as oxazolidone as the product. Generally all of the catalysts used for polyurethane industry could also be used to catalyze oxazolidone reactions such as alkyl imidazoles, quaternary ammonium and phosphonium salts, complexes of Lewis Acids such as aluminum chloride with tertiary amines, amides, phosphines, alkali metal carboxylates, carboxylates of heavy and transition metals. Among the Lewis Acid catalysts LiCl, $MgCl_2$, $ZnCl_2$, $FeCl_3$ are popular, and using these acids with Lewis Bases as a catalyst complex gives better results. Apart from them, triphenyl antimony iodide is an efficient catalyt as indicated in a Dow Patent. In recent years Ytterbium triflate and also Titanium, Zinc, Zirconium enolates have also been produced [31-34].

1.6. Isocyanate-Epoxy Reaction

Isocyanate-epoxy reaction is an unusual reaction of isocyanates and the reaction product is oxazolidone group. Oxazolidone synthesis and structure is shown in Figure 1.14, which can be considered as 5-membered ring contains urethane.

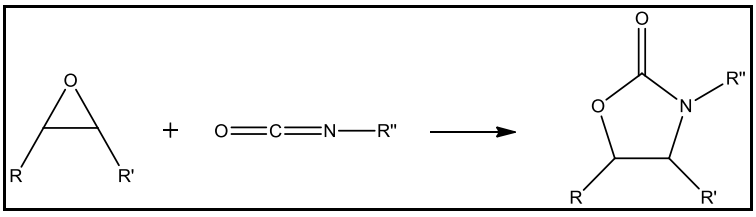

Figure 1.14. Synthesis of oxazolidone from epoxide and isocyanate and its general structure.

This reaction is accompanied by all the self reactions of the isocyanate group previously described.

When diepoxides and diisocyanates are used, polymers can be synthesized. Commercial DGBPA diepoxides and diisocyanate have been reacted to give polyoxazolidones.

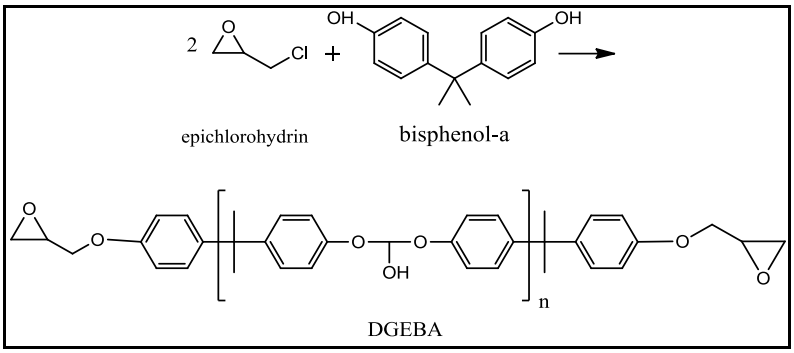

Figure 1.15. Synthesis of DGBPA.

Initial publication on polyoxazolidones was reported in 1958 by Speranza and Peppel. After that many publications were released two of them are going to be explained in detail.

J. S. Senger, I. Yilgor, and J. E. McGrath studied on polyoxazolidones with using MDI and diglycidyl ether of Bisphenol-A (DGBPA) as monomers and ethyl methyl imidazole (EMI) as a catalyst. Temperature was increased gradually up to 150 ^{o}C. Up to 70 ^{o}C, isocyanurate formation occurs and reaches its maximum then starts to decrease. At the same time at 70 ^{o}C oxazolidone formation starts and continues to increase above that temperature. They concluded that the isocyanurate is a reaction intermediate using FTIR as an identifier. They identified the absorption of isocyanate at 2270 cm^{-1}, oxazolidone carbonyl at 1754 cm^{-1}, isocyanurate carbonyl at 1710 cm^{-1}, and epoxide at 915 cm^{-1}. This study shows with EMI catalyst, oxazolidone formation was occured above 70 ^{o}C. Additionally, EMI is known to catalyze epoxy homopolymerization. DGBPA with EMI catalyst at 150 ^{o}C after 6 hours, 90% of DGBPA detected as unreacted. Additionally,

trimer of phenyl isocyanate was prepared and this trimer heated at 120 ^{o}C in the presence of DGBPA and EMI catalyst. Within 10 hours all the trimer compound disappeared [35].

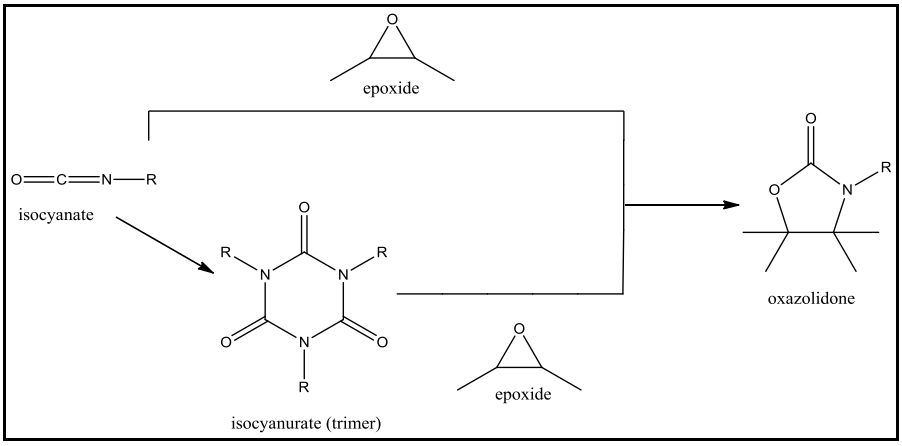

Figure 1.16. General scheme for the isocyanate-epoxy reaction.

Yeganeh et al. synthesized poly(urethane-oxazolidone) elastomer and characterized it. They have synthesized a model compound for oxazolidone with 1-methyl-1,3 diphenyl urea and 1,3 epoxy-3-phenoxypropane. Polymers were synthesized as an epoxy terminated polyurethane prepolymer and blocked HDI was used to minimize trimerization reaction. Temperature conditions for the polymer is 1 h at 100 ^{o}C, 1 h at 180 ^{o}C, 0.5 h at 200 ^{o}C in bulk. Crosslinked free model compound ATIR peaks were found at 1740 cm^{-1} due to oxazolidone carbonyl that was mixed with urethane carbonyl and esteric carbonyl arise from epoxy terminated polyurethanes (EUP) and blocked isocyanate (BIC). In ^{13}C NMR spectroscopy of model compound, carbonyl group of oxazolidone ring was appeared at 154 ppm and two other carbon atoms of oxazolidone ring were detected at 47.4, 83.0 ppm and 55.0, 68.0 ppm [36]. During isocyanate-epoxy reactions there are several side reactions. For DGBPA type of epoxides at temperatures below 100 ^{o}C, urethane formation was observed which gives a carbonyl stretching peak at about 1730 cm^{-1}. Urethane formation occurs due to the hydroxyl groups on DGPBA and reaction is shown in the Figure 1.17, in the same figure, additionally oxazolidones are formed this reactions generally occurs at elevated temperatures, followed by the trimerization reaction, isocyanurate formation.

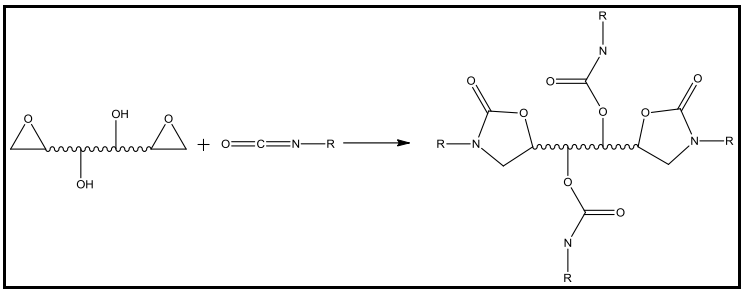

Figure 1.17. Urethane and Oxazolidone formation on the same compound.

TGA studies are important for the thermal degradation characterization of the functional groups in reaction product. General scheme declared the the order of thermal stability of main product and side products are;

isocyanurate > oxazolidone > carbodiimide > urea > urethane > biuret > allophanate

C. S. Lee, T. L. Ooi, C. H. Chuah, S. Ahmad reported the decomposition temperature of urea and urethane groups occurs between 200 ^{o}C-240 ^{o}C, oxazolidone ring 380 ^{o}C-430 ^{o}C, isocyanurate ring 450 ^{o}C-800 ^{o}C [37].

Kordomenos et al. however, stated these temperature ranges with a little difference and found that decomposition temperature of urethanes occurred at the temperature range of 260-360 ^{o}C, polyoxazolidones at 330-360 ^{o}C, polyisocyanurates at 380-420 ^{o}C [38].

Due to complex side product formation of the reaction, knowing the relative reactivity rates between the monomers and possible side products is important and could be seen in Table 1.7.

Table 1.7. Relative Reaction Rates of Active Hydrogen Compounds Against Isocyanates [39].

The Relative Reactivities of Isocyanates Against Different Hydrogen Active Compounds		
Hydrogen Active Compound	Formula	Relative Reaction Rate (non-catalyzed, 25 ^{o}C)
Primary Aliphatic Amine	$R\text{-}NH_2$	2500
Secondary Aliphatic Amine	$R_2\text{-}NH_2$	5000-1250
Primary Aromatic Amine	$Ar\text{-}NH_2$	5-7.5
Primary Hydroxy	$R\text{-}CH_2\text{-}OH$	2.5
Water	HOH	2.5
Carboxylic Acid	R-COOH	1
Secondary Hydroxyl	$R_2\text{-}CH_2\text{-}OH$	0.75
Urea	R-NH-CO-NH-R	0.375
Tertiary Hydroxyl	$R_3\text{-}C\text{-}OH$	0.0125
Phenolic Hydroxyl	Ar-OH	0.0025-0.0125
Urethane	R-NH-COOR	0.0025

Based on the reaction conditions and the catalyst type, amounts of side products differ. To identify these products could be important for characterization. Because of these are thermoset products, characterization is mainly based on FTIR spectroscopy and Table 1.8 shows the important peaks of both oxazolidone and side products. Additional to the Table 1.8, carbodiimide group has a characterictic sign at 2100-2200 cm^{-1}, biuret group has a characteristic sign at ~ 1081 cm^{-1}.

Petrovic et al. in US 6399698 B1 patent mentioned the oxazolidone synthesized from ESO. This reaction was conducted with a Lewis Acid catalyst and reaction was carried until the 50% of isocyanate was consumed. Several products such as oxazolidones, urethanes, amides, urea, isocyanurates, uretidinediones and esters are isolated from the

reaction. Due to these concerns ESO was not considered as an efficient monomer to synthesize oxazolidone polymers. Based on this situation this product was used as a prepolymer, for further synthesis of polyurethane [40].

Table 1.8. Common FTIR peaks of functional groups related with the oxazolidone and several side reactions of isocyanates [41,42].

FTIR IDENTIFICATION RELATED WITH THE SIDE PRODUCTS OF ISOCYANATE-EPOXY REACTION		
Functional Group	Carbonyl Stretch (cm^{-1})	C-N Stretch (cm^{-1})
Oxazolidone	1754-1736	1455
Aromatic Isocyanurate	1710	1410
Aliphatic Isocyanurate	1690	1465
Urea	1635-1655	1560-1510
Chain Imide	1790-1735/1750-1680 (2 bands)	1235-1165
Cyclic Imide	1740-1670	
Urethane	1760-1720	
Uretidinedione	1783-1776	
Allophonate and Biuret	1751-1709	1460-1416
Uretoneimine	1739	

2. RESEARCH OBJECTIVES

The aim of the project is to synthesize novel biobased thermoset poly(oxazolidone/isocyanaurate)s from epoxidized soybean oil and different monomeric diisocyanates such as MDI, TDI, IPDI, HDI which are shown in Table 2.1. The polymeric product will be identified by FTIR and NMR spectroscopy. Various tertiary amine and lewis acid catalysts will be used to maximize oxazolidone formation. The mechanical properties of the polymer will be determined by solvent uptake, surface hardness and compression tests. Thermal properties will be determined by TGA tests. The proposed reactions are shown in Figure 2.1, and the proposed mechanism is given in Figure 2.2.

Table 2.1. Abbreviations and Structures of Diisocyanates that used in this project.

Name of Diisocyanate	Abbreviation	Structure
Methylene diphenyl diisocyanate	MDI	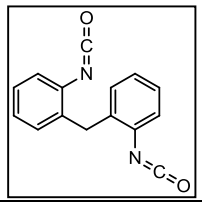
Toluene diisocyanate	TDI	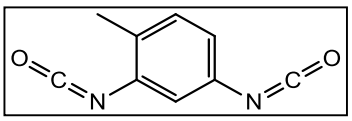
Hexamethylene diisocyanate	HDI	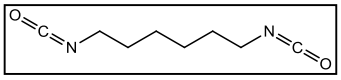
Isophorone diisocyanate	IPDI	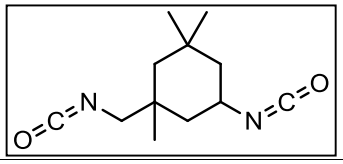

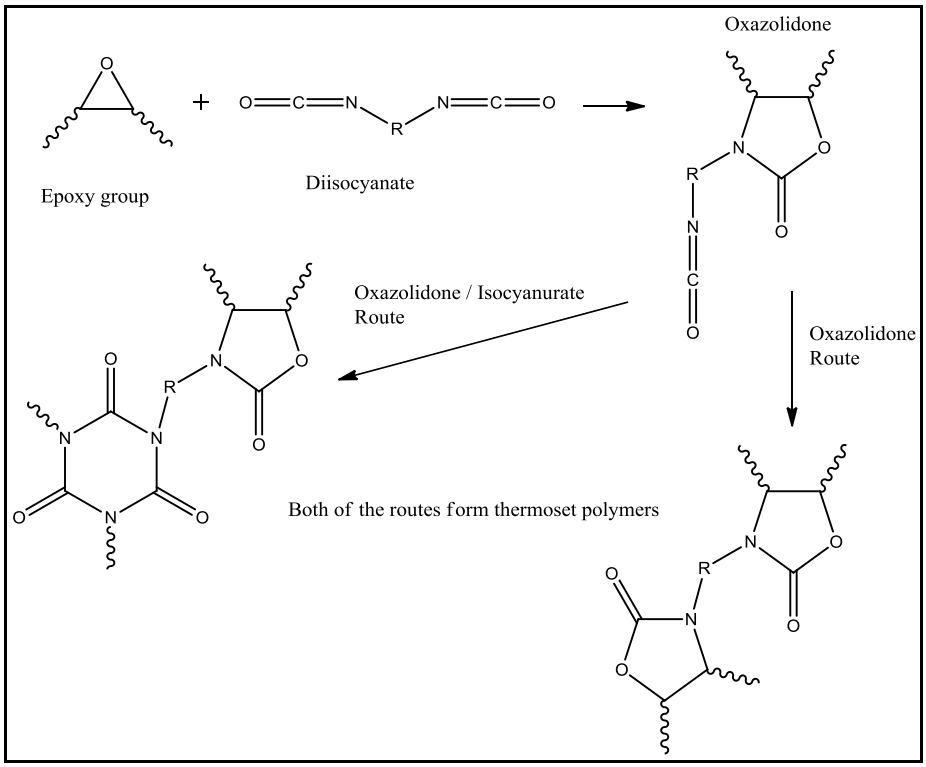

Figure 2.1. Main routes of diisocyanate-epoxy reaction.

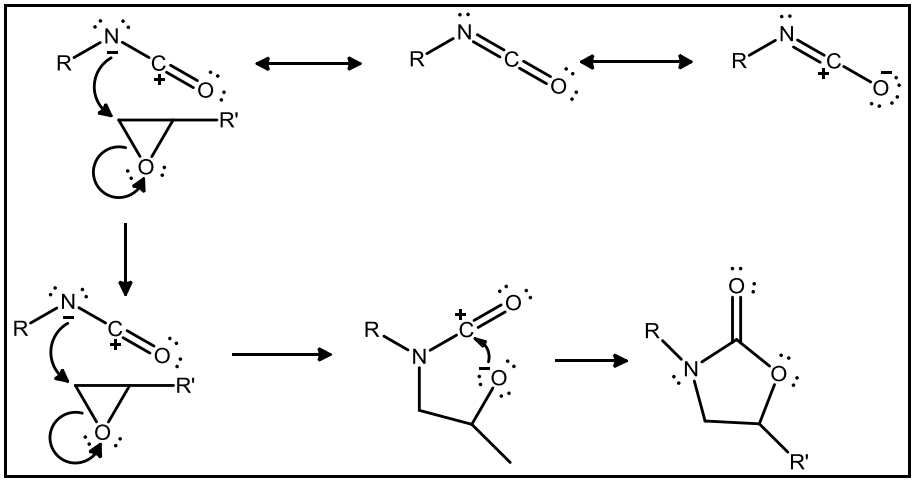

Figure 2.2. Proposed Mechanism of isocyanate–epoxy reaction.

3. EXPERIMENTAL

3.1. Materials and Apparatus

3.1.1. Materials

Epoxidized Soybean Oil was obtained from Akdeniz Kimya. Functionalizaton is 4.1 and used as it was obtained. Methylene diphenyl diisocyanate, Toluene diisocyanate, Isophorone diisocyanate and Hexamethylene diisocyanate, $SbCl_3$ were obtained from Fluka Chemical Corporation. Phenyl isocyanate and DABCO were obtained from Merck.

3.1.2. Apparatus

The ^{1}H NMR and ^{13}C NMR spectra were recorded on a Varian 400 MHz NMR instrument operating at a frequency of 399.986 MHz for ^{1}H NMR and 100.587 MHz for ^{13}C NMR and both of the spectras were given in ppm (δ).

The FTIR analysis were performed with Nicolet 380 FTIR Spectrometer with a Smart Diamond ATR.

Thermal Gravimetric Analysis of polymer products and model compounds was done with TA Instrument Q50. Temperature scans were performed with heating rate of 10 ^{o}C/min from room temperature to 700 ^{o}C.

Compression strength of polymers were obtained with Devotrans DVT TGP G NN instrument with a precision of ± 0.5 % according to ASTM D695 standard test.

Surface hardness data of polymers were obtained with Bareiss Shore D durometer according to ASTM D2240 standard test.

The swelling behavior of polymers was tested in hexane obtained from Merck Sharp & Dohme Corp. with solvent uptake method and weighings were taken with Shimadzu ATX 224 analytical balance.

3.2. ESO-Isocyanate Reaction Conditions

3.2.1. Reaction Conditions for the Preparation of Model Compounds

For preparing the model compounds, phenyl isocyanate was used with ESO as a monofunctional monomer. DABCO or $SbCl_3$ were used as catalysts. For the synthesis 0.1 g catalyst (3.3%) was used for 2.0 g ESO and 1.0 g phenyl isocyanate were used to provide 1:1 mole ratio. This corresponds to 4.1 moles of phenyl isocyanate to 1 mole of ESO. For first trials ESO was dried under vacuum at 110 ^oC for 6 hours and reactions were conducted under atmospheric conditions at 80 ^oC for 3 hours. Second trials were conducted with $SbCl_3$ under nitrogen. ESO was dried at 140 ^oC for 5 days and after, kept under nitrogen with the presence of molecular sieves. After weighing catalyst, reaction cell was closed and monomers were transferred with a syringe. Reactions were conducted at 65 ^oC and 140 ^oC for 1 day separately. FTIR, ^1H NMR, ^{13}C NMR characterization details are given in Section 4.

3.2.2. Reaction Conditions of Polymerization of ESO with Diisocyanates

Polymerization reactions were conducted with 1:1 mole ratio of isocyanate and epoxy groups. This corresponds to 2.05 moles of diisocyanate (functionality of isocyanate is 2) to 1 mole of ESO (functionality of ESO is 4.1). $SbCl_3$ was used as catalyst and it was used in varying amounts. The reactants were mixed and stirred at room temperature. Then mixture was placed in a test tube which was placed under vacuum to remove gas bubbles until an increase in viscosity was observed. Then the mixture was placed in an oven and heated for 12 hours at the chosen temperature.

For TDI, 1.5 g diisocyanate and 4.0 g ESO were used. Polymerization reactions were conducted at 100 ^oC, 110 ^oC, 120 ^oC. For each temperature 3 different catalyst amounts

were used. These amounts are 0.2 g, 0.3 g and 0.4 g. Their weight percentages are 3.6%, 5.5%, 7.3% duration of vacuum was 10, 5 and 2 minutes respectively.

Only for TDI-based polymers both $SbCl_3$ and DABCO were used to synthesize the specimens. Polymers synthesized with DABCO were only used for Surface Hardness Test and the reactions conducted at 80, 100, 120 ^oC with the identical catalyst amounts.

For IPDI, 1.9 g diisocyanate and 4.0 g ESO were used. Polymerization reactions were conducted under 70 ^oC, 80 ^oC, 90 ^oC. Above 90 ^oC isophorone diisocyanate vaporizes and creates bubbles in the polymer parts. For each temperature 2 different catalyst amounts were used. These amounts are 0.3 g, 0.4 g, 0.5 g and their weight percentages are 5.1%, 6.8%, 8.5%, duration of vacuum was 30, 10 and 2 minutes respectively.

For MDI, 2.1 g diisocyanate and 4.0 g ESO were used. Polymerization reactions were conducted under 90 ^oC, 100 ^oC, 110 ^oC. For each temperature 3 different catalyst amounts were used. These amounts are 0.2 g, 0.3 g, 0.4 g and their weight percentages are 3.2%, 4.9%, 6.5%, duration of vacuum was 5, 2 and 1 minute(s) respectively.

Compression and Hardness tests were done with the same polymer parts as it was indicated before. According to ASTM D695 standart test for compression tests, polymer parts could be in rectangular prism or cylindirical shape with a width or diameter to height ratio is 1:2. The diameter of sample was 11 mm and the height was 22 mm. For such polymers containing heterogeneous crosslinking dispersion, obtaining the parts without cracks is very difficult therefore the process was applied as A stage for viscosity increase and B stage for completion the polymerization reactions.

FTIR characterization details are given in Section 4.

3.2.3. Caution

Proper precautions must be observed when samples are cut. The sawdust created was found to be a mild skin irritant.

3.3. Procedures for Mechanical Tests

3.3.1. Shore (D) Hardness Test

Shore Hardness Tests were applied according to ASTM D2240 standard test. Polymer samples should have at least 6 mm width. For every catalyst ratio and temperature condition three sampleswere synthesized and six data points were obtained from each sample. Thus an average of 18 data points were calculated and reported.

3.3.2. Compression Test

Compression Tests were applied according to ASTM D695 standard test. Height of specimens was twice of the diameter of samples (22 mm x 11 mm). Surface cross-sectional area was 0.95 cm^2. For every catalyst ratio and temperature condition three samples were synthesized and three data were obtained and average of these data were used.

3.4. Swelling Test

Swelling tests were done in hexane. The initial weights of polymers were recorded. Afterwards samples were put in closed containers which contained 25 ml of hexane. Increase in weight was recorded for one hour time intervals until the solvent uptake ceased and swelling reached to equilibrium. Data was presented graphically and as the equilibrium solvent uptake.

3.5. Thermogravimetric Analysis (TGA)

TGA samples were used from the samples that were synthesized for compression and surface hardness tests. Both weight vs. temperature and derivative of weight vs. temperature graphs were obtained and examined.

4. RESULTS AND DISCUSSION

4.1. Characterization and Analysis of ESO

Characterization of ESO was done with ^{1}H NMR, ^{13}C NMR and FTIR. Quantitative analysis of the functionality of ESO was done with ^{1}H NMR. ESO is a known compound, still careful spectral analysis was required so that the product spectra could be interpreted.

Figure 4.1 shows the chemical structure and ^{1}H NMR spectrum of ESO and Table 4.1 shows the interpretation of the peaks in ^{1}H NMR.

Table 4.1. ^{1}H NMR Interpretation of ESO [43].

Number of Hydrogen	Chemical Shift (ppm)	Integration
1	4.23-4.04	4.02
2	5.18	1.01
3	2.25-2.03	6.02
4	1.73-0.97	74.01
5	3.04-2.81	8.20
6	0.97-0.79	9.00

In order to calculate the average number of epoxy groups present in one molecule of ESO, the ratio of integral value of methyl protons of ESO (peak 6) to the integral value of the peaks corresponding to the –CH –CH– protons of epoxy groups (peak 5) was calculated. From that ratio it was concluded that there are 4.1 epoxy functional groups per triglyceride on average.

Soybean oil from which ESO is synthesized does not have a fixed composition of fatty acids. Therefore it is impossible to calculate the molecular weight of ESO. ^{1}H NMR integration gives 950 g/mole but most publications take the molecular weight as 1000 g/mole. This is the value accepted in this work.

^{13}C NMR spectra of ESO is shown in Figure 4.2. Table 4.2, shows the relationship between the chemical structure and the signals in ^{13}C NMR spectra of ESO.

Table 4.2. Interpretation of ^{13} C NMR spectra of ESO.

Number of Carbon	Chemical Shift (ppm)
1	62.1
2	68.8
3	33.9
4	24.8-24.7
5	27.1-26.8
6	56.9-54.2
7	26.1/27.8-27.7
8	14.1-13.9
9	29.6-28.9
10	173.4
11	31.6
12	22.6-22.5

FTIR Spectrum of ESO is shown in Figure 4.3. Interpretation of the peaks are listed in Table 4.3 [44].

Table 4.3. Interpretation of the FTIR peaks of ESO [44].

Frequency (cm^{-1})	Chemical Structure	Interpretation
823	C-O-C (Epoxy Ring)	Symmetric Ring Deformation
846	C-O-C (Epoxy Ring)	Asymmetric Ring Deformation
1241	C-O-C (Epoxy Ring)	Asymmetric Ring Stretching
1463	C-H (CH2,CH3)	Bending (Scissoring)
1379	C-H (CH2,CH3)	Symmetric Bending
1155	C-O	Asymmetric Stretching
724 (Reference peak)	C-H (CH2)	Rocking

4.2. Synthesis and Characterization of Model Compounds

ESO-diisocyanate products necessarily give crosslinked, insoluble products. Therefore model compounds with a monoisocyanate; phenyl isocyanate, were synthesized to determine the structure of the products.

Model Compounds were synthesized with ESO and phenyl isocyanate using two different catalysts DABCO and $SbCl_3$ at different temperatures. These experiments showed that $SbCl_3$ was a better catalyst and $SbCl_3$ was chosen for synthesis of the polymers. Soluble products could be obtained and NMR analysis became possible.

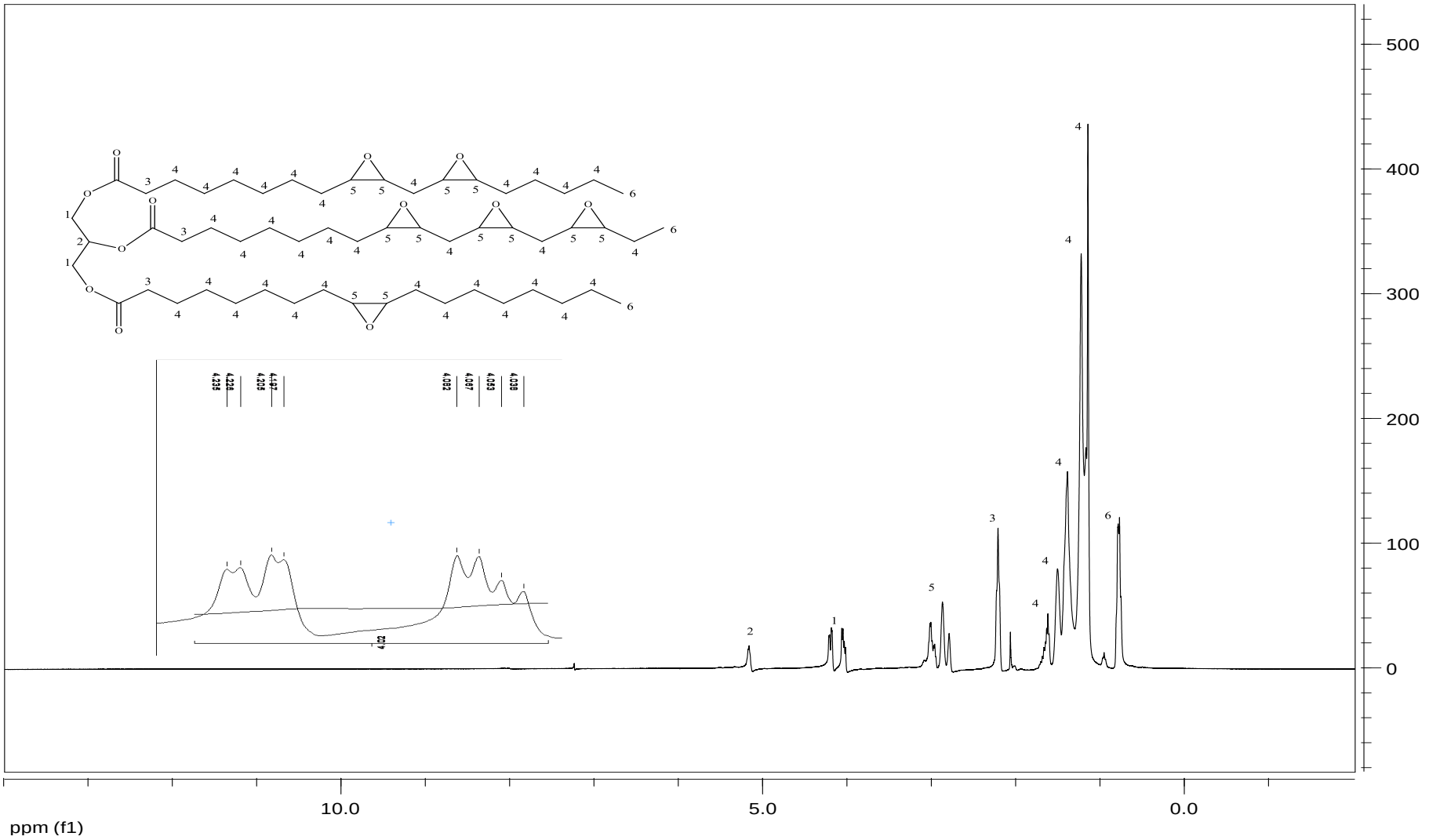

Figure 4.1. ^{1}H NMR Spectrum of ESO.

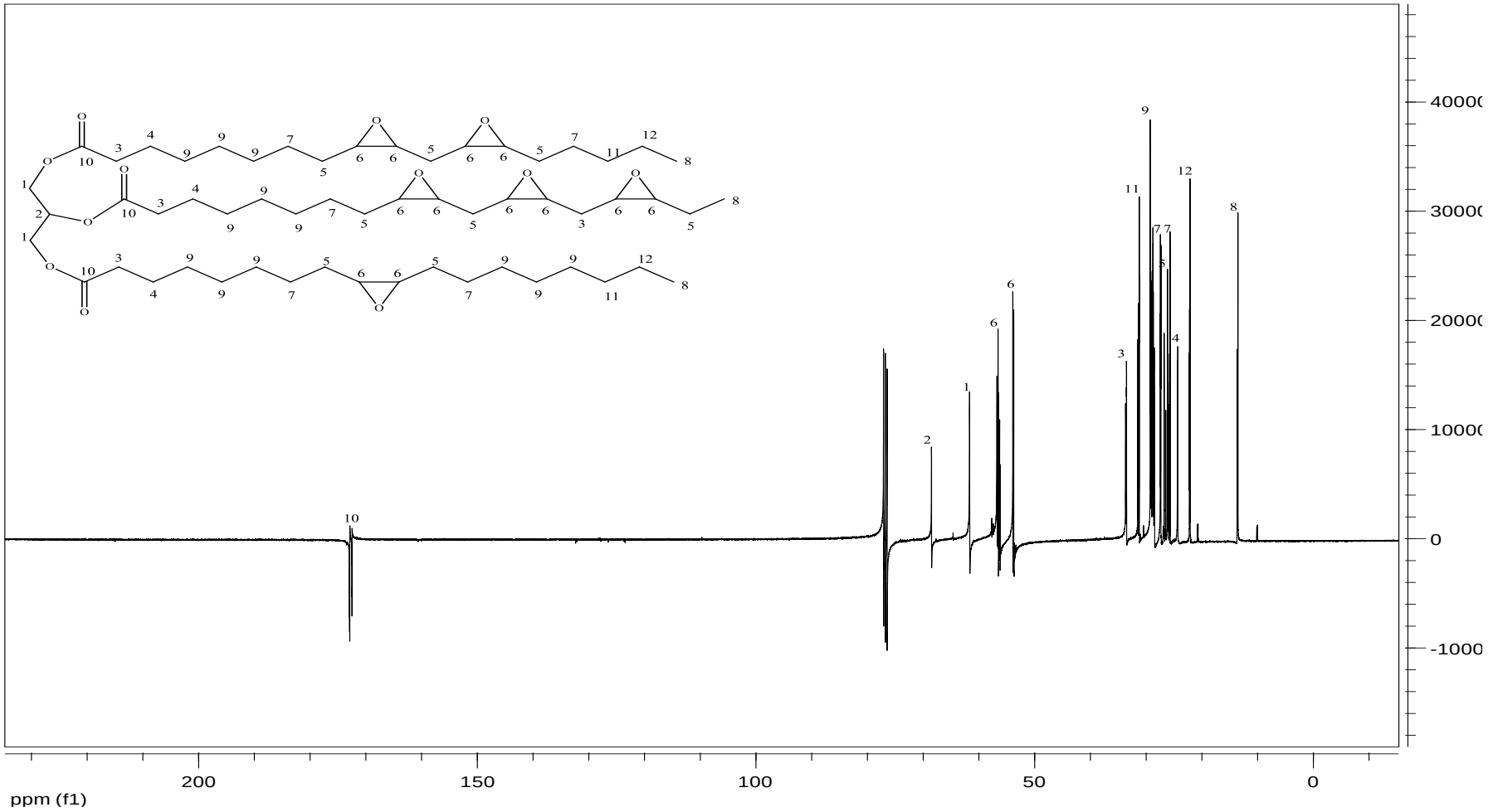

Figure 4.2. ^{13}C NMR spectrum of ESO.

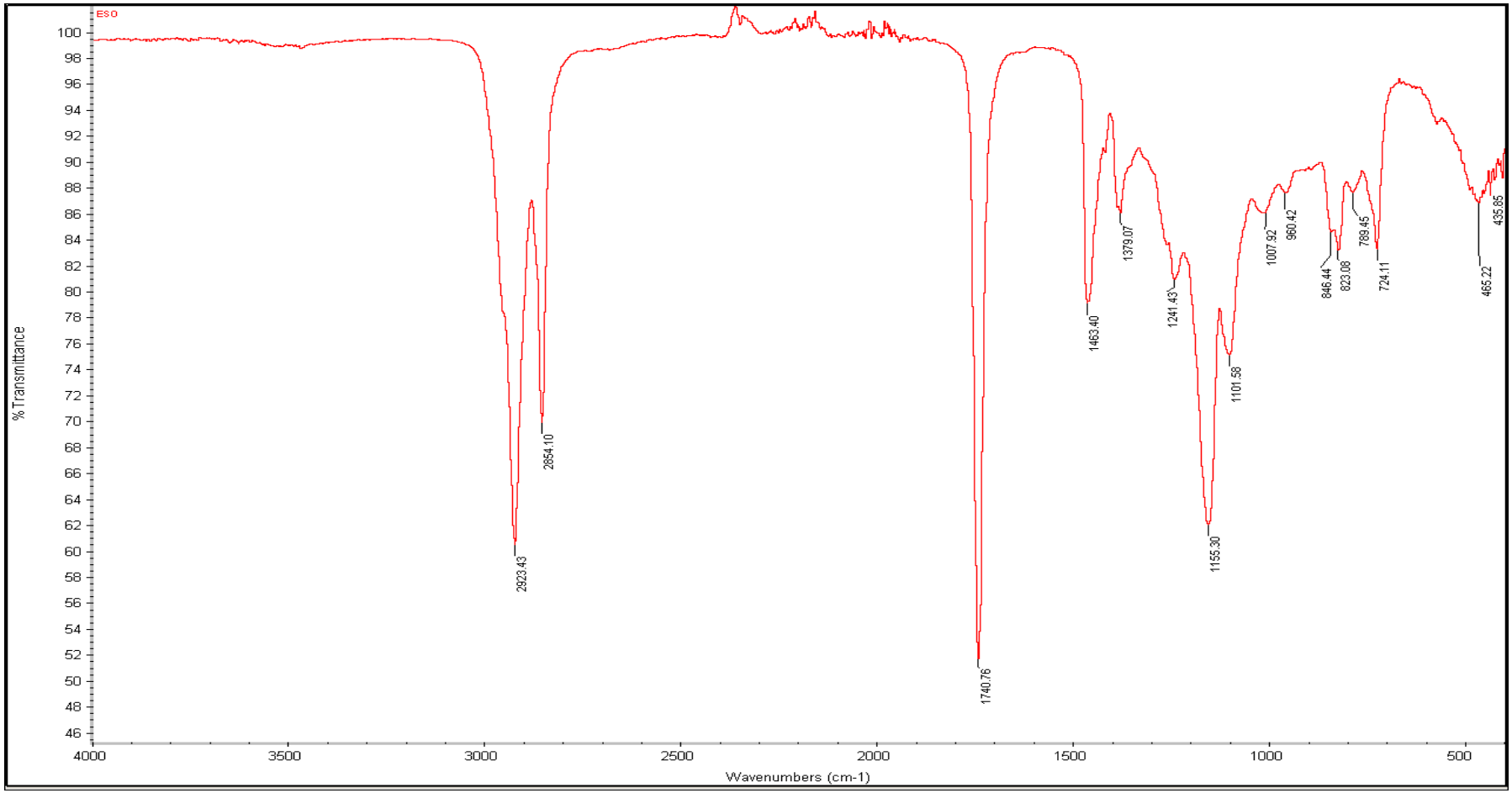

Figure 4.3. FTIR Spectrum of ESO.

Figure 4.4 shows the reactions that take place with isocyanate-epoxy reaction.

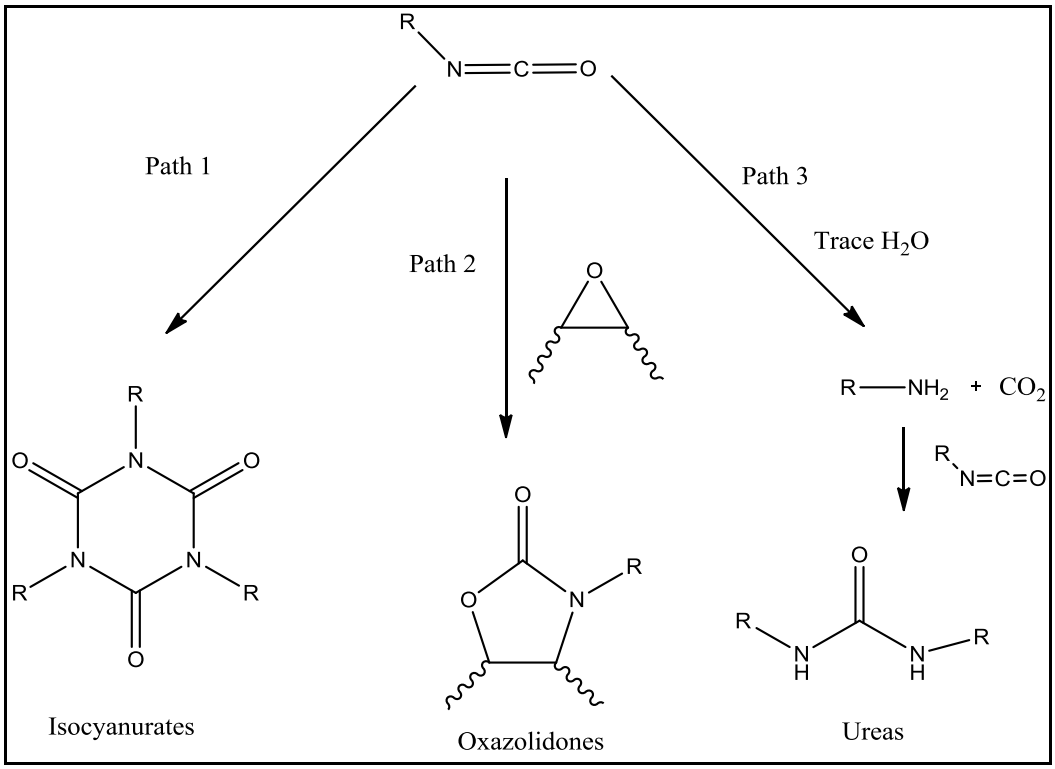

Figure 4.4. Possible side reaction pathways for isocyanate-ESO reaction.

4.2.1. Model Compounds under Atmospheric Conditions at 80 °C

4.2.1.1. Trial 1. In the DABCO catalyzed reaction of phenyl isocyanate with ESO the color of oil got darker and a white precipitate was formed during the reaction which is a sign of isocyanurate formation. The crude reaction mixture was extracted with hexane to remove unreacted ESO. The remainder was extracted with toluene which dissolved the reaction product but did not dissolve the isocyanurate by-product. The isocyanurate was dissolved in acetone and recrystallized at -18 °C. Its ^{1}H NMR and ^{13}C NMR anf FTIR spectra were examined. ^{1}H NMR can be seen in Figure 4.5, ^{13}C NMR can be seen in Figure 4.6 and Table 4.4 shows the ^{1}H NMR and ^{13}C NMR interpretation of this solid by-product. Spectral analysis confirmed that the structure of the white solid was the trimeric isocyanurate of phenyl isocyanate which is shown as Path 1 in Figure 4.4.

Table 4.4. ^{1}H NMR–^{13}C NMR interpretation of white solid.

Types of Hydrogen	Chemical Shift for ^{1}H NMR	Integration
Aromatic Hydrogens (Isocyanurate)	7.52-7.39	4.23
Acetone Hydrogens	2.16	1.02
Types of Carbon	Chemical Shift for ^{13}C NMR	Number of Hydrogen
Aromatic Carbons (Isocyanurate)	148.7	1
	133.6	2
	129.3	4
	128.4	3, 5
Acetone Carbons	30.9	

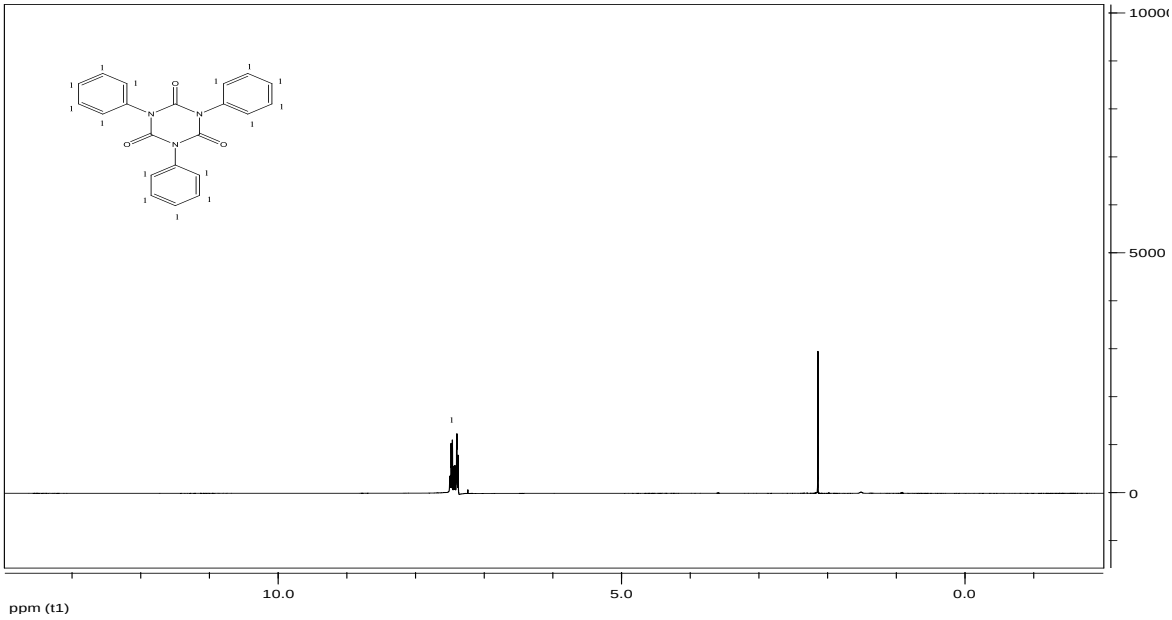

Figure 4.5. ^{1}H NMR of the white solid product.

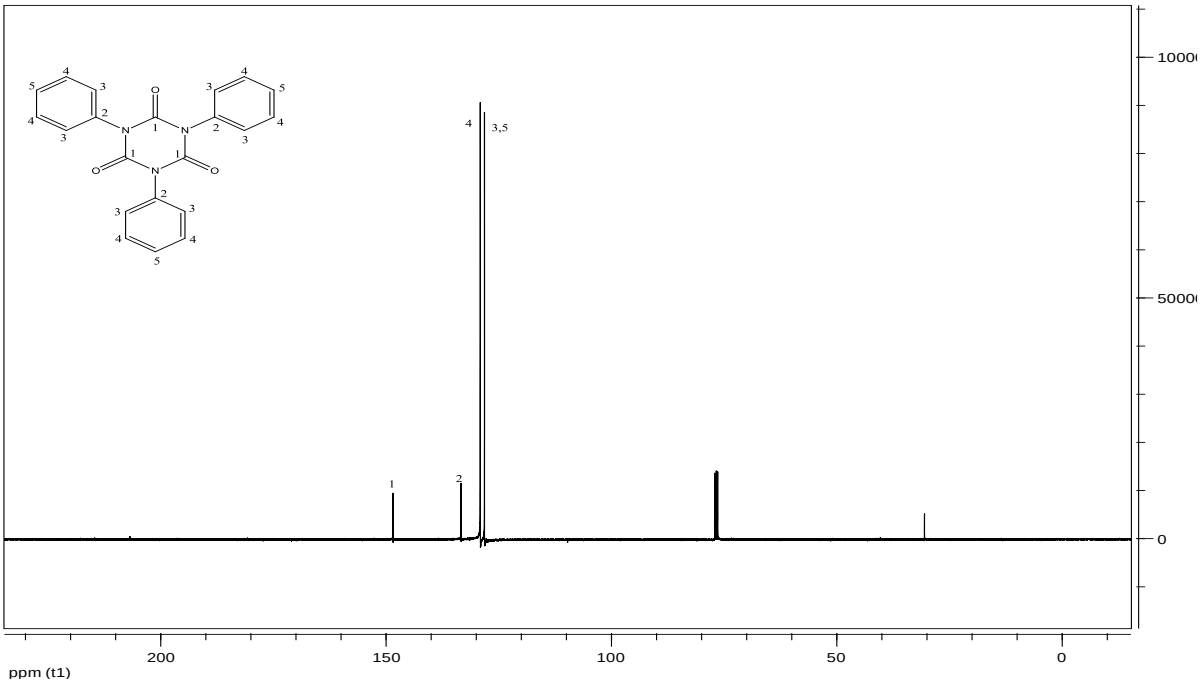

Figure 4.6. ^{13}C NMR of the white solid product.

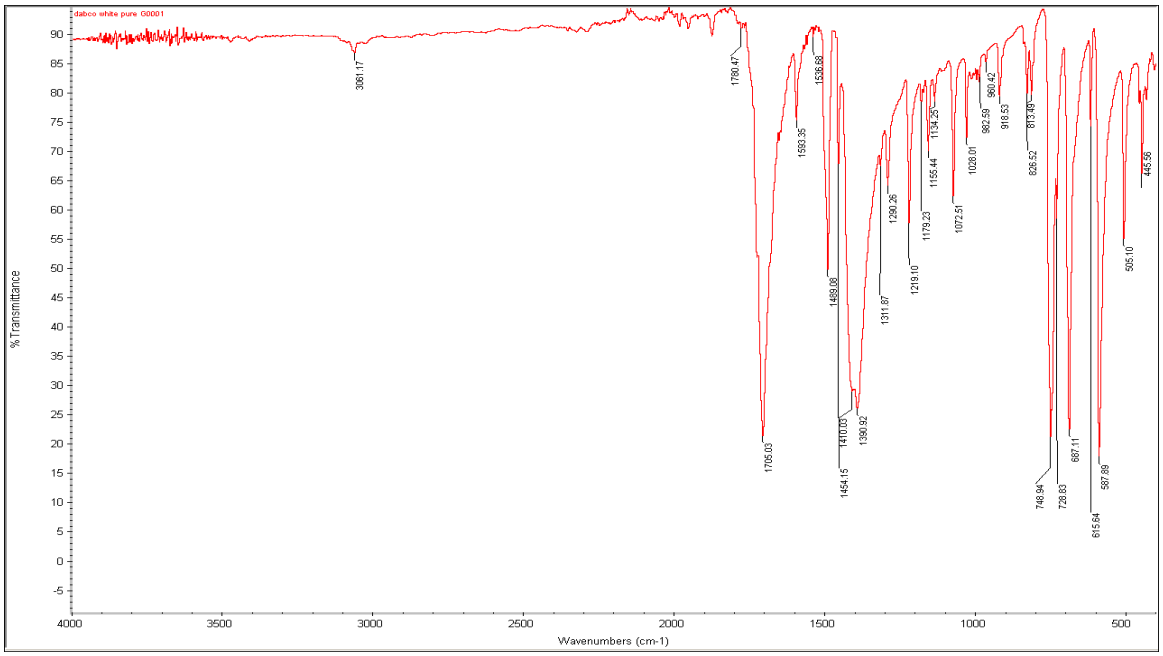

Figure 4.7. FTIR spectrum of white solid (triphenyl isocyanurate) product.

Figure 4.7 shows the FTIR spectrum of isocyanurate product. The peak at 1705 cm^{-1} shows the carbonyl stretching of isocyanurate which is close to literature data (1710 cm^{-1}), 1410 cm^{-1} shows triazine ring stretching and 813 cm^{-1} shows the triazine out of plane bending. This data indicates that DABCO catalyzed reaction of epoxides and phenyl isocyanate gives mostly the isocyanurate of phenyl isocyanate (Figure 4.8) and reaction with the epoxy group proceeds only to a small extent.

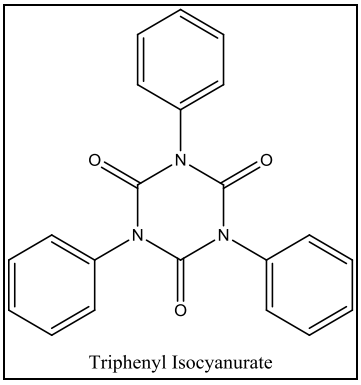

Figure 4.8. Triphenyl Isocyanurate.

The toluene soluble but hexane insoluble part of the product was isolated. Its ^{1}H NMR and ^{13}C NMR was examined. Several reaction products were observed. Figure 4.9 shows the FTIR spectrum of the main product and Table 4.5 shows the FTIR interpretation of the main product. FTIR in Figure 4.9 proved the peak at 1538 cm^{-1} belongs to urethane –NH bend and at 1444 cm^{-1} belongs to urethane C-N stretch. The peak broadening at 1755 cm^{-1} clearly shows the oxazolidone formation. Open chain-urethane and oxazolidone formation occurred together.

Table 4.5. FTIR interpretation of the main product obtained from second model compound.

Position of the Peak (cm^{-1})	Interpretation
1755	Oxazolidone Carbonyl Stretch
1731	Urethane carbonyl stretch
1538	Urethane N-H bend
1457	Isocyanurate C-N stretch
1444	Urethane C-N stretch
1404	Isocyanurate ring deformation
846-823	Epoxy ring deformations (Decreased)
1240	Epoxy ring deformation (shifted and decreased)
722	Alkyl -CH rocking (Reference Peak)

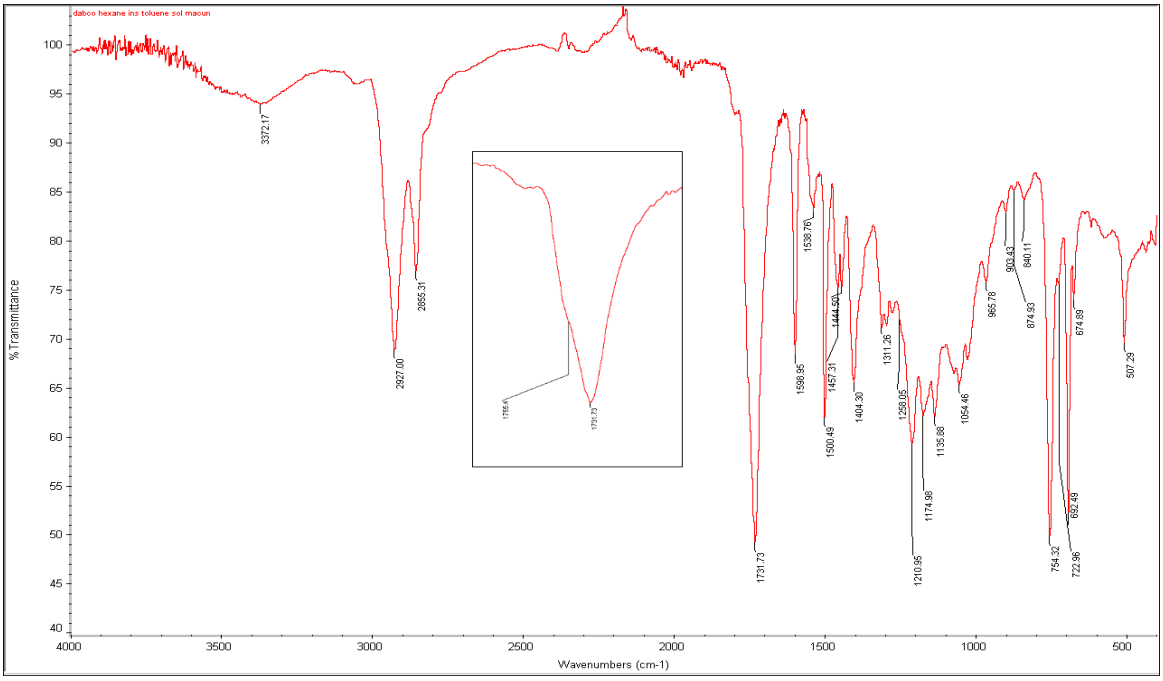

Figure 4.9. FTIR Spectrum of the main product obtained from second model compound.

In ^{13}C NMR of the main product there are two new carbonyl peaks at 153.5 and 155.9 ppm. One of which could be related with the urethane carbonyl and the other one could be related with the oxazolidone. Due to 5-membered strained ring, 155.9 ppm is more realistic to associate with the oxazolidone than urethane. Chemical shifts of other carbons of oxazolidones are close to (–CHO) ~60 ppm, (-CHN) ~40 ppm in literature [45-48].

Table 4.6 shows the ^{13}C NMR interpretation of the main functional groups in main product. All of the peaks could not be identified but some logical identification was done. Figure 4.4 shows the possible side reactions.

Table 4.6. ^{13}C NMR interpretation of functional groups observed in phenyl isocyanate-ESO compound after separation of isocyanurate.

Number and Type of Carbon	Chemical Shift (ppm)
1 (Oxazolidone carbonyl)	155.9
2 (CHO-Oxazolidone)	64.5
3 (CHN- Oxazolidone)	45.1
4 (Urethane carbonyl)	153.5
5 (OCH_2) Urethane	61.6

From ^{13}C NMR, glycerol carbon peaks at 68 and 62 ppm are invisible due the unidentified reaction. Figure 4.10 shows the ^{13}C NMR spectrum of the model compound.

Figure 4.11 shows ^{1}H NMR of the separated product shows complex side reactions. Table 4.7 shows the logical interpretation of ^{1}H NMR spectrum of product.The first peak

of oxazolidone is between 3.70 and 3.65 ppm and splits into four peaks. The splitting of other oxazolidone hydrogen peak is not clear due to the complex side reactions.

Table 4.7. ^{1}H NMR interpretation of the model compound.

Number of Hydrogen	Chemical Shift (ppm)	Integration
1	4.30-4.26	0.71
2	3.70-3.65	0.60
3	8.60	0.28
4	0.93-0.84	9

To eliminate the possibility of ring opening homopolymerization of ESO; ESO was heated in the presence of DABCO. FTIR spectrum shown in Figure 4.12 shows that no change was observed on the epoxy peaks which are at 823 and 846 cm^{-1} with respect to the reference peak at 724 cm^{-1} which belongs to –C-H rocking (for –CH,CH_2,CH_3). This proves that DABCO does not catalyze the epoxy homopolymerization reaction.

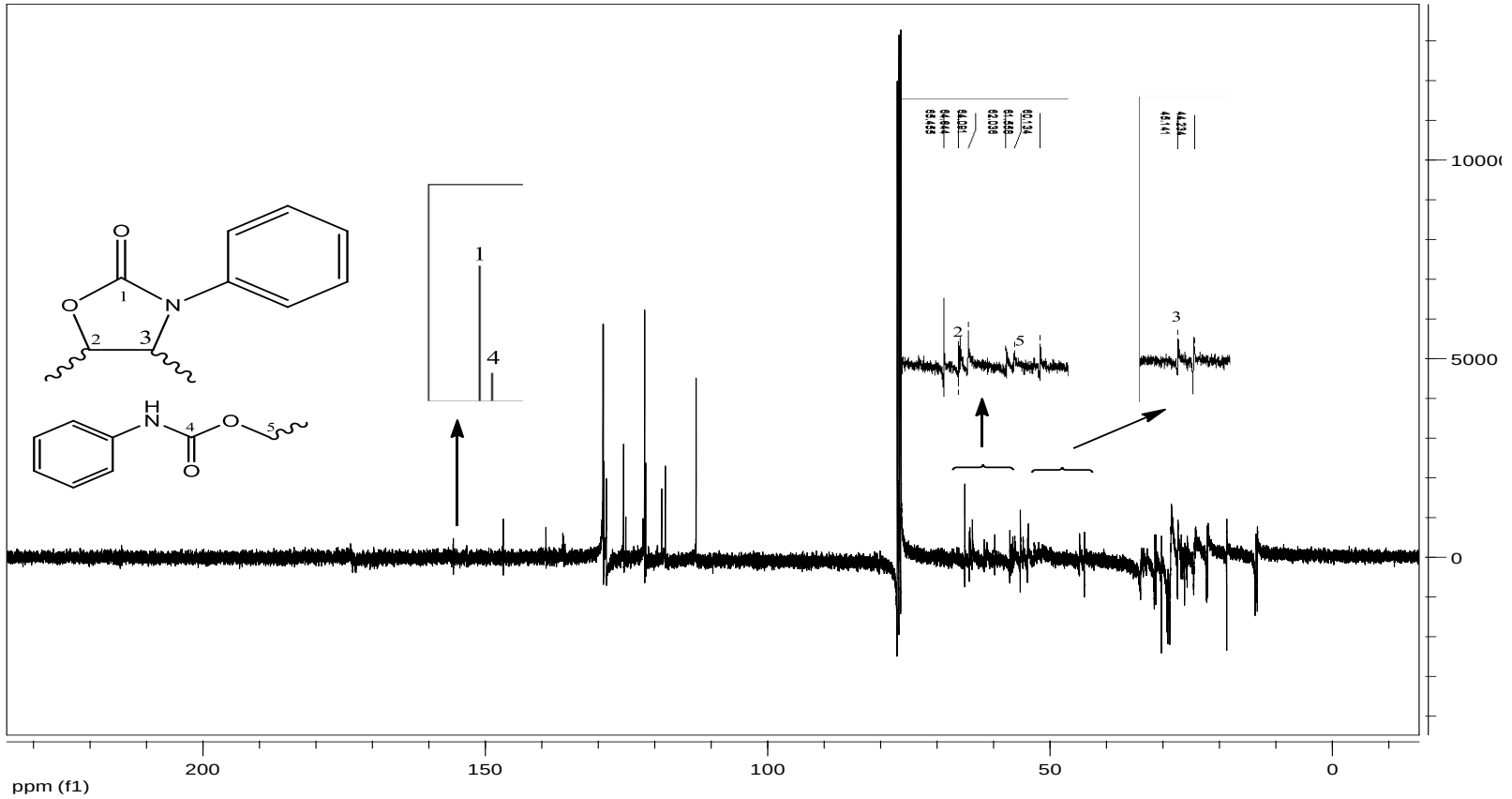

Figure 4.10. ^{13}C NMR spectrum of the second model compound.

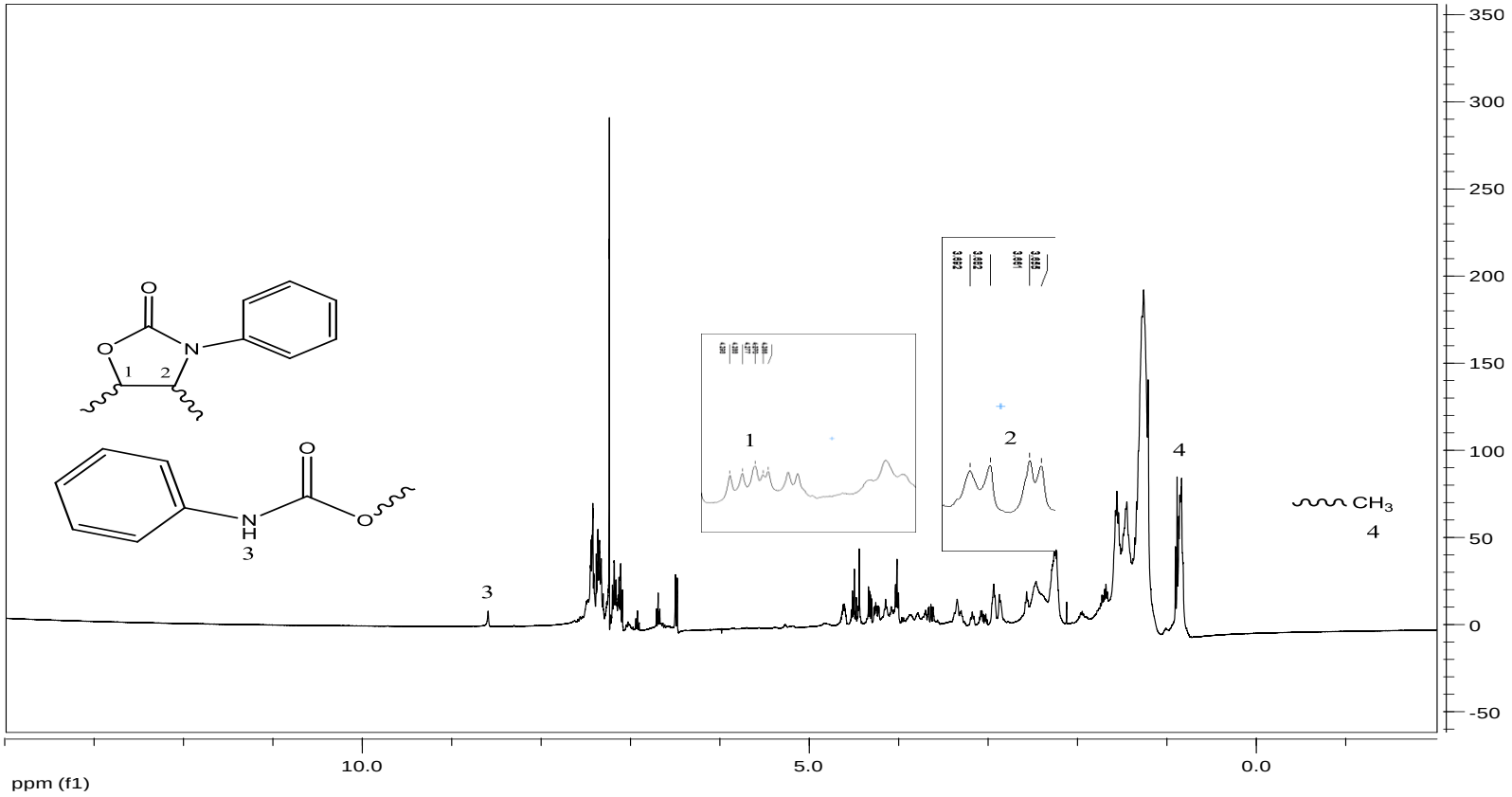

Figure 4.11. ^{1}H NMR spectrum of the second model compound.

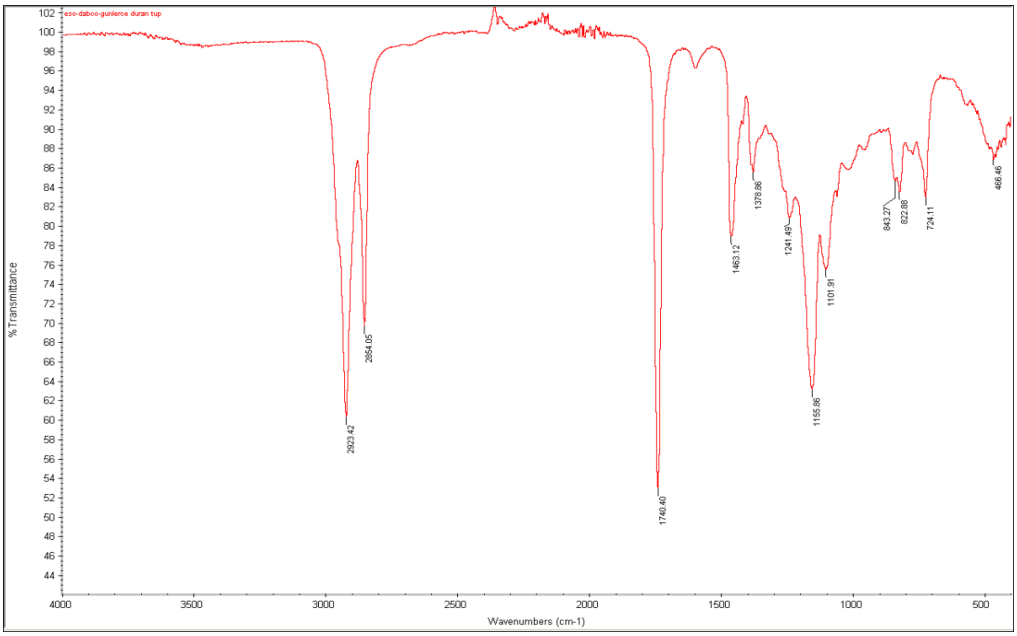

Figure 4.12. FTIR spectrum of ESO-DABCO reaction.

4.2.1.2. Trial 2. The second catalyst used in this work was $SbCl_3$. Surprisingly under atmospheric conditions product was a crosslinked, insoluble polymer.

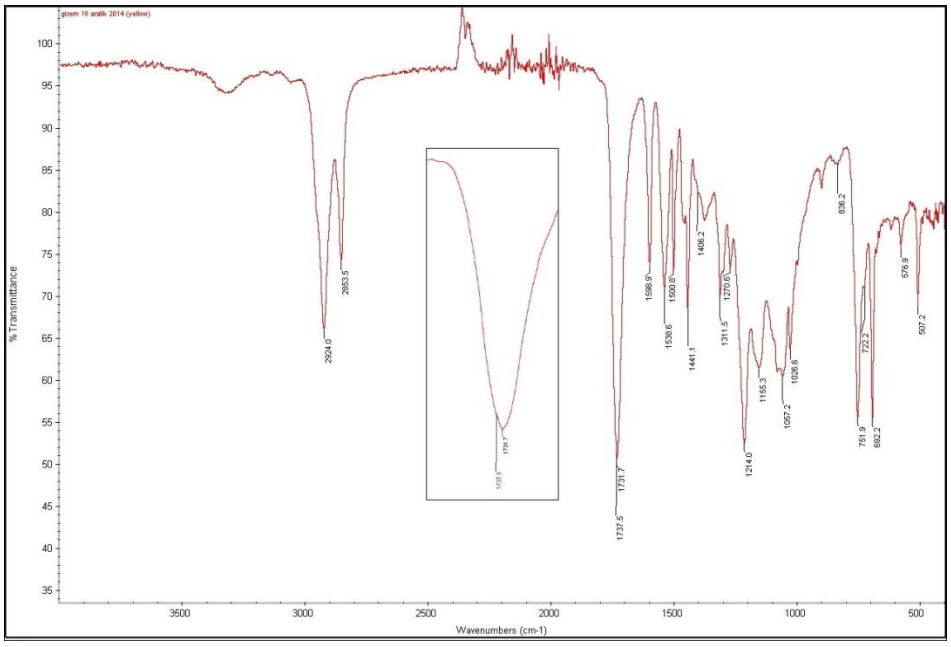

Figure 4.13. FTIR Spectrum of Crosslinked compound obtained from ESO, phenyl isocyanate reaction in the presence of $SbCl_3$.

In Figure 4.13, at 1057 cm^{-1} a new peak was observed corresponds to C-O stretching of the epoxy homopolymerization product. $SbCl_3$ in air and with trace amounts of water catalyzes ring opening homopolymerization of ESO to a crosslinked product.

Table 4.8. FTIR Interpretation of Crosslinked Product.

Position of the Peak (cm^{-1})	Interpretation
1737	ESO ester carbonyl stretch
1731	Urethane carbonyl stretch
1538	Urethane N-H bend
1441	Urethane C-N stretch
1406	Isocyanurate ring deformation
836	Epoxy ring deformations (Decreased)
1240	Epoxy ring deformation (disappeared)
722	Alkyl -CH rocking (Reference Peak)

4.2.2. Model Compound Preparation Under Nitrogen in the presence of $SbCl_3$

4.2.2.1. Trial 3. Due to the crosslinking problem observed with the $SbCl_3$, model compounds were synthesized under nitrogen with ESO monomer carefully dried for 3 days at 140 ^oC and kept under nitrogen in the presence of molecular sieves. First trial was done at 65 ^oC for 24 hours to eliminate the possibility of allophonate and biuret formation. Allophonate and biuret formation is observed at high temperatures starting at 90 ^oC and but the product reverses to the isocyanate over 150 ^oC [49-51].

There were three components in the reaction product one of which is unreacted ESO which was removed by the hexane extraction. The other one is the main reaction product and the third part is white crystalline solid. The main product was examined with ^1H NMR, ^{13}C NMR and FTIR whereas the side product was only examined by FTIR.

First of all under nitrogen and in absolutely dry conditions, crosslinking was prevented and characterization of model compound by NMR, became possible. By-products due to isocyanate–water reaction (aniline/urea) were formed in trace amounts. ^{13}C NMR spectrum of the compound is shown in Figure 4.14.

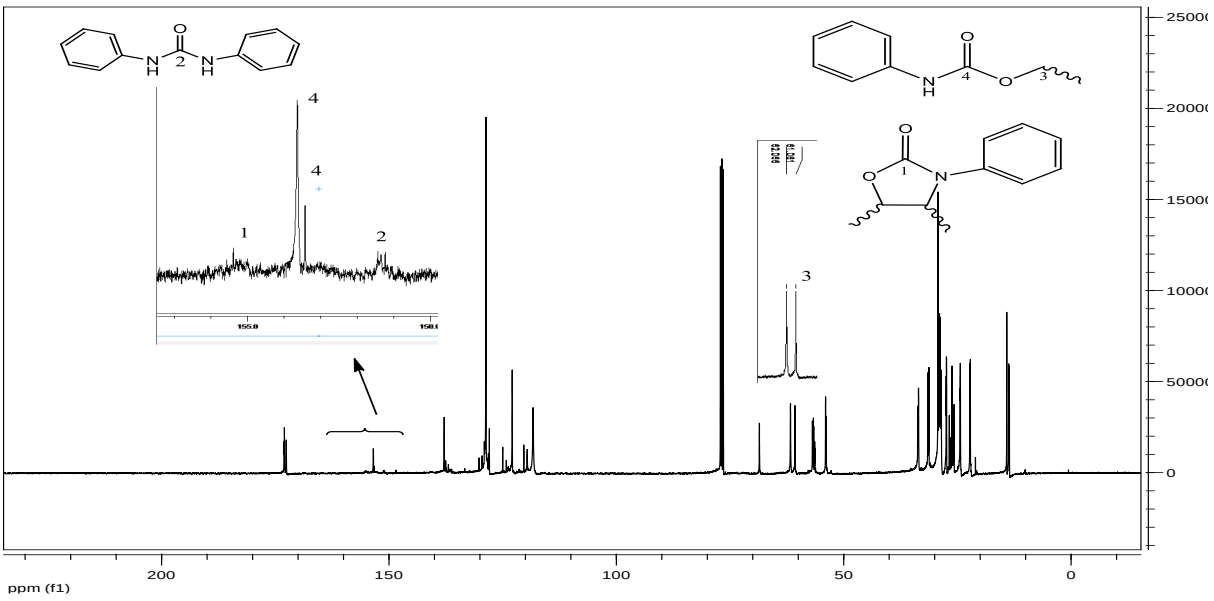

Figure 4.14. ^{13}C NMR of the model compound synthesized from ESO+phenyl isocyanate in the presence of $SbCl_3$ under nitrogen.

Table 4.9 shows the simple ^{13}C NMR interpretation of the functional groups.

Table 4.9. The simple ^{13}C NMR interpretation of the functional groups of the model compound synthesized from ESO+phenyl isocyanate in the presence of $SbCl_3$ under nitrogen.

Number and Type of Carbon	Chemical Shift (ppm)
1 (Oxazolidone carbonyl)	155.4
2 (Urea Carbonyl)	151.5-151.3
3 (OCH_2) Urethane	61.1
4 (Urethane carbonyl)	153.7-153.4

Figure 4.15 shows the ^1H NMR of the model compound synthesized from ESO-phenyl isocyanate in the presence of $SbCl_3$.

As it was expected from the literature at lower temperatures like 65 ^oC, apart from the small peak at 155.4 ppm, no other carbon peaks of oxazolidone were observed from ^{13}C NMR. In the Table 4.10, ^1H NMR interpretation could be obtained.

Table 4.10. ^1H NMR Interpretation of the model compound synthesized from ESO-phenyl isocyanate in the presence of $SbCl_3$.

Chemical Shift (ppm)	Integration	Assignments
0.84-0.78	9.00	$-CH_3$ (Reference peak)
1.18-1.74	76.21	Fatty acid alkyl (CH_2)
2.27-2.22	6.84	CH_2 at the α-position of ester carbonyl
3.07-2.84	4.12	Epoxy Hydrogens
4.24-4.05	6.96	Glycerol (CH_2)+Urethane (CH_2O)
5.19	0.83	Glycerol -CH
7.49-6.92	17.20	Ar-H
8.90	0.04	Urea NH
10.77	0.35	Urethane NH

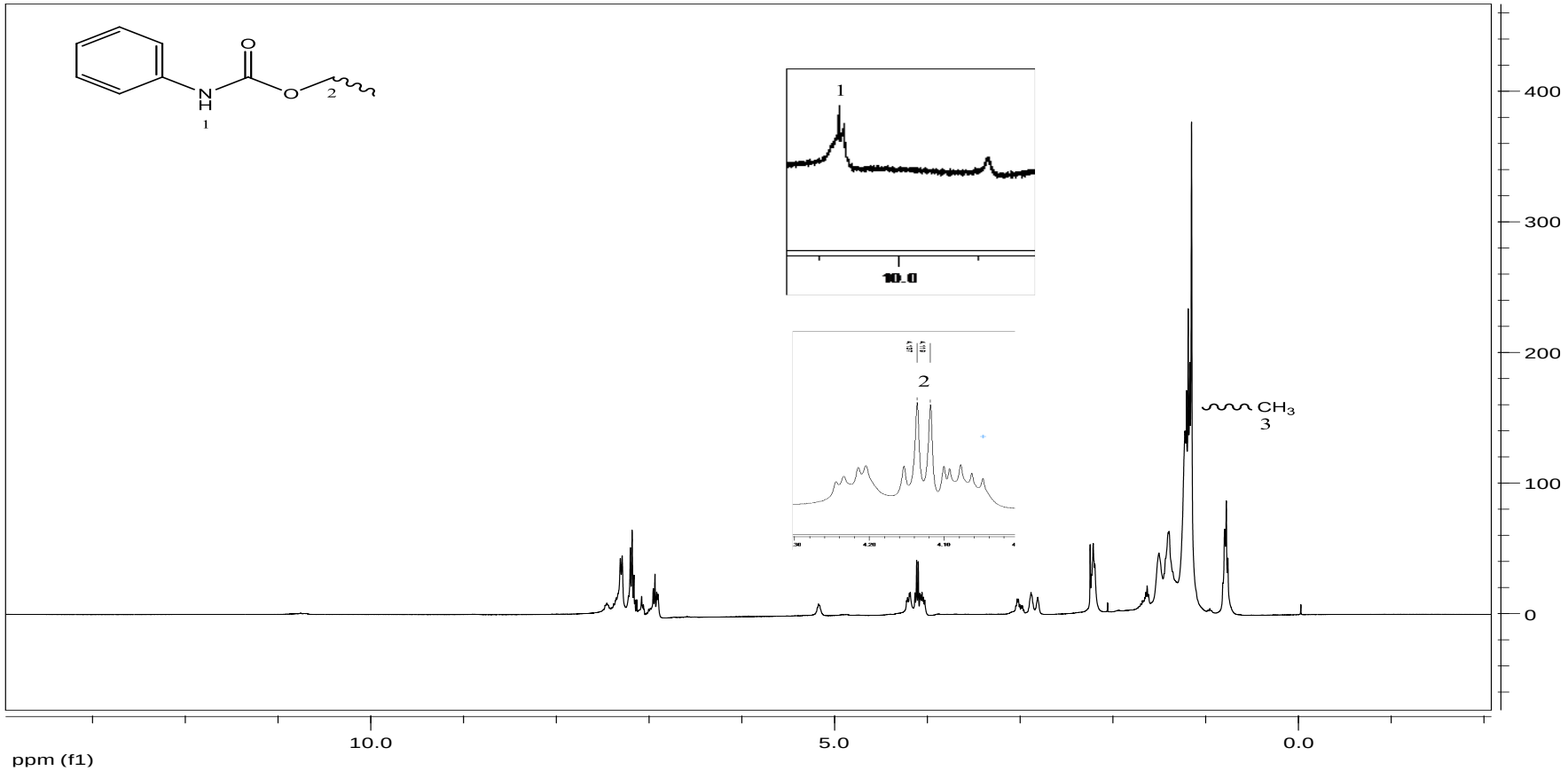

Figure 4.15. ^{1}H NMR of the model compound synthesized from ESO-phenyl isocyanate in the presence of $SbCl_3$.

The FTIR spectrum of the compound could be seen in Figure 4.16 and the Table 4.11 shows the interpretation.

Table 4.11. FTIR Interpretation of model compound synthesized from ESO+phenyl isocyanate in the presence of $SbCl_3$.

Position of the Peak (cm^{-1})	Interpretation
1737	ESO ester carbonyl stretch
1732	Urethane based carbonyl stretch
1539	Urethane N-H bend
1456	Isocyanurate C-N stretch
1444	Urethane C-N stretch
1416	Isocyanurate ring deformation
842-823	Epoxy ring deformations (Decreased)
1240	Epoxy ring deformation (shifted)
726	Alkyl -CH rocking (Reference Peak)

Combination of ^{1}H NMR and ^{13}C NMR and FTIR spectra shows that,

- Trace amount of urea formation exists.
- Oxazolidone ring exists.
- Open chain urethane formation predominates.
- Higher temperatures are required for higher oxazolidone formation.
- Epoxy groups are consumed by ring opening homopolymerization in addition to reaction with isocyanate.

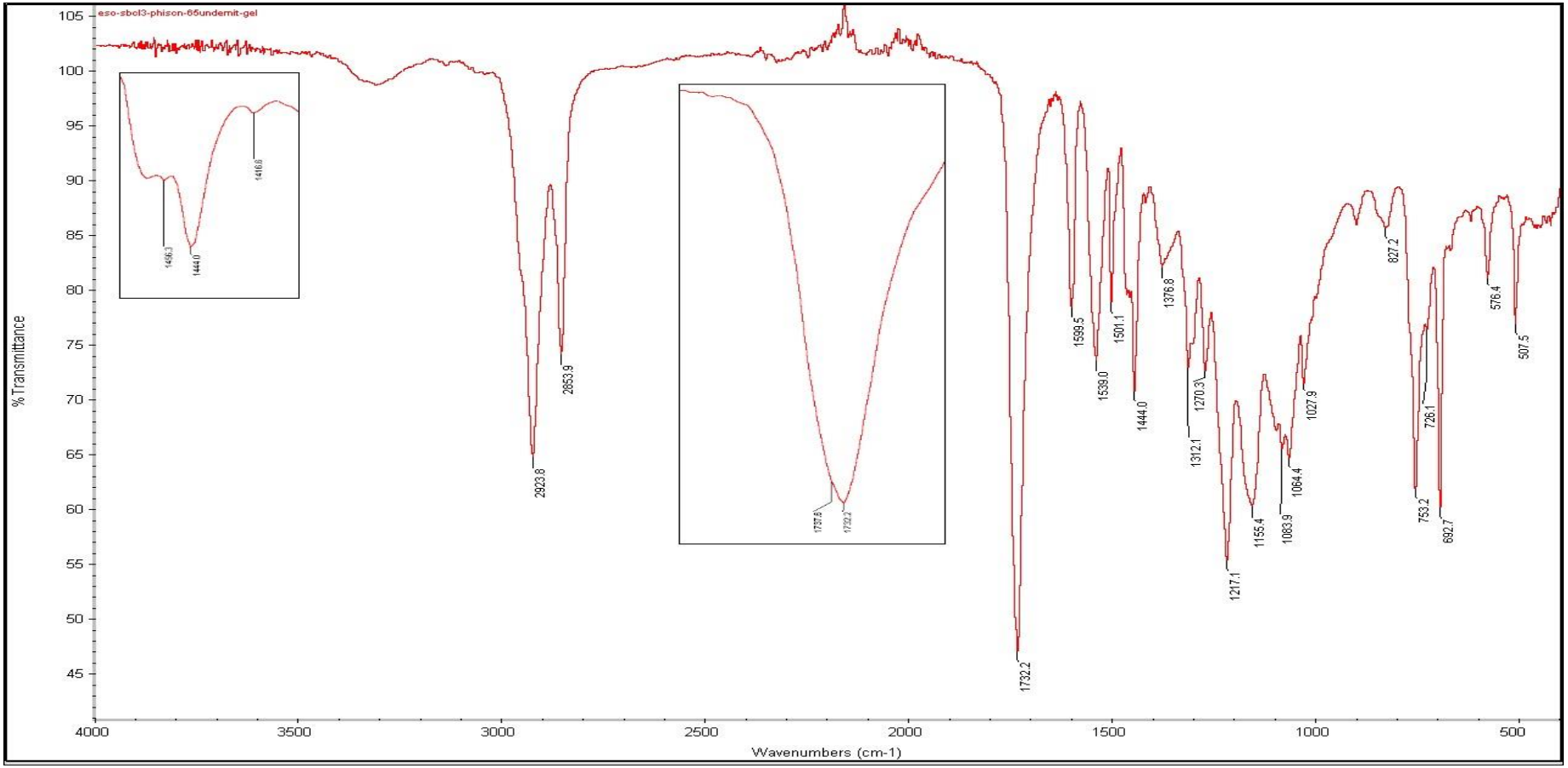

Figure 4.16. FTIR spectrum of the model compound synthesized from ESO+phenyl isocyanate in the presence of $SbCl_3$.

As a side product a white crystalline solid was obtained 3% by weight of the total mass of monomers. The side product has different FTIR spectrum than the isocyanurate side product from the reactions conducted by DABCO. Figure 4.17 shows the FTIR spectrum of this side product. Table 4.12 shows the FTIR interpretation of side product.

Table 4.12. FTIR Interpretation of the white crystalline solid side product.

Position of the Peak (cm^{-1})	Interpretation
1754	Oxazolidone Carbonyl Stretch
1737	ESO ester carbonyl stretch
1732	Urethane carbonyl stretch
1714	Biuret or allophonate carbonyl stretch
1541	Urethane N-H bend
1454	Isocyanurate C-N stretch
1437	Urethane C-N stretch
1432	Oxazolidone C-N stretch
842-823	Epoxy ring deformations (decreased)
1240	Epoxy ring deformation (invisible)
724	Alkyl -CH rocking (Reference Peak) Invisible due to 750 cm^{-1} peak because of the intensity of aryl groups are high

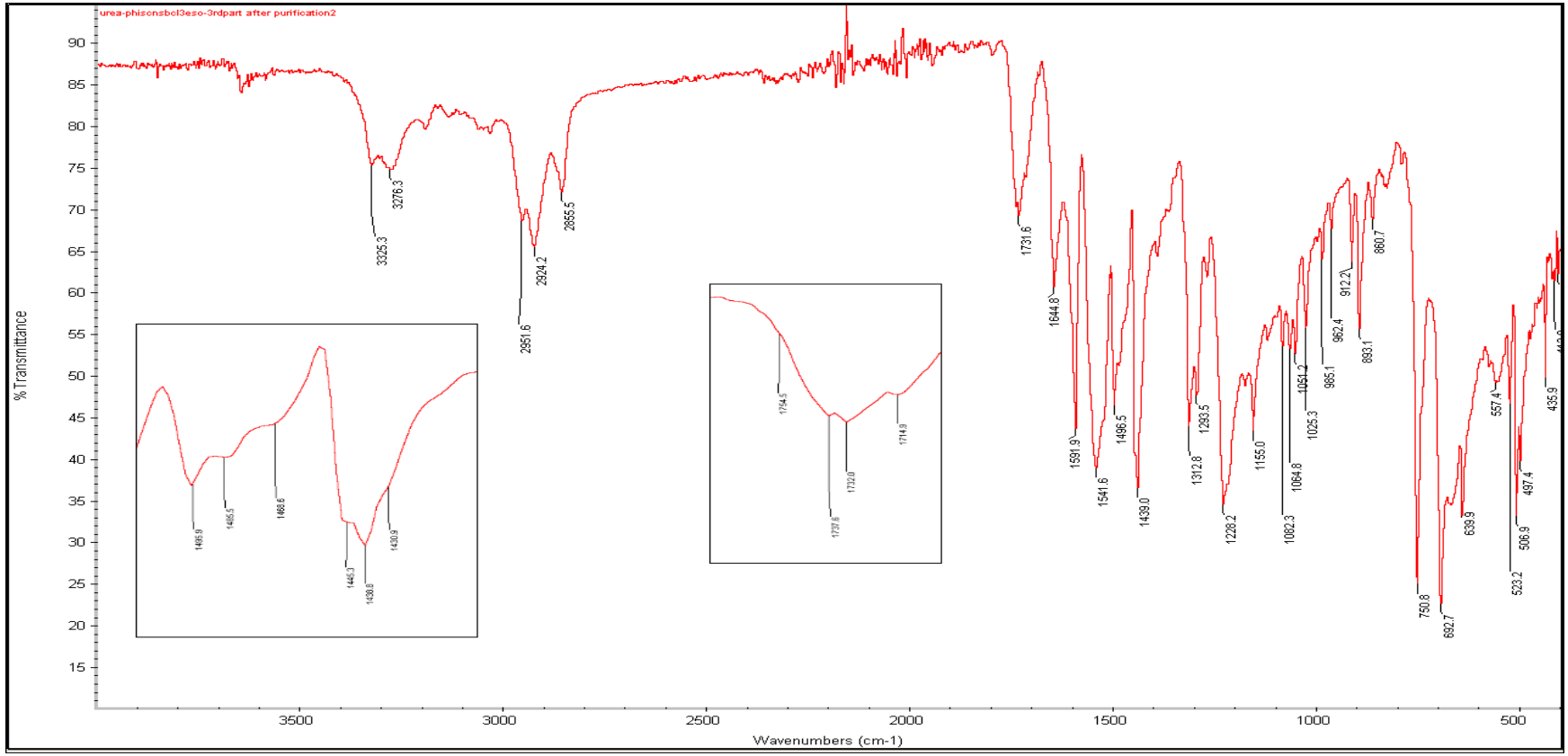

Figure 4.17. FTIR Spectrum of side product of the reaction conducted at 65 ^{o}C with $SbCl_3$ under Nitrogen.

4.2.2.2. Trial 4. With the lessons learned from the previous three trials a fourth trial was run in dry conditions at higher temperatures. Reaction was run at 120 ºC for 22 hours and then at 140 ºC for the last 2 hours. Color of the product is dark brown. Figure 4.18 shows the FTIR spectrum of the product and the Table 4.13, gives the interpretation.

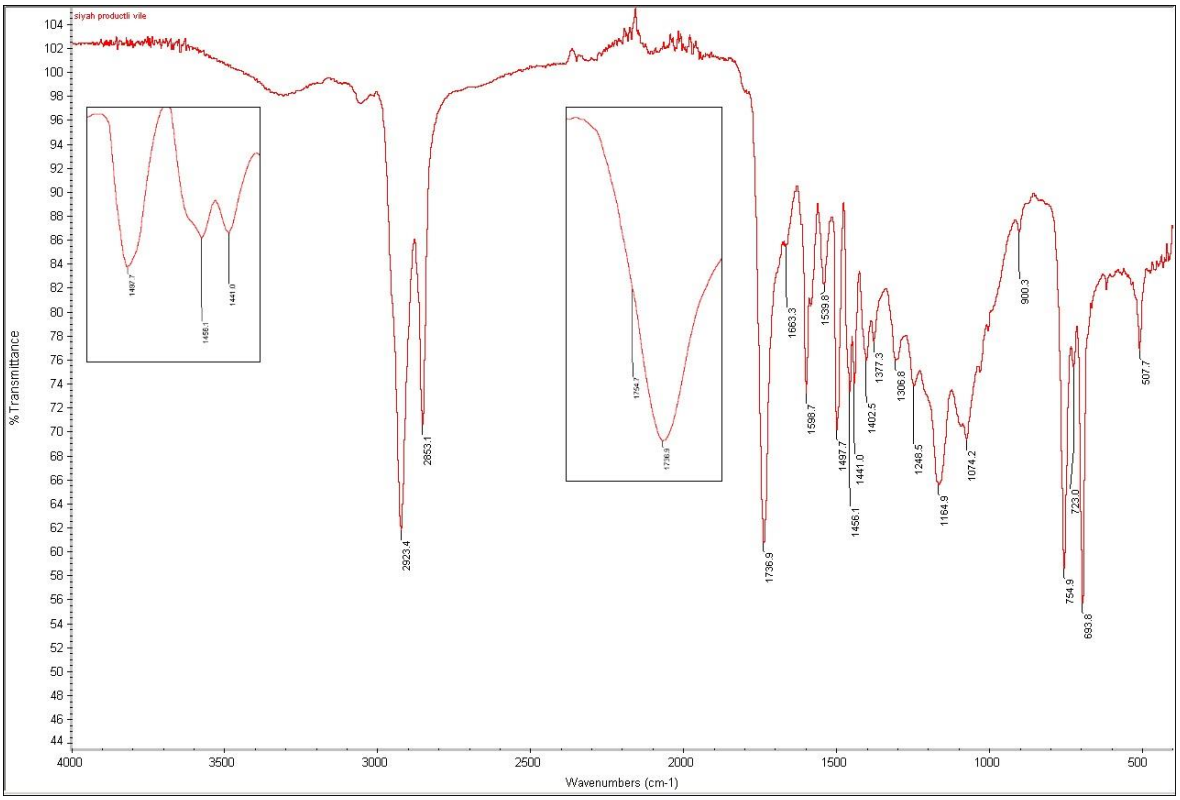

Figure 4.18. FTIR spectrum of the ESO+phenyl isocyanate product with $SbCl_3$ at high temperature.

Table 4.13. FTIR interpretation of the ESO+phenyl isocyanate product with $SbCl_3$ at high temperature.

Position of the Peak (cm^{-1})	Interpretation
1754	Oxazolidone Carbonyl Stretch
1736	ESO ester carbonyl stretch together with urethane carbonyl stretch
1539	Urethane N-H bend
1456	Isocyanurate C-N stretch
1441	Urethane C-N stretch together with oxazolidone C-N stretch
1402	Isocyanurate ring deformation
842-823	Epoxy ring deformations (invisible)
1240	Epoxy ring deformation (shifted)
723	Alkyl -CH rocking (Reference Peak)
815	Triazine oop bending (Invisible)

FTIR spectrum shows that at high temperature isocyanurate reverses back to the isocyanate and additionally oxazolidone formation occured. Thus at high temperature both undesirable side reactions, isocyanurate formation and epoxy homopolymerization can be minimized and oxazolidone formation can be maximized.

^{13}C NMR spectrum is showed in Figure 4.19. From this figure, new carbonyl peaks were observed at 155.3 and 154.3 ppm. One of which belongs to urethane carbonyl at 154.3 ppm and the other one belongs to oxazolidone carbonyl carbon at 155.3 ppm. Table 4.14 shows the simple interpretation.

If comparison of Figure 4.16 and 4.18 is done, intensity of the peak at 1541-1539 cm^{-1} which belongs to urethane N-H bending, seriously decreased. This shows the ring closure of oxazolidone occured more easily at high temperatures.

Table 4.14. Simple ^{13}C NMR interpretation of ESO+phenyl isocyanate product with $SbCl_3$ at high temperature.

Number and Type of Carbon	Chemical Shift (ppm)
1 (Oxazolidone carbonyl)	155.3
2 (OCH Oxazolidone)	65.0
3 (NCH Oxazolidone)	44.9
4 (Urethane carbonyl)	154.3
5 CH_2O (Urethane)	61.1

Between 3.04-2.81 ppm there is no distinguished peak which shows the complete consumption of epoxy groups was reached.

Last information is related with –CHN group of oxazolidone. The peak at 3.63-3.68 is observed at the begining of model compound analysis. This peak appears at the same region in Figure 4.11 which belongs to the model compound synthesized with DABCO at 80 ^oC. ^1H NMR spectrum of the model compound synthesized with $SbCl_3$ at high temperature is shown in Figure 4.20.

Characterization of model compounds was done [52], accordingly.

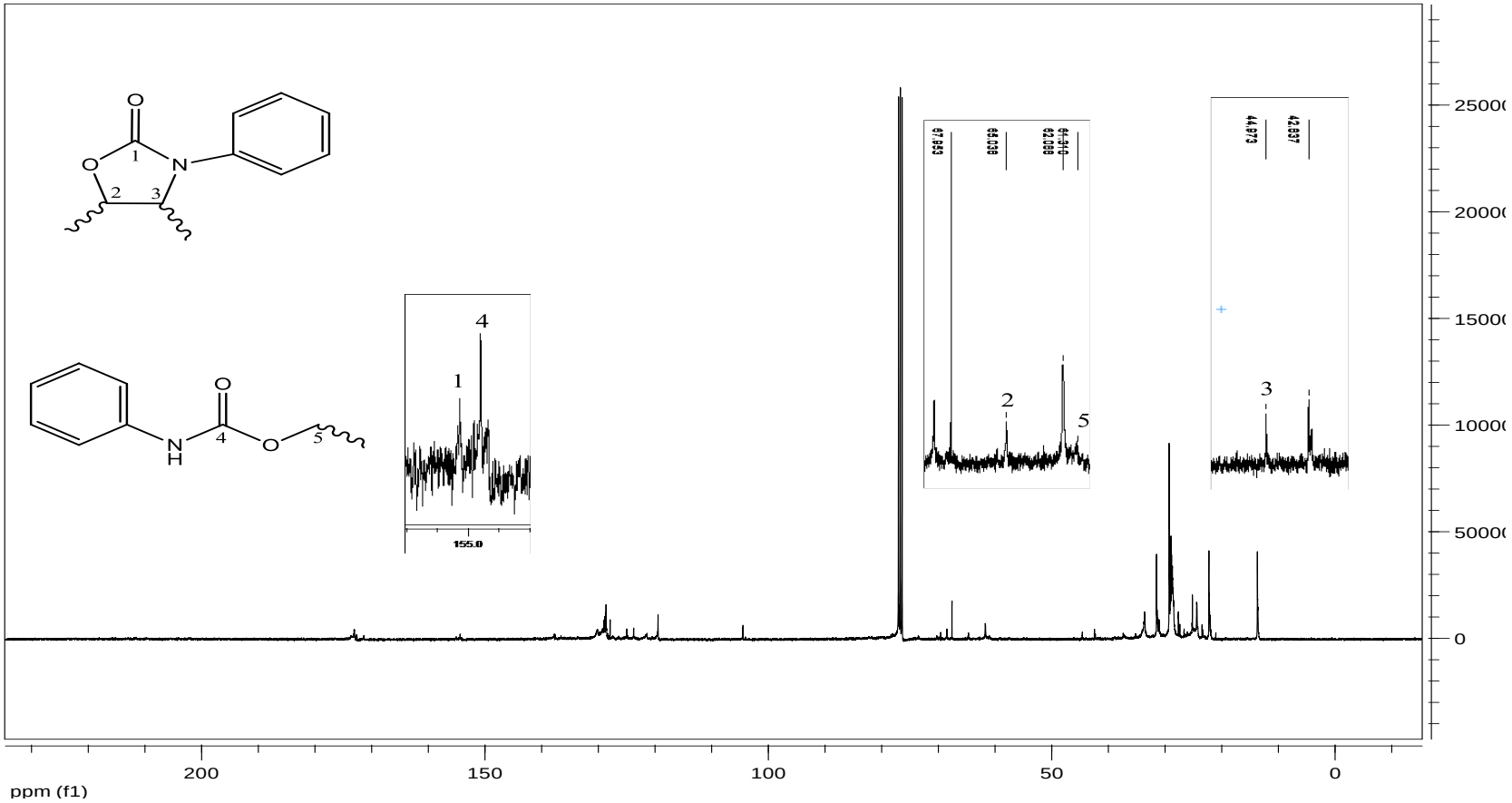

Figure 4.19. ^{13}C NMR of ESO+phenyl isocyanate product with $SbCl_3$ at high temperature.

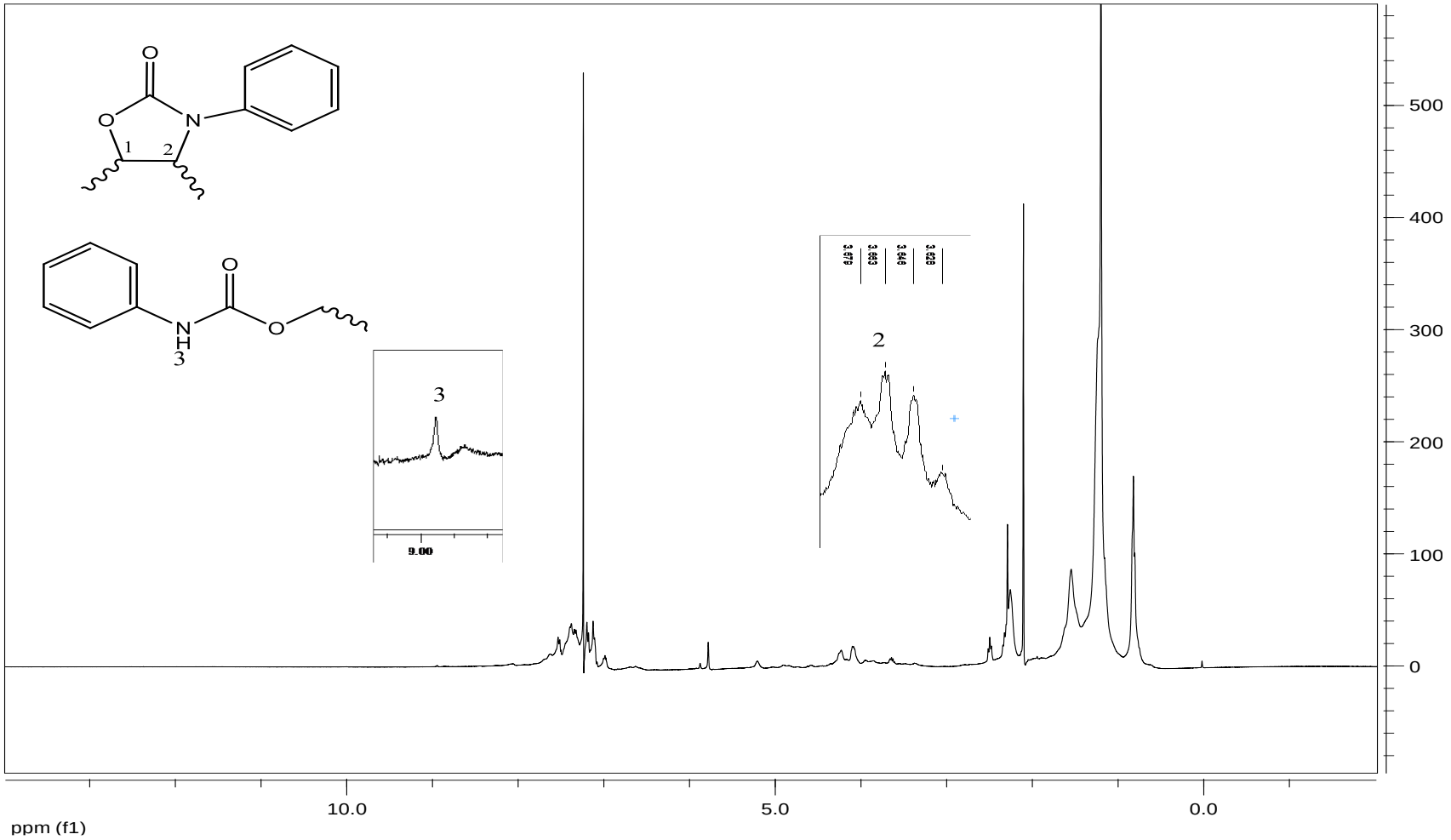

Figure 4.20. ^{1}H NMR spectrum of ESO+phenyl isocyanate product with $SbCl_3$ at high temperature.

Because the ^{1}H NMR of the model compound is not understandable at high temperatures, epoxy homopolymerization with $SbCl_3$ should be considered. Since $SbCl_3$ is insoluble in ESO, ESO and $SbCl_3$ were dissolved in toluene under atmospheric conditions. Reaction was conducted at 120 ^{o}C for 5 hours and gellation occured. Product's FTIR spectra showed in Figure 4.21.

For monomeric ESO, there are three peaks for C-O stretching. 1241 cm^{-1} indicates the epoxy ring, 1155 cm^{-1} and 1101 cm^{-1} indicate the ester -C-O stretching. For polymer, additional peak which is at 1170 cm^{-1} was observed. The peaks at 846 cm^{-1} and 823 cm^{-1} are not observable, additionally intensity of the peak at 1241 cm^{-1} decreased which shows the epoxy consumption.

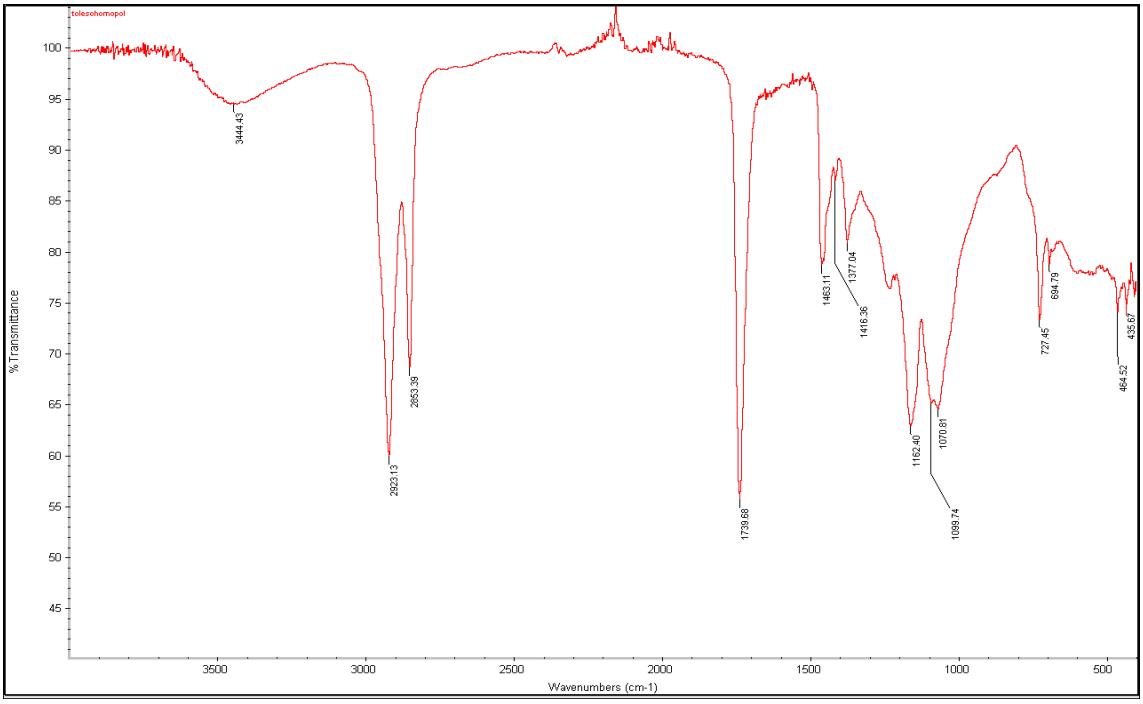

Figure 4.21. FTIR spectrum of ESO pre-homopolymer.

Comparison of DABCO and $SbCl_3$, is given in Table 4.15.

Table 4.15. Comparison of DABCO and $SbCl_3$ as catalysts.

	DABCO	$SbCl_3$
Epoxy Homopolymerization	Not observed	Observed
Isocyanurate Formation	74% of isocyanate monomer consumed to give isocyanurate	Untraceable
Isocyanate-Water Reaction	No solid proofs for urea formation	3% by total weight of monomers
Oxazolidone Formaton	Low (Not observed)	High (Observed)

4.2.3. Synthesis and Characterization of Polymeric Model Compounds

4.2.3.1. Synthesis and Characterization of A187 Epoxy Silane/TDI-based Model Compound. Due to the complications of preparing model compounds with using polyfunctional molecule such as ESO; a monoepoxide, propyltrimethoxy silyl glycidol (A187) was used to prepare a model compound, to understand the reaction mechanism for simplicity. The structure of A187 could be found in Figure 4.22.

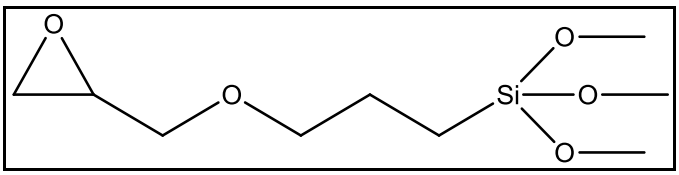

Figure 4.22. Structure of A187.

Because A187 does not contain any carbonyl group in its structure to its reaction with isocyanate is easier to follow. The reaction of A187 with TDI was examined in the

presence of $SbCl_3$ catalyst. $SbCl_3$ was dissolved in TDI and was added to A187 at room temperature. The reaction was followed by FTIR . Figure 4.24 shows a new carbonyl peak appearence as the reaction proceeded. The carbonyl peak started to appear at 1734 cm^{-1}, and later the peak separated into two peaks at 1745 cm^{-1} and 1736 cm^{-1}. This is a proof for oxazolidone formation at room temperature in the presence of $SbCl_3$ catalyst. 1745 peak is evidence for oxazolidone formation but the peak at 1734 cm^{-1} which was also observed in the polymers is due to urethane formation. This could help to understand the peak at 1731 cm^{-1} for the polymers that were synthesized with $SbCl_3$.

Another reaction was conducted again with TDI and A187 at 100 ^oC for 24 hours. Figure 4.25 shows the FTIR spectrum of this product. A peak appears at 1704 cm^{-1} which shows isocyanurate formation could easily seen. The peak at 1732 cm^{-1} for urethane (allophonate) formation, and 1754 cm^{-1} shows the oxazolidone formation. At higher temperatures, isocyanurate and urethane (allophanate) formation predominates.

Also the TGA of the product is shown in Figure 4.23 as the derivative of percent weight according to the temperature. From literature, the peak at 260 ^oC shows the degradation temperature of urea and urethane, peaks at 343 and 376 ^oC shows the degradation temperature of oxazolidone, and final peak at 445 ^oC shows the degradation temperature of isocyanurate functional group.

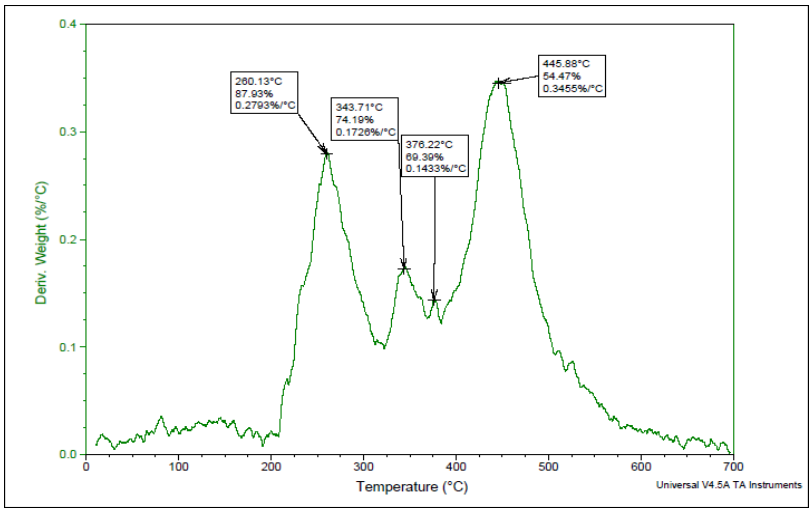

Figure 4.23. TGA of A187/TDI product synthesized at 100 ^oC for 24 hours.

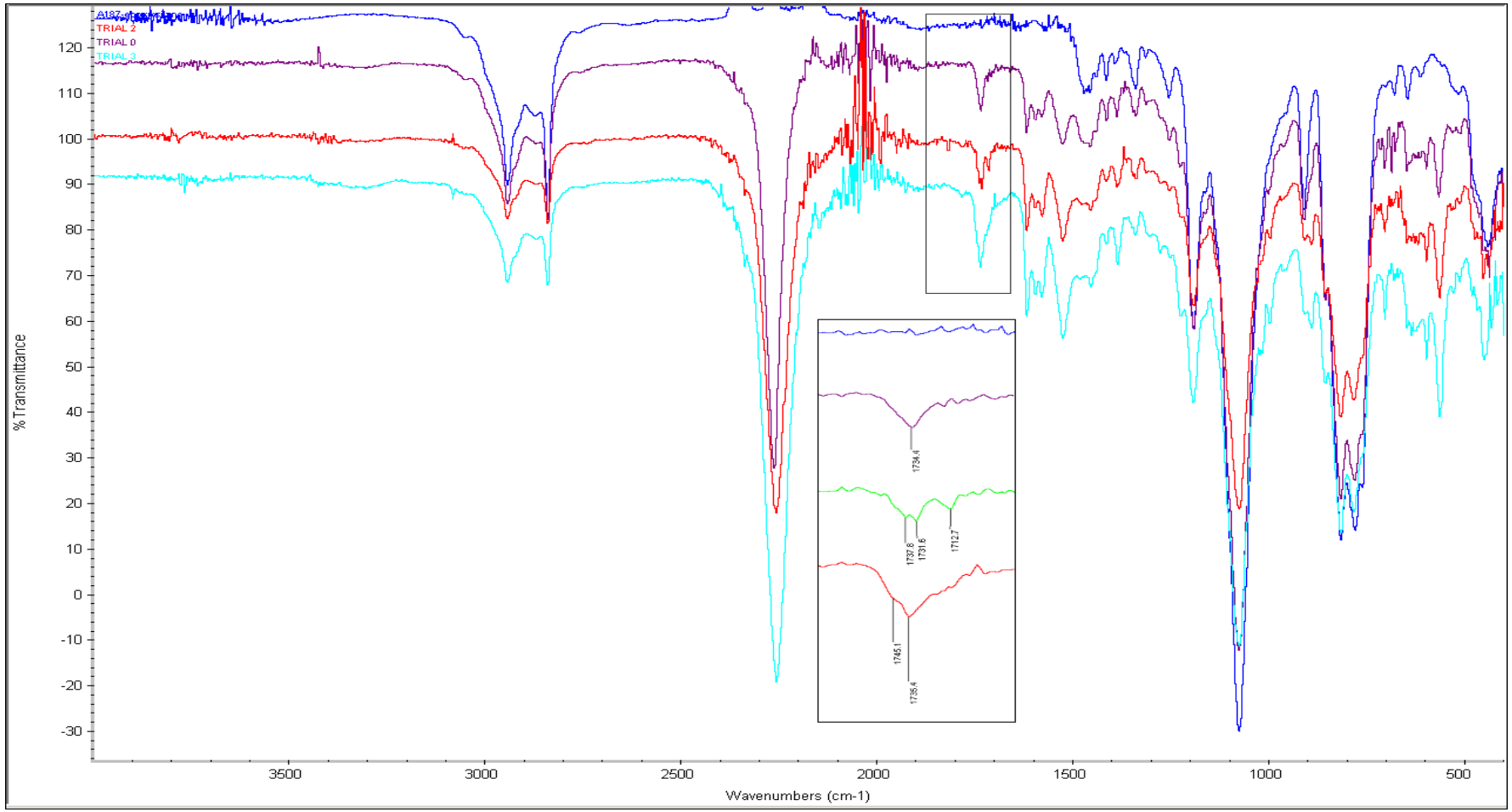

Figure 4.24. Evolution of novel carbonyl peaks from A187, concurrently the addition of TDI.

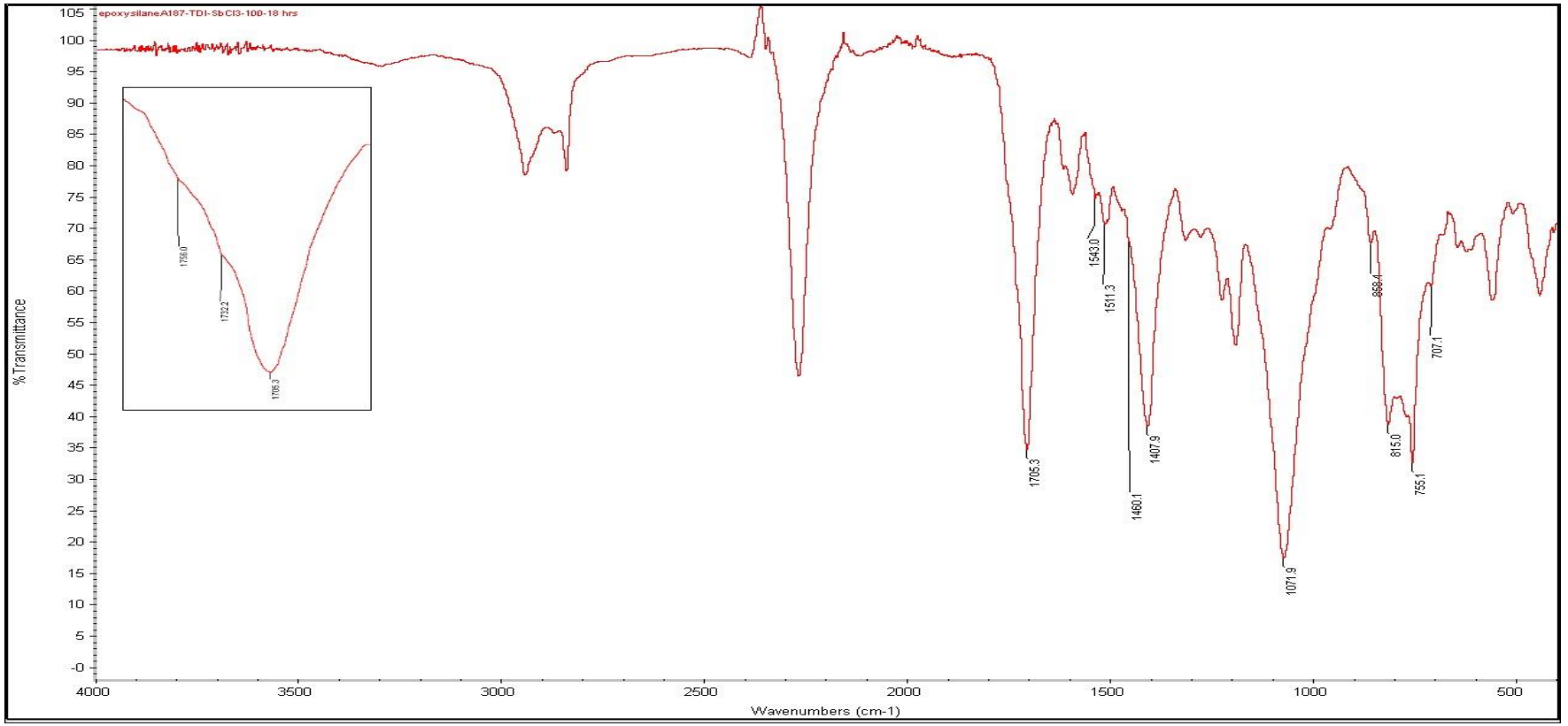

Figure 4.25. FTIR spectrum of A187/TDI product sythesized at 100 ºC for 24 hours.

4.2.3.2. Synthesis and Characterization of DEG/TDI-based Model Compound. Another model compound preparation was done with diethylene glycol and TDI in the presence of $SbCl_3$ at room temperature. Diethylene glycol is already a reactive monomer than ESO, with the catalyst reaction time was about less than a minute and it was highly exothermic. Reaction can be seen in Figure 4.26.

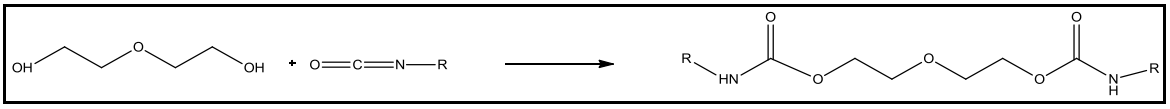

Figure 4.26. Reaction of DEG and isocyanate with their product as urethane.

In the FTIR spectrum of the product two different carbonyl peaks at 1719 cm^{-1} and 1703 cm^{-1} were observed meaning that the urethane carbonyl and isocyanurate had formed. FTIR spectrum of the compound can be seen in Figure 4.28, Table 4.16 indicates the FTIR interpretation for the model compound synthesized with DEG and TDI.

Table 4.16. FTIR Interpretation of the urethane compound.

Position of the Peak (cm^{-1})	Interpretation
3295	NH, OH stretch
1719	Urethane carbonyl stretch
1703	Isocyanurate carbonyl stretch
1530	Urethane N-H bend
1446	Urethane C-N stretch
1414	Isocyanurate ring deformation

TGA of the compound in Figure 4.27, indicates the degradation temperature of the funcional products are at 293, 318, 419 ºC which confirms the literature as the urethane groups have the degradation temperature at the range of 260-360 ºC and the peak at 419 ºC indicates the small amount of isocyanurate formation.

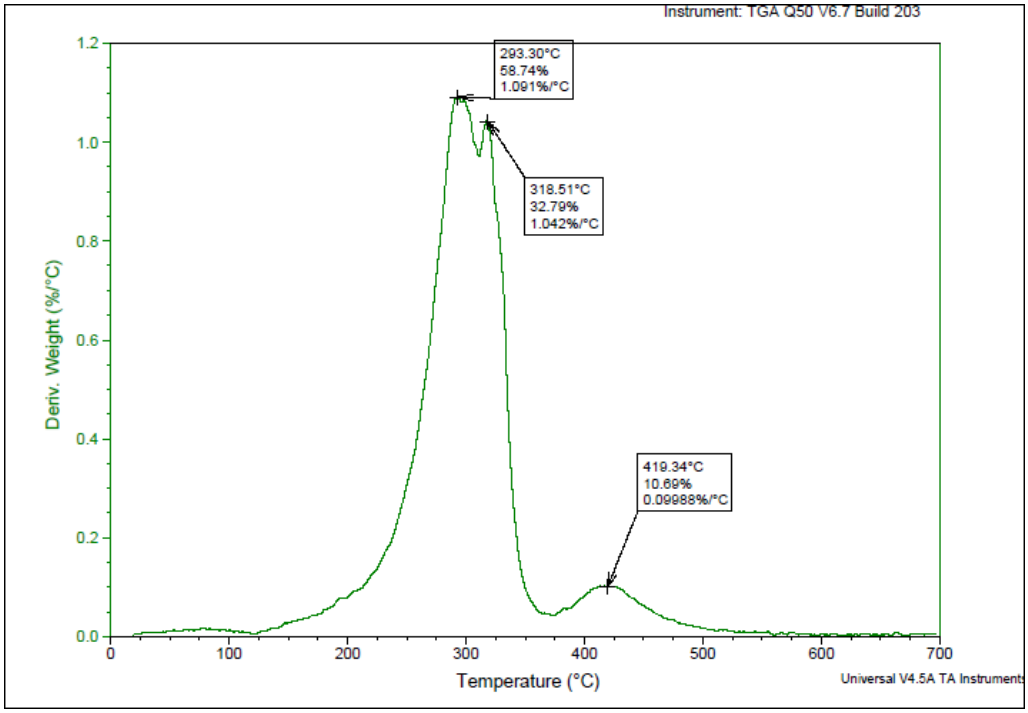

Figure 4.27. TGA of DEG-TDI reaction product.

The time spent with two model compounds was well spent. This allows accurate assignment of the carbonyl peaks of urethane, allophanate, isocyanurate, oxazolidone and urea type carbonyls observed in the polymers synthesized.

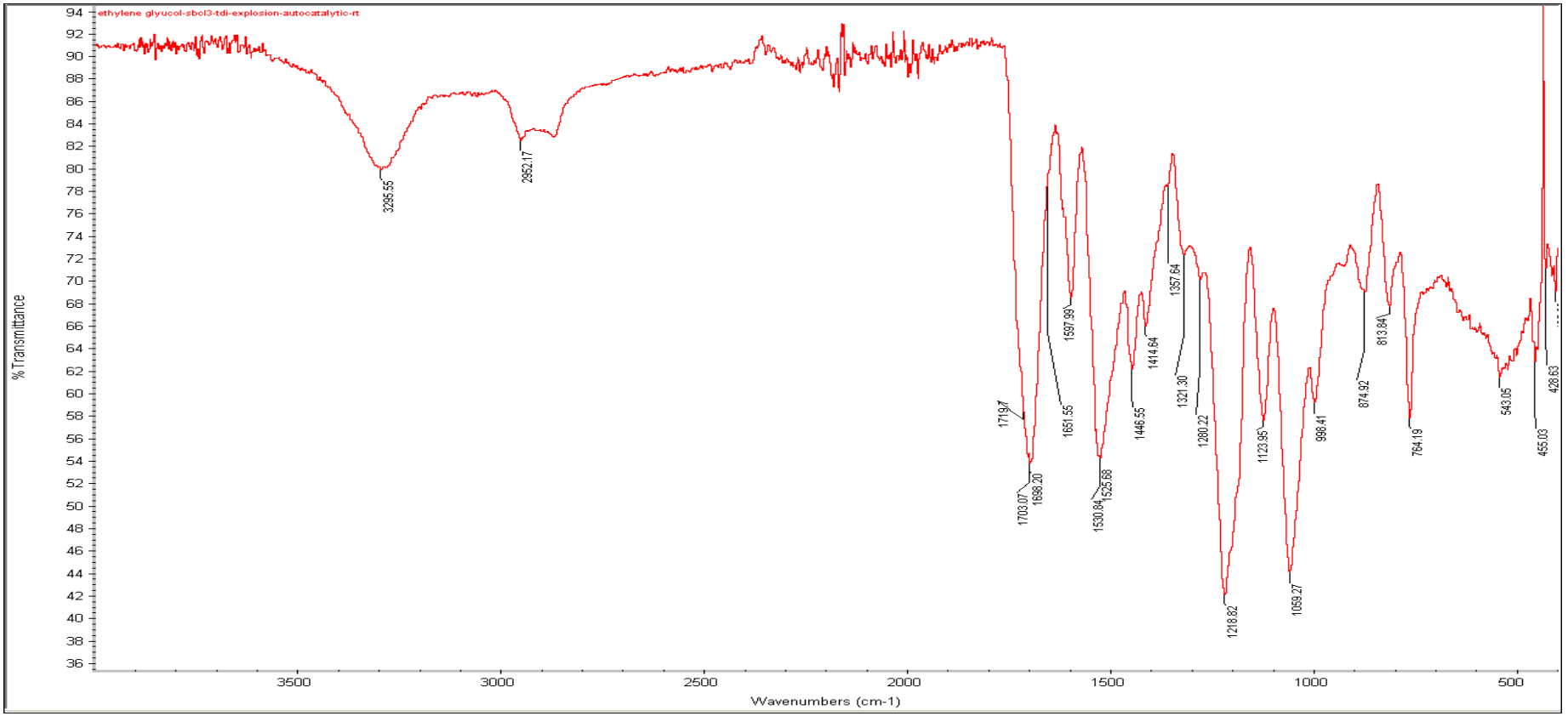

Figure 4.28. FTIR spectrum of urethane product synthesized from DEG and TDI.

4.2.3.3. Synthesis and Characterization of DGBPA/TDI-based Model Compound. Diglycidyl ether of Bisphenol-A (DGBPA) type oxazolidones are well-known in literature. Reaction conditions such as temperature, monomer ratio, catalyts type were examined by different groups [53-59].

For the $SbCl_3$ catalyst detailed examination does not exist. But it is known that triphenyl antimony iodide catalyst was used for the reaction. Luckily, $SbCl_3$ is soluble in monomeric diisocyanates. The minimum reaction temperature that was known to give oxazolidone is 70 ^oC. For $SbCl_3$ at room temperature, from the previous model compounds the product has an FTIR peak at 1739 cm^{-1} which is claimed to be the oxazolidone carbonyl stretch for one group by one group of scientists. The other group claimed oxazolidone carbonyl stretch peak is at 1754 cm^{-1}. For the present study it was important to know which research group is correct. When DGBPA and TDI were reacted between 50–110 ^oC, the peak corresponding to oxazolidone carbonyl appeared at 1754 cm^{-1}. Thus this model compound allowed definitive identification of oxazolidone carbonyl peak by FTIR spectrometry. It should be noted that as the polymers synthesized as thermoset polymers and therefore insoluble, FTIR is the only tool availiable for structure determination. For having an idea about the required temperature for oxazolidone formation, trials were conducted with high catalyst ratios. One example of the DGBPA type model compounds will be explained. From 50 ^oC to 110 ^oC temperature started to increase by 10 ^oC for each 30 minutes. At the end of the 60 ^oC period, in the FTIR spectrum, oxazolidone peak was started to be observed at 1754 cm^{-1}. Figure 4.29 shows the FTIR spectrum of the compound after reacting at 50 ^oC for 30 minutes and after 60 ^oC for 30 minutes.

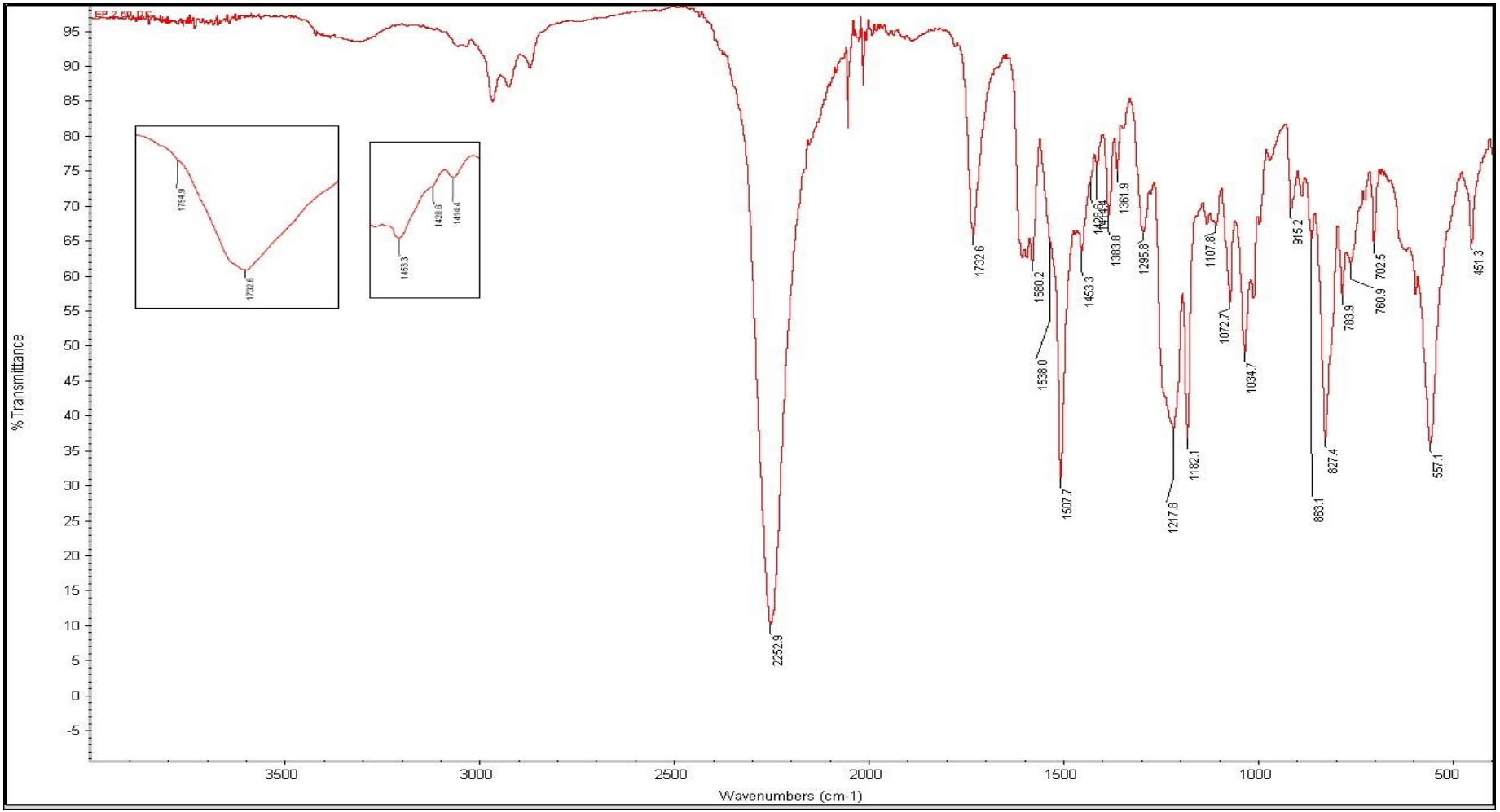

Figure 4.29. FTIR spectrum of DGBPA/TDI polymer after reacting at 60 ºC.

4.3. FTIR Examination of Polymers Synthesized with $SbCl_3$

Due to high effectiveness of $SbCl_3$ as a catalyst polymer samples for mechanical testing, were made with $SbCl_3$. The oxazolidone peak expected at 1754 cm^{-1} was most prevalent in MDI-polymers with the other monomers TDI and IPDI this peak was burried under the peak at 1740 cm^{-1} fatty ester carbonyl peaks.

Figure 4.30 shows the MDI-based polymer synthesized with 0.2 grams of $SbCl_3$ catalyst at 90 ^oC. This is the only spectrum that the 1754 cm^{-1} carbonyl stretching peak was observed with $SbCl_3$ catalyst.

Interpretation of the spectrum is shown in Table 4.17.

Table 4.17. Interpretation of the 0.2 MDI 90 ^oC sample.

Position of the Peak (cm^{-1})	Interpretation
1754	Oxazolidone Carbonyl Stretch
1738	ESO ester carbonyl stretch
1731	Urethane based carbonyl stretch
1713	Biuret/Allophonate carbonyl stretch
1704	Isocyanurate carbonyl stretch
1537	Urethane N-H bend
1455	Isocyanurate C-N stretch
1448	Urethane C-N stretch
1436	Oxazolidone C-N stretch
1411	Isocyanurate ring deformation
842-823	Epoxy ring deformations (Invisible)
1240	Epoxy ring deformation (decreased)
812	Isocyanurate out of plane bending
722	Alkyl -CH rocking (Reference Peak)

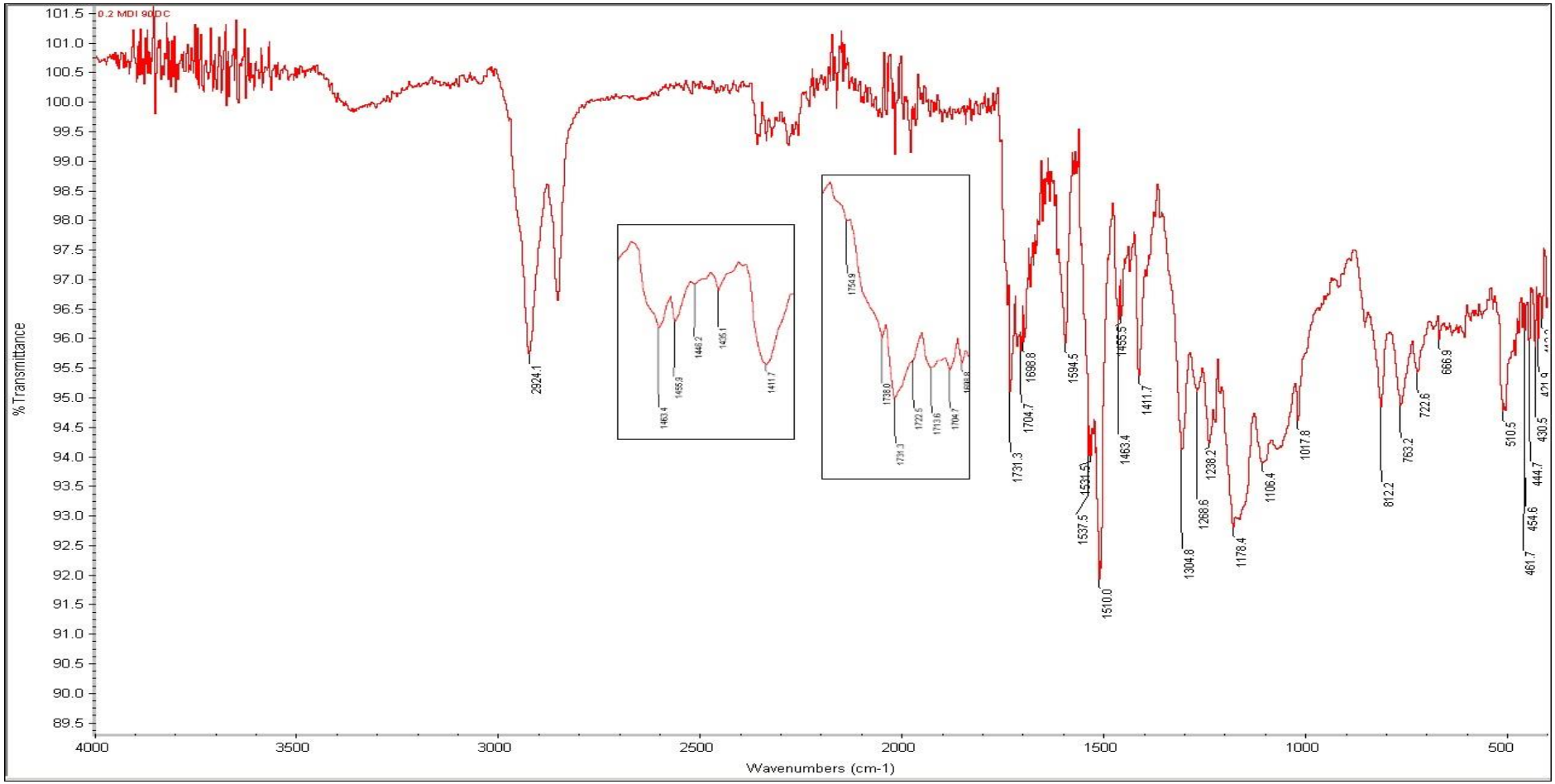

Figure 4.30. FTIR spectrum of 0.2 MDI 90 ^{o}C.

The following spectra belongs to TDI based polymer which was synthesized with 0.2 g catalyst at 100 ºC. Interpretation of the spectra is showed in Table 4.18.

Table 4.18. FTIR Interpretation of 0.2 TDI 100.

Position of the Peak (cm^{-1})	Interpretation
1754	Oxazolidone carbonyl stretch
1737	ESO ester carbonyl stretch
1731	Urethane carbonyl stretch
1716	Biuret/Allophonate carbonyl stretch
1704	Isocyanurate Carbonyl Stretch
1537	Urethane N-H bend
1455	Isocyanurate C-N stretch
1446	Urethane C-N stretch
1434	Oxazolidone C-N stretch
842-823	Epoxy ring deformations (Invisible)
1240	Epoxy ring deformation (Invisible)
815	Isocyanurate out of plane bending
722	Alkyl -CH rocking (Reference Peak)

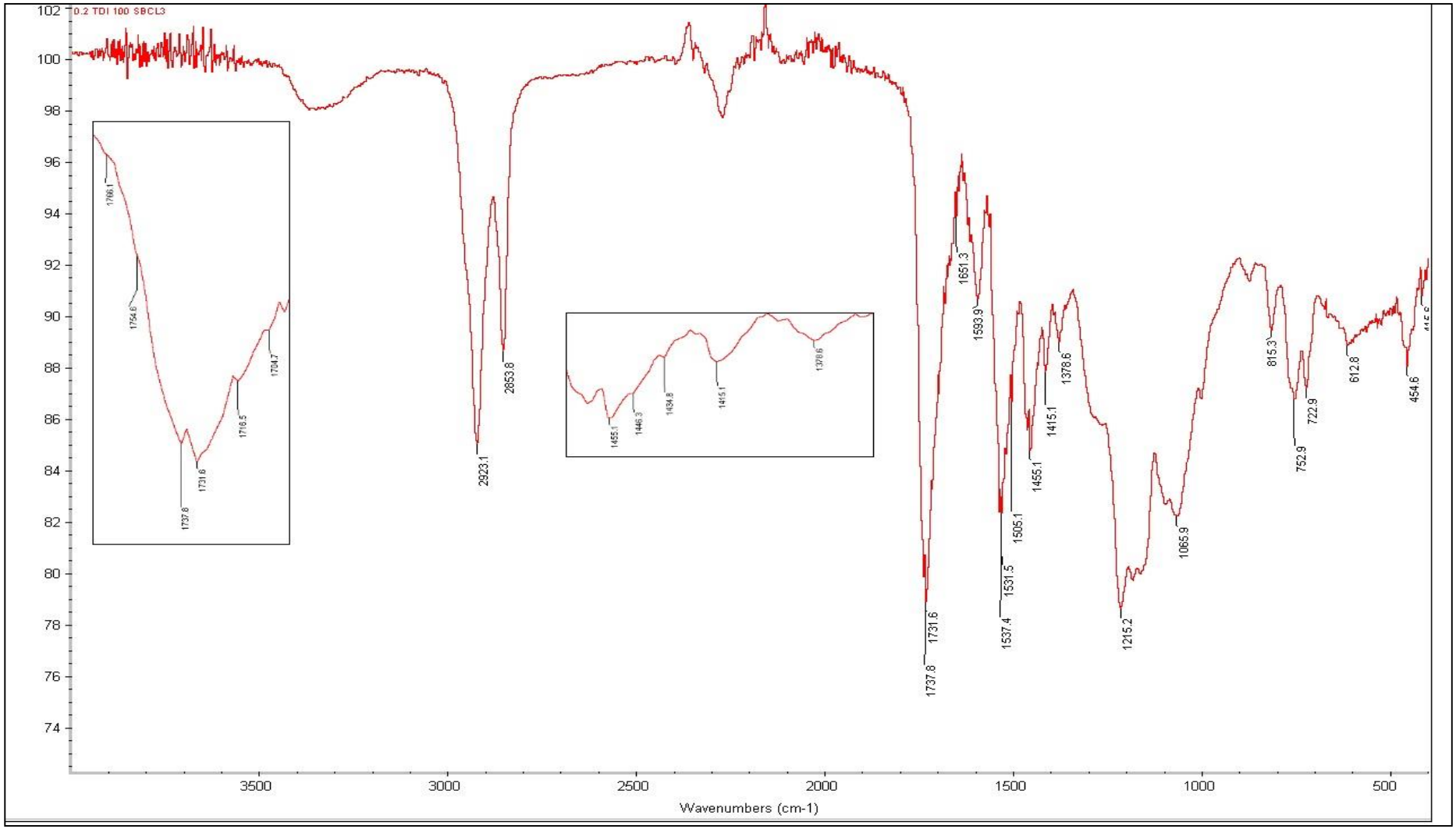

Figure 4.31. FTIR Spectrum of 0.2 TDI 100.

Third FTIR interpretation was done for an IPDI-based polymer, which is an aliphatic diisocyanate. Because isophorone diisocyanate has a lower boiling point than other diisocyanate monomers, IPDI based polymers were done 90 ^{o}C at maximum.There is a peak broadening towards 1754 cm^{-1} shows the oxazolidone formation.

Figure 4.32 shows the FTIR spectrum of the polymer which was done with 0.5 IPDI 90. Table 4.19 shows the interpretation of its spectrum.

Table 4.19. FTIR interpretation of the 0.5 IPDI 90.

Position of the Peak (cm^{-1})	Interpretation
1755	Oxazolidone Carbonyl Stretch (as peak broadening)
1737	ESO ester carbonyl stretch
1732	Urethane carbonyl stretch
1716	Biuret/Allophonate carbonyl stretch
1699	Isocyanurate carbonyl stretch
1519	Urethae/Allophonate/Biuret N-H bend
1455	Isocyanurate C-N stretch
1434	Oxazolidone C-N stretch
1402	Isocyanurate ring deformation
842-823	Epoxy ring deformations (Invisible)
1240	Epoxy ring deformation (invisible)
725	Alkyl -CH rocking (Reference Peak)

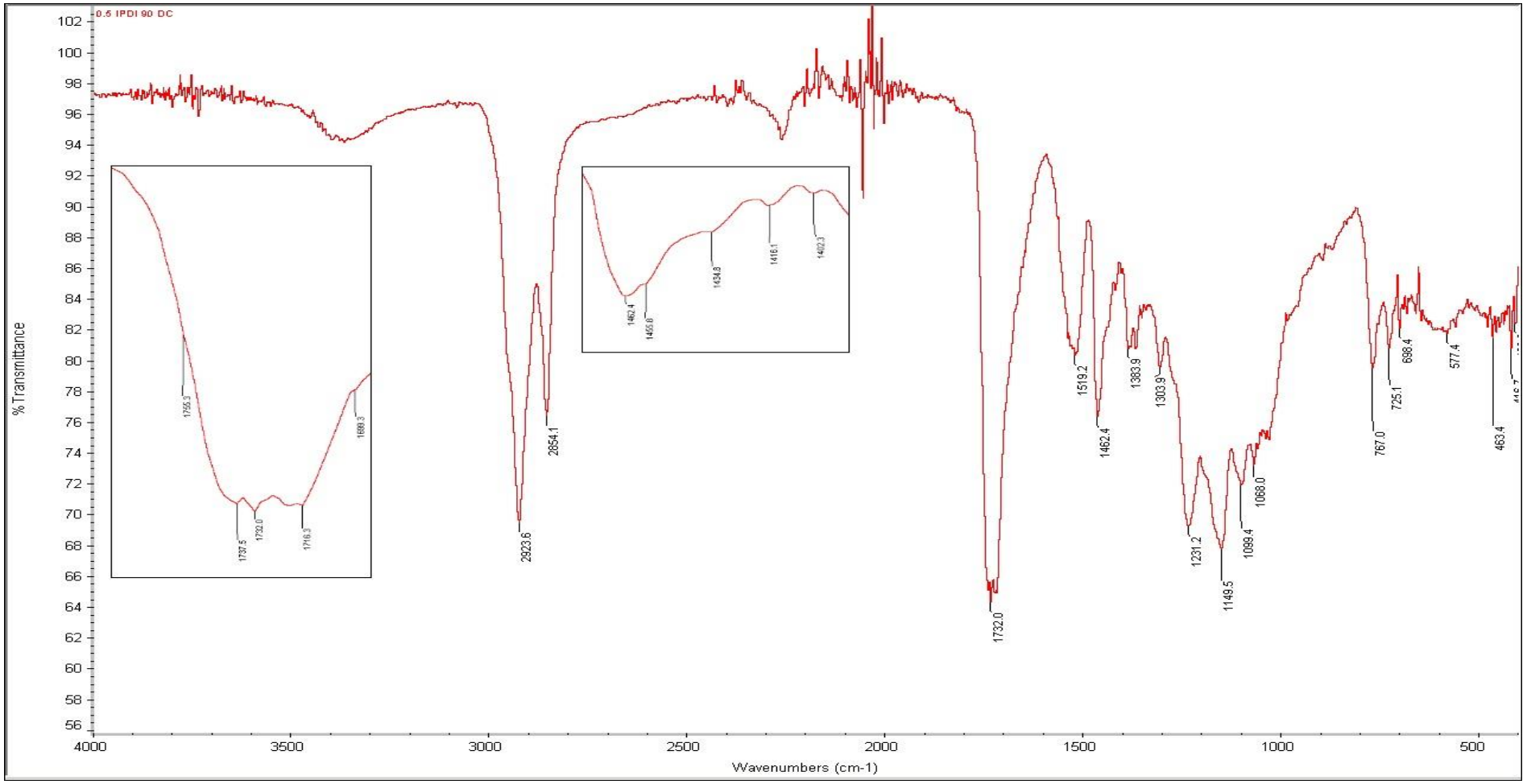

Figure 4.32. FTIR Spectrum of 0.5 IPDI 90.

4.4. Physical Characterization of ESO/Diisocyanate Polymers

4.4.1. Swelling Test

Crosslinked polymers swell in suitable solvents. As crosslink density or connectivity increases the retractive forces created by the crosslinks becomes equal to the solvation forces and swelling stops. This point is called the equilibrium swelling ratio and is good indicator of crosslink density. Equilibrium swelling ratio could be found with following equation:

$$q = V/V_0 = (L/L_0)^3 \qquad \text{volumetric swelling}$$

$$q' = m/m_0 \qquad \text{solvent uptake}$$

When the polymer sample is not homogeneous volume measurement becomes unreliable. A simpler method is to measure solvent uptake gravimetrically. This is done by weighing the polymer before and during swelling until it reaches the equilibrium point. From this data, one can find the swelling ratio, by using the density of the polymer, and density of solvent. When a number of different crosslinking reactions are possible, the density of the crosslinked product is not constant but shows local heterogeneity. Therefore, it is better to measure equilibrium solvent uptake rather than equilibrium swelling ratio. If the solvent choice is not suitable, fragmentation of polymer is observed. Lightly crosslinked regions of the polymer are fragmented by solvent. For soy-based poly(oxazolidone-isocyanurate)s dichloromethane and chloroform immediately cause fragmentation. Toluene is a better solvent but it also causes fragmentation for the some samples synthesized with lower catalyst amount and lower temperatures.

For each type of isocyanate one example of the weight increase by swelling vs. time graphs are shown in Figure 4.33, 4.34, 4.35.

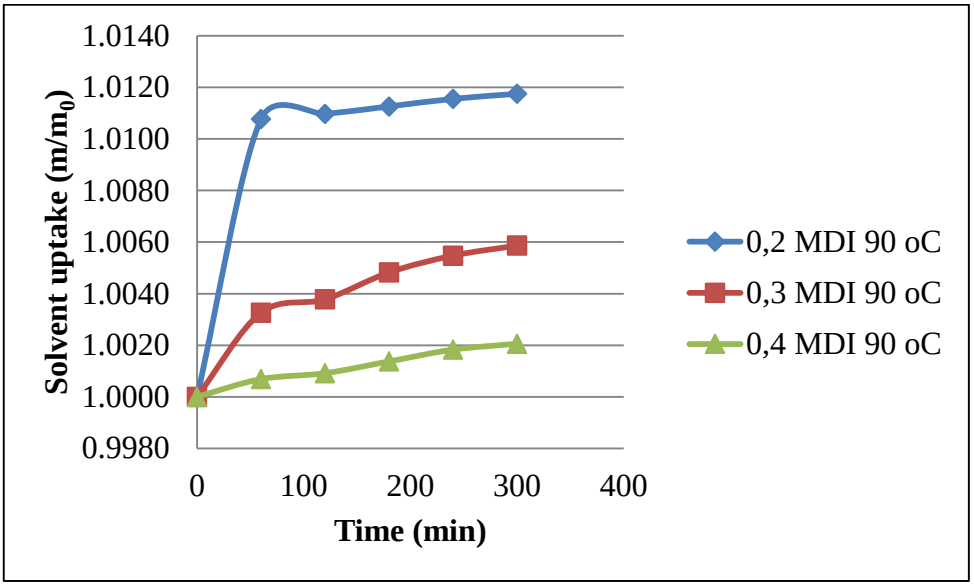

Figure 4.33. Solvent uptake vs. Time for MDI samples synthesized at 90 ºC with different catalyst ratios.

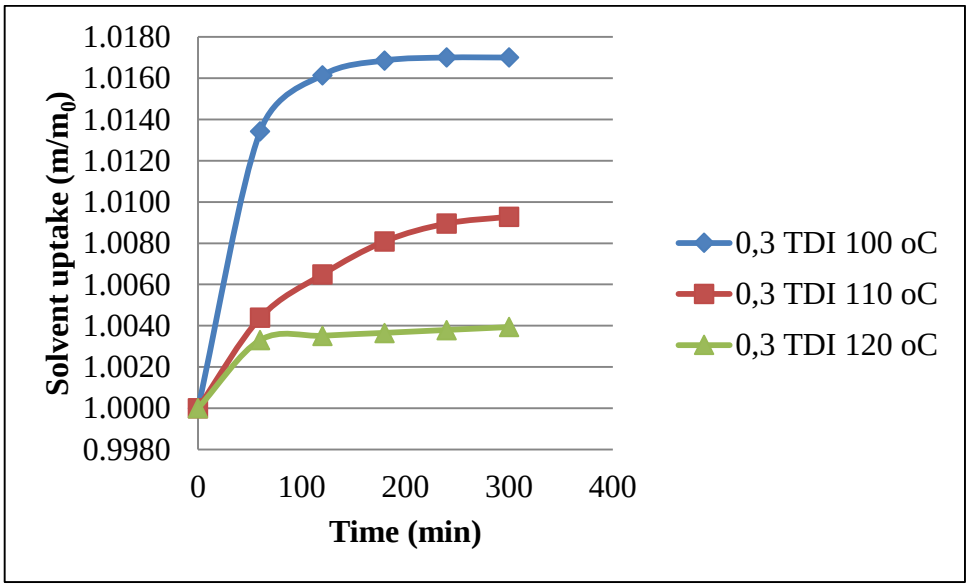

Figure 4.34. Solvent uptake vs. Time for TDI samples synthesized with the same catalyst ratio at different temperatures.

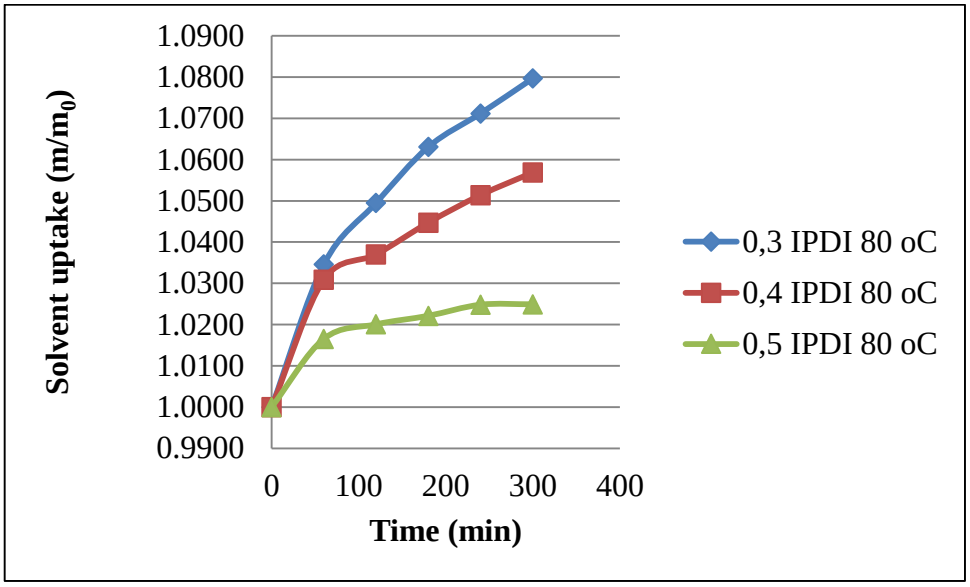

Figure 4.35. Solvent uptake vs. Time for IPDI samples synthesized at 80 ºC with different catalyst ratios.

In the Table 4.20 equilibrium solvent uptake of all test specimens are listed. The number at the begining of the column indicates the weight of catalyst used in polymerization in grams, and the number at the end of the column indicates the polymerization temperature, and the letters refer to the isocyanate used. Thus, 0.3 IPDI 70 means that 0.3 g of catalyst used with isophorone diisocyanate at 70 ºC.

Table 4.20. Equilibrium weights of test specimens.

Number	Property of Test Specimen	Equilibrium weight (gr)	Property of Test Specimen	Equilibrium weight (gr)	Property of Test Specimen	Equilibrium weight (gr)
1	0.3 IPDI 70	1.0825	0.2 MDI 90	1.0118	0.2 TDI 100	1.0203
2	0.4 IPDI 70	1.0614	0.3 MDI 90	1.0059	0.3 TDI 100	1.0170
3	0.5 IPDI 70	1.0376	0.4 MDI 90	1.0021	0.4 TDI 100	1.0071
4	0.3 IPDI 80	1.0797	0.2 MDI 100	1.0048	0.2 TDI 110	1.0101
5	0.4 IPDI 80	1.0569	0.3 MDI 100	1.0024	0.3 TDI 110	1.0093
6	0.5 IPDI 80	1.0249	0.4 MDI 100	1.0013	0.4 TDI 110	1.0053
7	0.3 IPDI 90	1.0607	0.2 MDI 110	1.0032	0.2 TDI 120	1.0042
8	0.4 IPDI 90	1.0526	0.3 MDI 110	1.0014	0.3 TDI 120	1.0039
9	0.5 IPDI 90	1.0155	0.4 MDI 110	1.0011	0.4 TDI 120	1.0038

Figure 4.36, 4.37, 4.38, shows the equilibrium weight difference in different polymer specimens which is the graph form of Table 4.20. Figure 4.39 shows the comparison of average solvent uptake data for each type of diisocyanate.

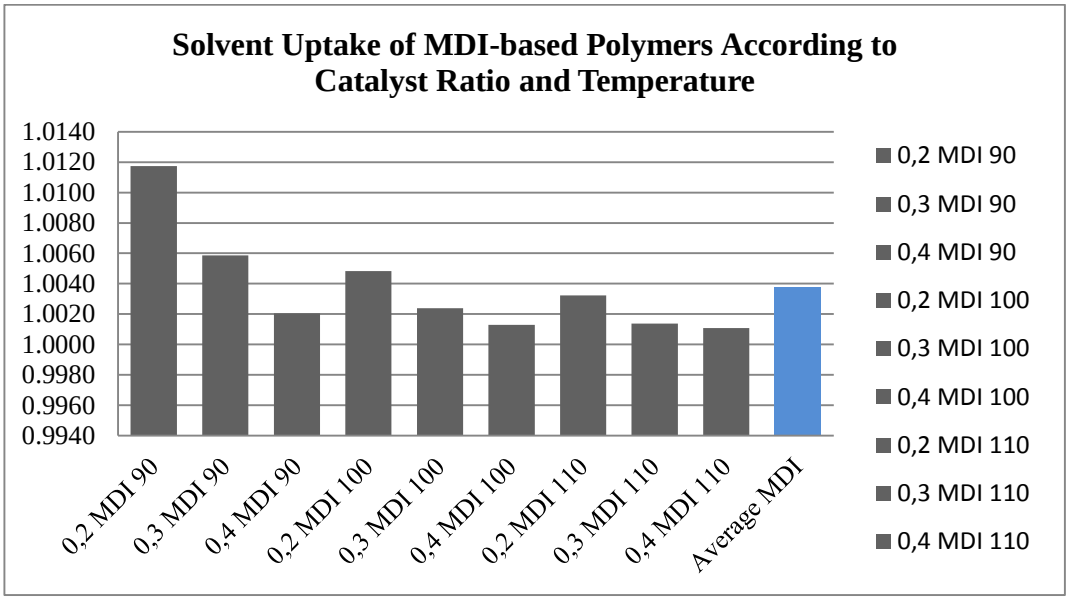

Figure 4.36. Equilibrium solvent uptake values for all MDI-based samples and their average.

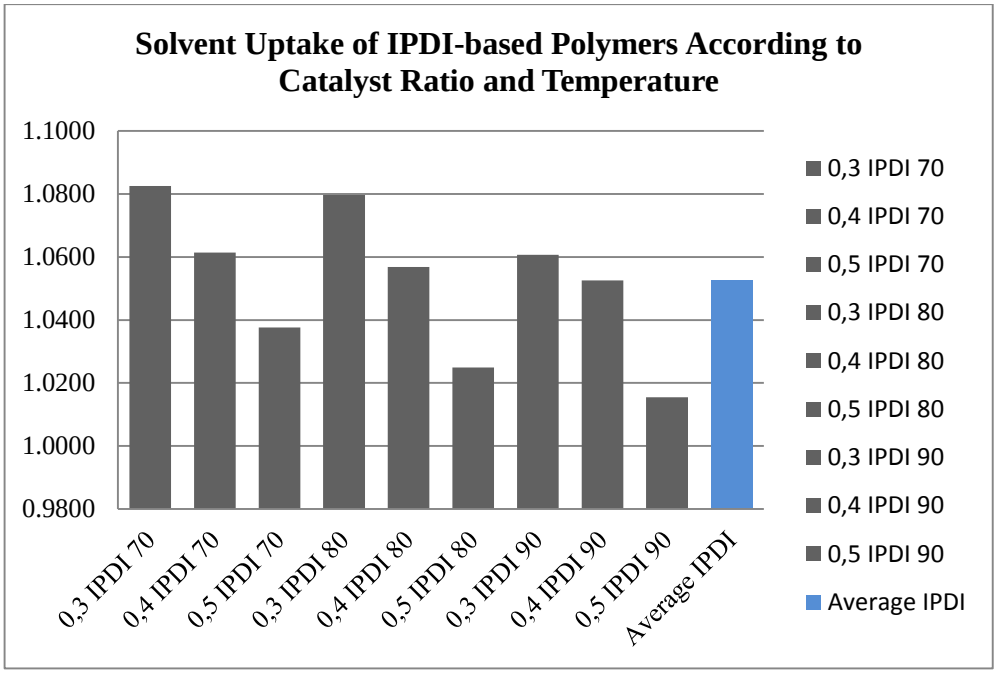

Figure 4.37. Equilibrium solvent uptake values for all IPDI-based samples and their average.

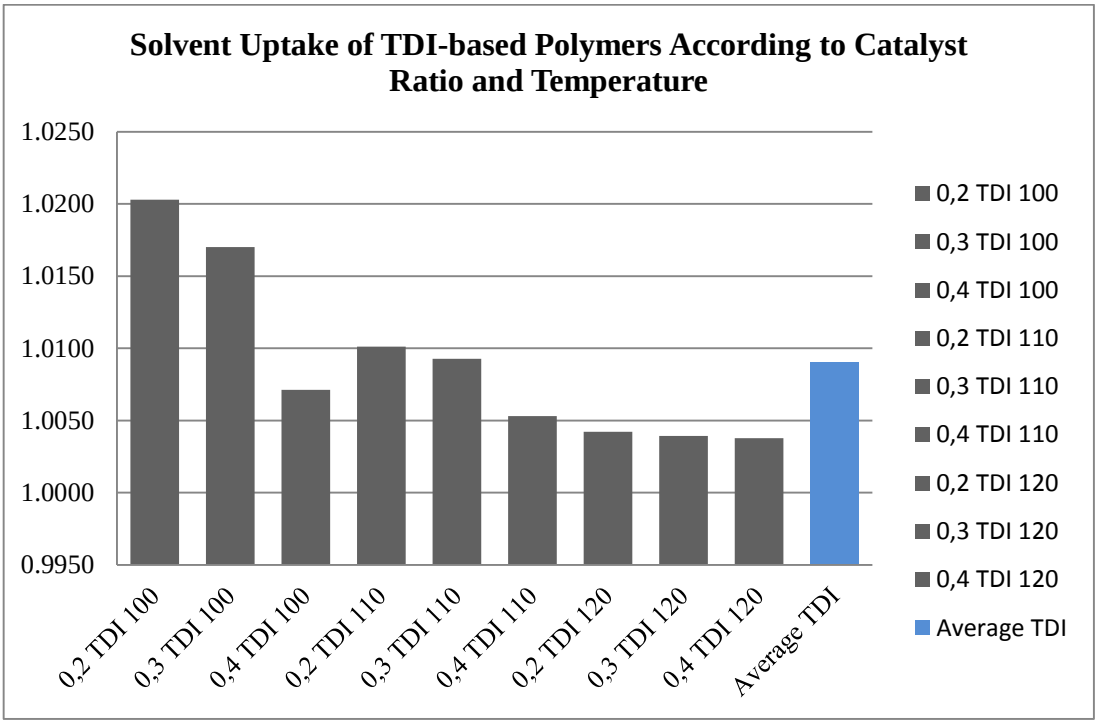

Figure 4.38. Equilibrium solvent uptake values for all TDI-based samples and their average.

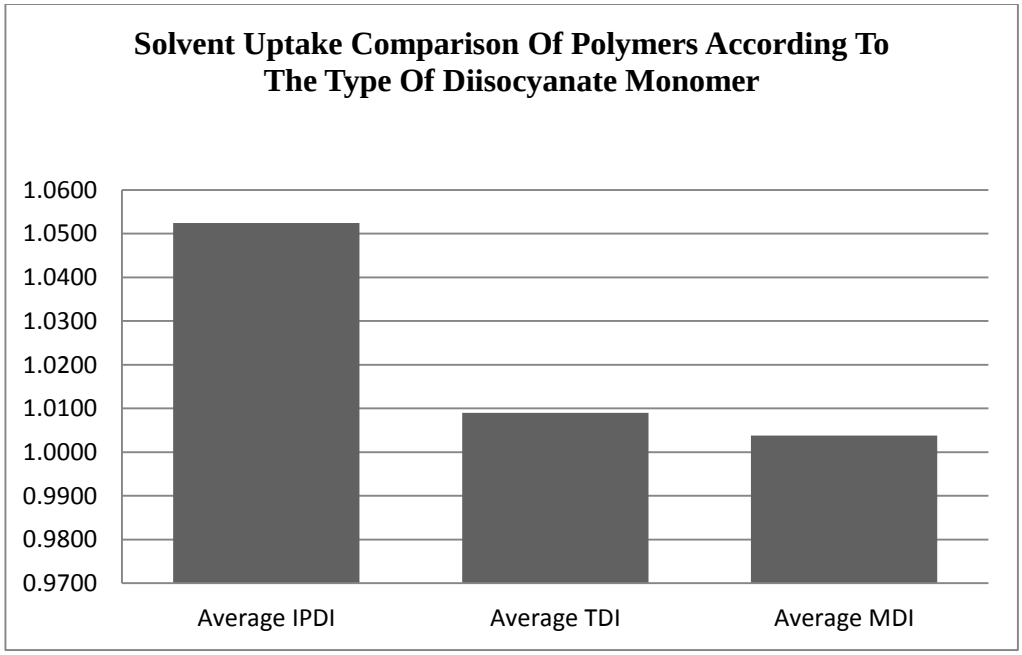

Figure 4.39. Comparison of average solvent uptake values according to the type of diisocyanate.

In conclusion, hexane was found to be the best solvent for the swelling tests. The graphs show that the solvent uptake is higher when catalyst ratio is low and synthesis temperature of the polymer is low. This indicates that at lower catalyst ratios and at lower temperatures crosslinking density is lower. With increasing catalyst ratio and reaction temperature solvent uptake decreased which indicates increasing crosslinking density. Also it changes according to the diisocyanate monomer, for aliphatic isocyanate IPDI, solvent uptake is highest. The solvent uptake test allows the choice of best reaction conditions in terms of catalyst ratio and reaction temperature in order to achieve the highest crosslink ratio.

4.4.2. Surface Hardness Test

Hardness tests measure the resistance of material against indentation, scratching, cutting or bending. For rigid polymers surface deformation could be considered as plastic deformation whereas for elastomers it is elastic deformation. Surface hardness test is a nondestructive test even if the marks or indentations are produced by the test. Results of surface hardness test do not necessarily correlate between the other mechanical behaviours of polymers but it gives a clue to understand the tensile strength, yield strength, work hardening properties of polymers. In this project Shore Hardness Test was applied to the polymers according to ASTM D2240, with Shore D durometer. For each catalyst and temperature condition of polymer, three different polymer samples were used. Six data points were obtained from each specimen such that for each reaction condition 18 data points were taken from three polymer samples synthesized under the same experimental conditions. Results are shown in Table 4.21 as an average of 18 data for each specimen and indicate that surface hardness of polymers are increased with increasing catalyst amount and increasing temperature. In Figures 4.40, 4.41, 4.42 surface hardness results shown as a graph according to the type of diisocyanate monomer, finally in Figure 4.43,comparison of hardness values of polymers was done for type of diisocyanates.

Table 4.21. Average Surface Hardness values for each polymer.

Property of Test Specimen	Average Surface Hardness	Property of Test Specimen	Average Surface Hardness	Property of Test Specimen	Average Surface Hardness
0.2 MDI 90	64	0.2 TDI 100	59	0.4 IPDI 70	60
0.3 MDI 90	70	0.3 TDI 100	67	0.5 IPDI 70	65
0.4 MDI 90	73				
0.2 MDI 100	65	0.2 TDI 110	60	0.4 IPDI 80	66
0.3 MDI 100	71	0.3 TDI 110	69	0.5 IPDI 80	67
0.4 MDI 100	74				
0.2 MDI 110	65	0.2 TDI 120	68	0.4 IPDI 90	69
0.3 MDI 110	74	0.3 TDI 120	71	0.5 IPDI 90	73
0.4 MDI 110	77				

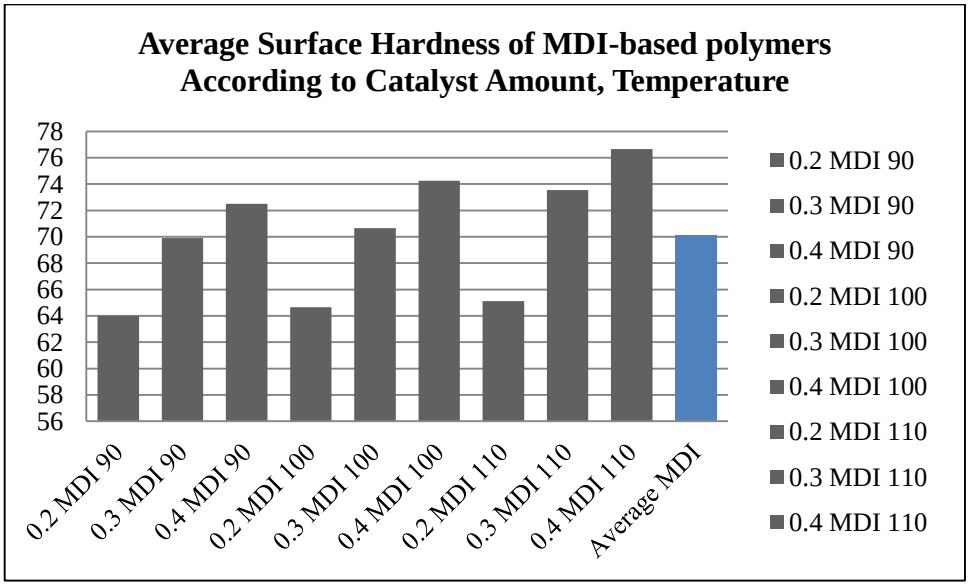

Figure 4.40. Average Surface Hardness values for all MDI-based samples and their average.

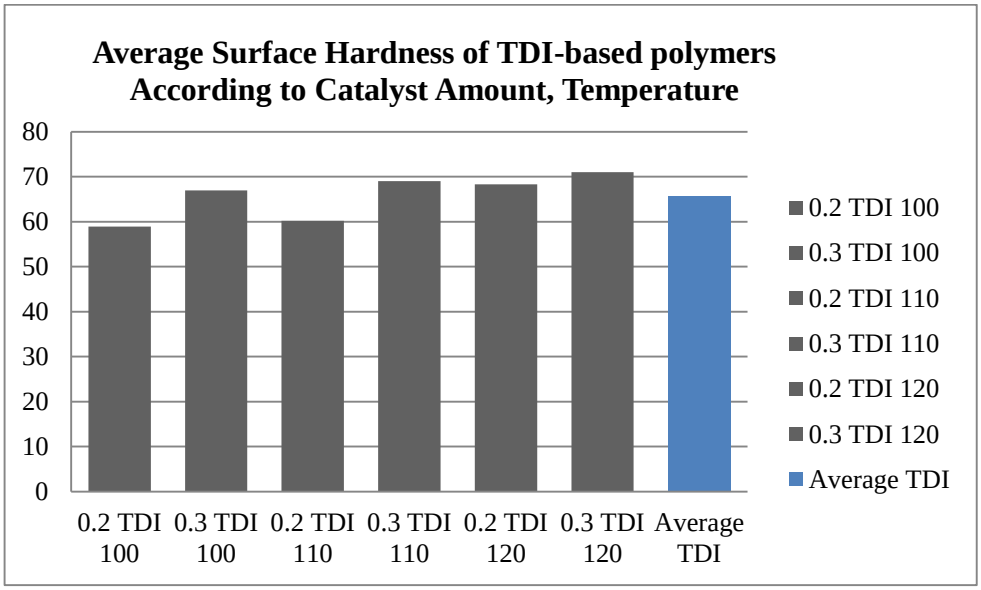

Figure 4.41. Average Surface Hardness values for all TDI-based samples and their average.

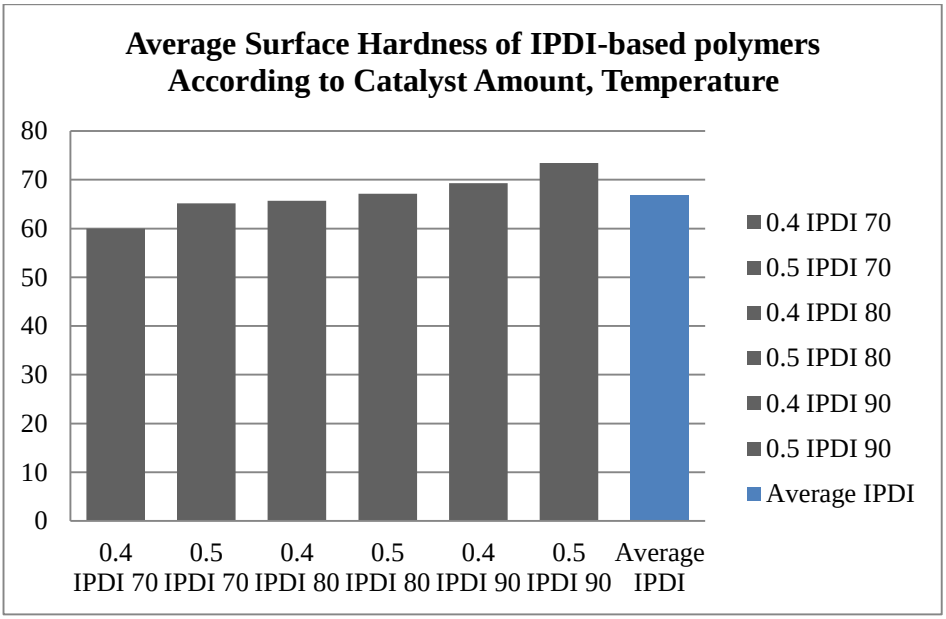

Figure 4.42. Average Surface Hardness values for all IPDI-based samples and their average.

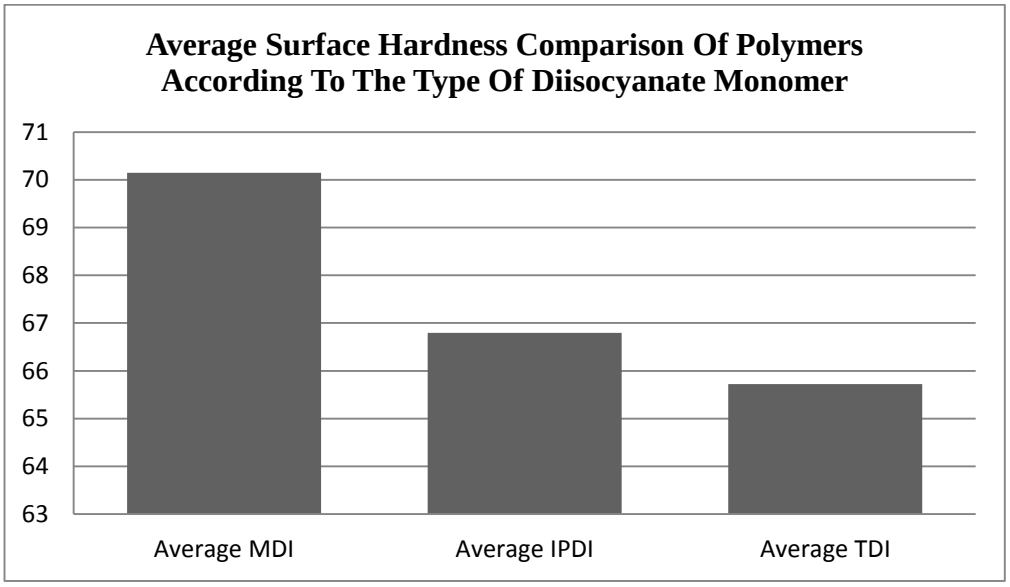

Figure 4.43. Average Surface Hardness comparison acccording to the type of diisocyanate monomer.

As a conclusion, several samples were made with ESO and TDI in the presence of DABCO catalyst instead of $SbCl_3$ catalyst. Results were similar with the polymers synthesized with $SbCl_3$ catalyst, average surface hardness values increased by increasing temperature and increased catalyst amount. $SbCl_3$ gave better results probably because it promotes oxazolidone formation. The hardness values for DABCO catalyzed samples were on the avarage lower than $SbCl_3$ catalyzed samples. Thus we conclude that DABCO, which promotes isocyanurate formation over oxazolidone formation is not the best choice as a catalyst. When isocyanurates are formed a large percentage of isocyanate groups are wasted and are no longer available for crosslinking. Table 4.22 shows the average surface hardness results of TDI samples synthesized with DABCO catalyst.

Table 4.22. Average Surface Hardness Values for polymers synthesized with DABCO catalyst.

Property of Test Specimen	Average Surface Hardness
0.2 TDI 80	51
0.3 TDI 80	52
0.4 TDI 80	54
0.2 TDI 100	53
0.3 TDI 100	54
0.4 TDI 100	60
0.2 TDI 120	55
0.3 TDI 120	60
0.4 TDI 120	62
Average TDI-DABCO	56

4.4.3. Compression Test

Compression test is reverse tensile test only strain is increase in length in tensile test whereas in compression test strain is decrease in length. For this project static compression test was applied to polymer parts where compressive force is increased and the sample length is measured. But there are three problems two of which is technical and the other one is related with the heterogeneity of polymers. To obtain the similar compressive strength results specimens should have perfectly parallel surfaces with only 0.025 mm deviation is accepted, but since the polymer specimens used are not fabricated parts, deviation from parallelity could not be measured. The other problem was the shape of polymer at break when it was broken. Some of the polymers buckle instead of compressing uniformly. In this case instead of uniformly breaking, specimens were fractured through small area (or volume) and the compression test machine registered this fracture as failure.

The third and the most important problem is heterogeneity. These samples were synthesized by bulk polymerization according to ASTM D695 standard but they have heterogeneous crosslink density. Uneven crosslink distribution caused cracking of in some samples. To prevent cracking monomers and catalyst were first mixed in a test tube and allowed to polymerize for some time and transferred to other mold before gellation occurred. This process is similar to A stage and B stage polymerization which is widely used industrially but has drawback of molding a resin that has already reacted high viscosity. Figure 4.44 shows a typical stress-strain curve for 3 identical samples. Here the three samples show very similar compression strengths.

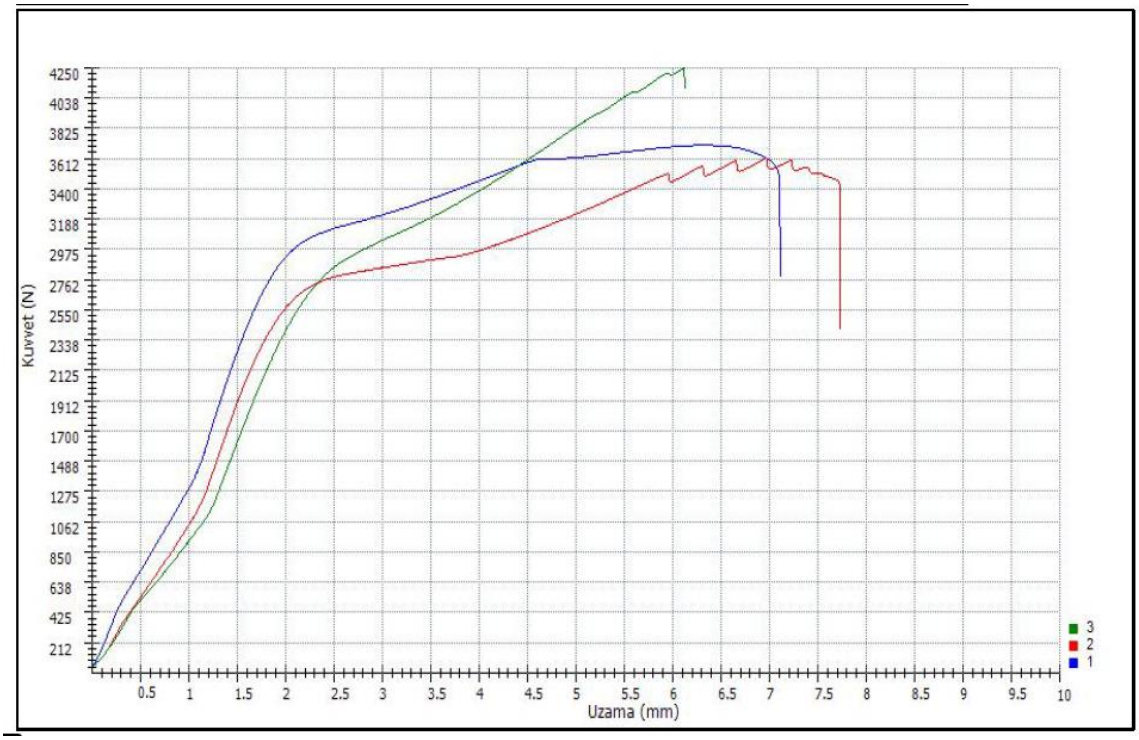

Figure 4.44. Successful example of compression test of 0.3 TDI 100 sample cross section area was 0.95 cm^2.

Figure 4.45 shows another set of 3 identical samples. Here the compression strengths are not at all similar. Such discrepancies made the compression test unreliable.

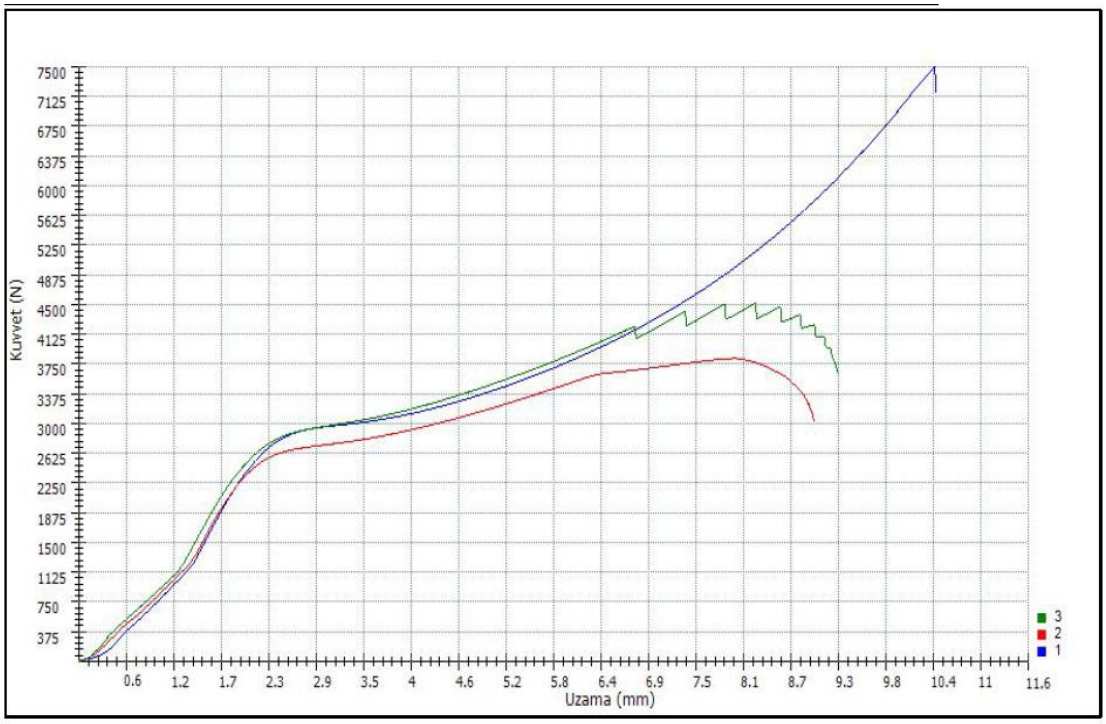

Figure 4.45. Unsuccessful example of compression test for 0.2 MDI 110 sample cross sectional area is 0.95 cm^2.

Polymer specimens are generally shows both elastic and plastic behaviors. At first stress and strain is in linearly related which is related the elastic behavior of polymer. This is where the modulus; the slope of the stress-strain curve, is usually measured. Some samples give a camber in graph which indicates yield, plateau in graphs which indicates the elastic recovery. After that densification starts meaning the plastic deformation occurs just before the sample fails.

Table 4.23 shows the average values of compressive strength of specimens in (MPa). Table 4.24 shows the average compressive modulus of specimens in (MPa). The data is an average obtained from three identical samples.

Table 4.23. Average Compressive Strength values in MPa for all samples.

Property of Test Specimen	Average Compressive Strength (MPa)	Property of Test Specimen	Average Compressive Strength (MPa)	Property of Test Specimen	Average Compressive Strength (MPa)
0.2 MDI 90	48	0.2 TDI 100	53	0.4 IPDI 70	39
0.3 MDI 90	62	0.3 TDI 100	41	0.5 IPDI 70	35
0.4 MDI 90	42	0.2 TDI 110	44	0.4 IPDI 80	59
0.2 MDI 100	38	0.3 TDI 110	56	0.5 IPDI 80	41
0.3 MDI 100	66	0.2 TDI 120	34	0.4 IPDI 90	54
0.4 MDI 100	54	0.3 TDI 120	50	0.5 IPDI 90	60
0.2 MDI 110	56				
0.3 MDI 110	74				
0.4 MDI 110	56				
Averge MDI	55	Average TDI	46	Averge IPDI	48

Table 4.24. Average Compressive Modulus (MPa) for all samples.

Property of Test Specimen	Average Compressive Modulus (MPa)	Property of Test Specimen	Average Compressive Modulus (MPa)	Property of Test Specimen	Average Compressive Modulus (MPa)
0.2 MDI 90	255	0.2 TDI 100	213	0.4 IPDI 70	158
0.3 MDI 90	267	0.3 TDI 100	303	0.5 IPDI 70	234
0.4 MDI 90	268	0.2 TDI 110	226	0.4 IPDI 80	184
0.2 MDI 100	211	0.3 TDI 110	336	0.5 IPDI 80	268
0.3 MDI 100	329	0.2 TDI 120	265	0.4 IPDI 90	208
0.4 MDI 100	371	0.3 TDI 120	270	0.5 IPDI 90	306
0.2 MDI 110	282				
0.3 MDI 110	350				
0.4 MDI 110	434				
Average MDI	308	Average TDI	269	Average IPDI	226

Unlike compressive strength data in Table 4.23, compressive modulus data in Table 4.24 gives meaningful results except for 3 data points (shown bold on the Table 4.24) out of 21 data points. Compressive modulus increases by catalyst ratio and temperature. Figure 4.46, 4.47, 4.48, shows the compressive modulus results shown as a graph according to the type of diisocyanate monomer, finally in Figure 4.49 comparison of compressive modulus of polymers was done for type of diisocyanates.

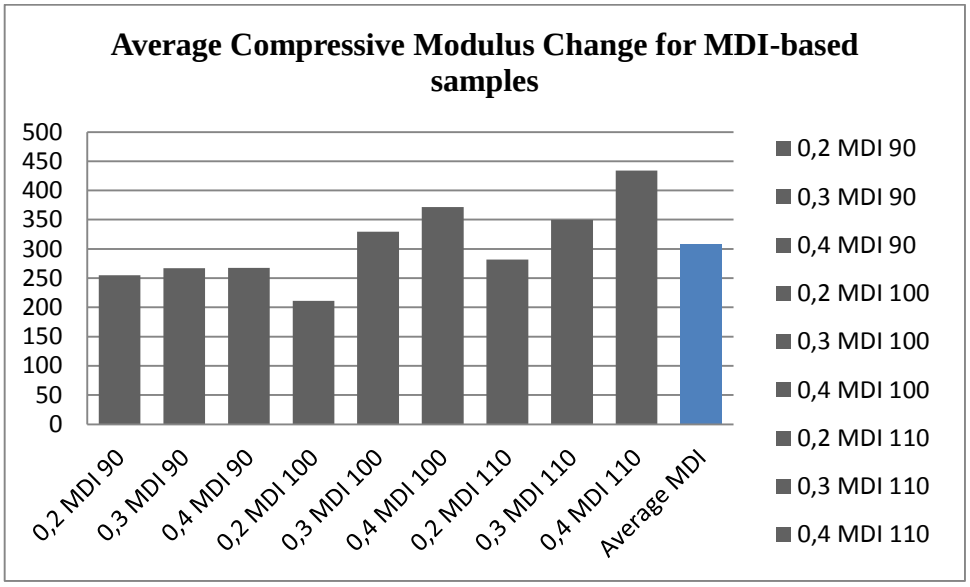

Figure 4.46. Average Compressive Modulus values for all MDI-based samples and their average.

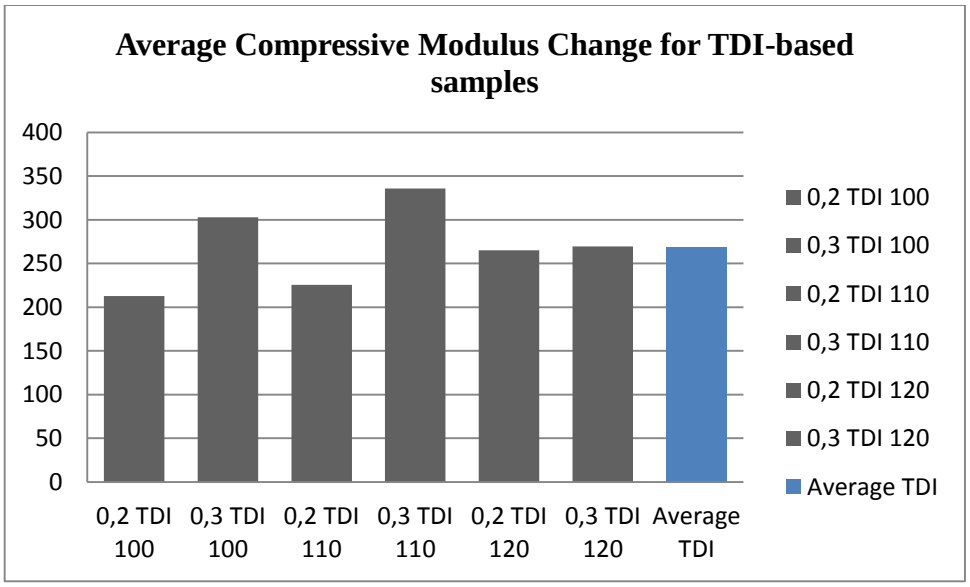

Figure 4.47. Average Compressive Modulus values for all TDI-based samples and their average.

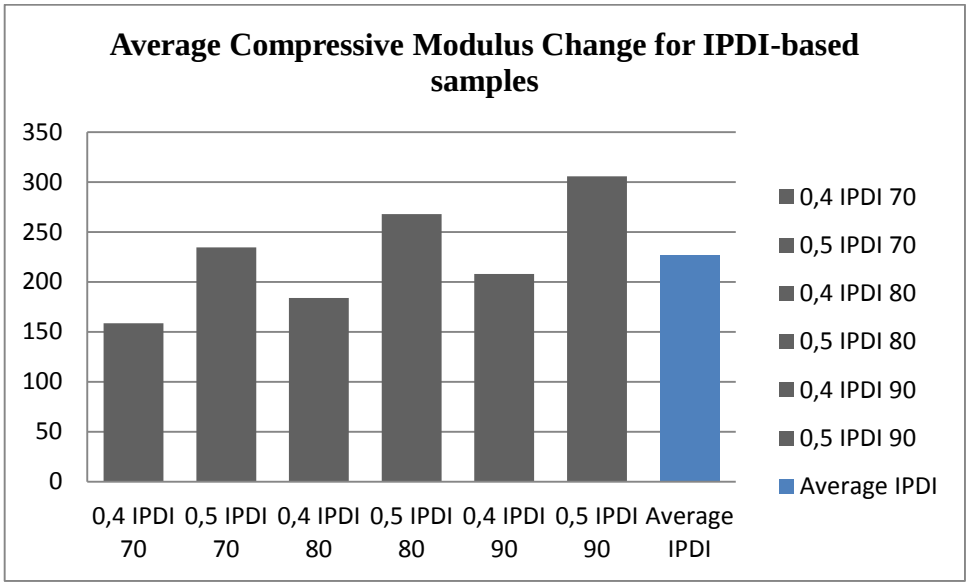

Figure 4.48. Average Compressive Modulus values for all IPDI-based samples and their average.

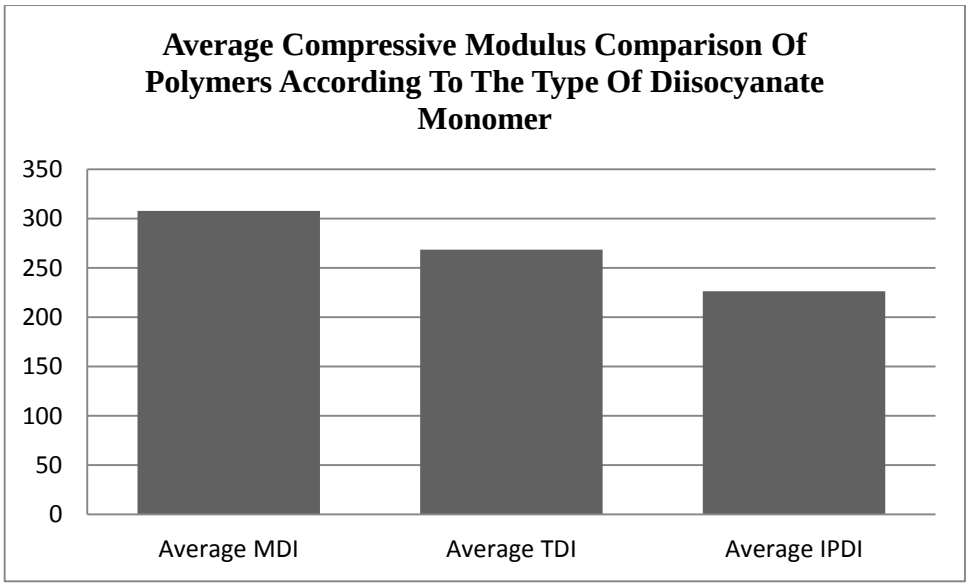

Figure 4.49. Average Compressive Modulus comparison acccording to the type of diisocyanate monomer.

Unlike surface hardness and swelling experiments it is impossible to correlate compression strength with reaction conditions. However the compression strength and modulus is the highest among 18 different ESO based thermosets synthesized and

published by this research group. These values compare very favorable with commercial liquid molding resins as shown in Table 4.25.

Table 4.25. Comparison Compressive Strength and Modulus of Commercial Polymers with ESO–diisocyanate polymers [60,61].

Type of Polymer	Compression Strength (MPa)	Compression Modulus (MPa)
ESO-MDI	55	308
ESO-TDI	46	269
ESO-IPDI	48	226
Commercial Unsaturated Phtallate Polyester	65	1000
Commercial BPA Epoxy Resin	125	3400

4.5. Leaching Test

When new thermoset polymers are synthesized it is important to determine the amount of unreacted monomers or short, uncrosslinked chains in the poymer sample. Polymers synthesized with $SbCl_3$ swells in many solvents such as hexane, toluene, chloroform and dichloromethane. Toluene was chosen as a solvent to remove extractables because it swells the sample faster. For the leaching tests the solvent was replaced by fresh solvent 5 times and the extracts were combined. Evaporation of toluene showed that 2.7% of a typical sample was extractable.

Figure 4.50 shows the FTIR spectrum of extractables and Table 4.26 shows the interpretation of the spectrum. 0.2 TDI 110 sample was used for the leaching test.

Table 4.26. FTIR Interpretation of extractables.

Position of the Peak (cm^{-1})	Interpretation
1754	Oxazolidone Carbonyl Stretch (as peak broadening)
1737	ESO ester carbonyl stretch
1709-1705	Isocyanurate carbonyl stretch
1536	Urethane N-H bend
1455	Isocyanurate C-N stretch
1438	Oxazolidone C-N stretch
1415	Isocyanurate ring deformation
842-823	Epoxy ring deformations (Invisible)
1240	Epoxy ring deformation (invisible)
815	Isocyanurate out of plane bending

Figure 4.50 shows the FTIR spectrum of the polymer part after leaching test and Table 4.27 shows the interpretation of the FTIR spectrum.

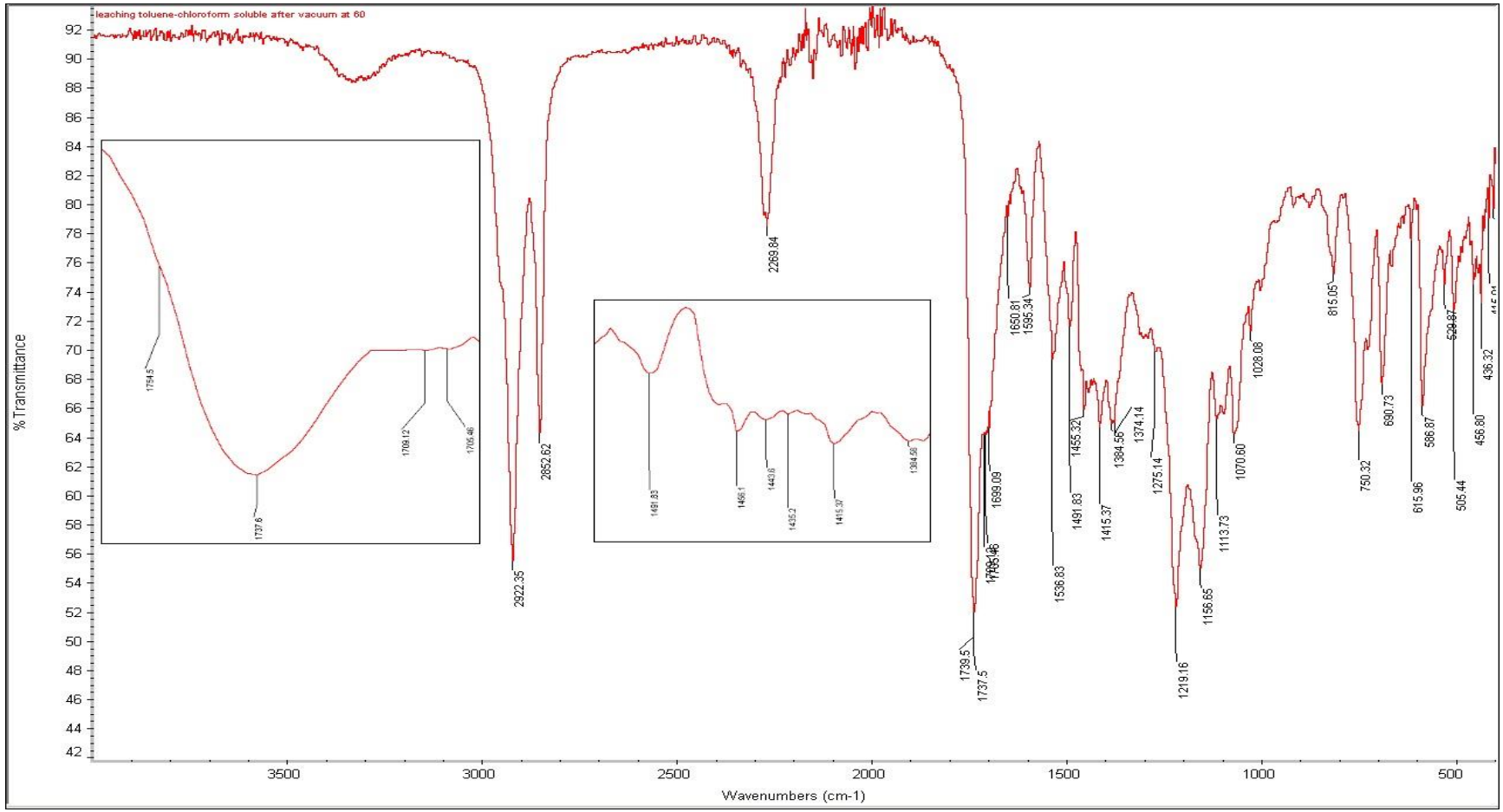

Figure 4.50. FTIR Spectrum of extractables.

Table 4.27. FTIR Interpretation of the polymer after removal of extractables.

Position of the Peak (cm^{-1})	Interpretation
1754	Oxazolidone Carbonyl Stretch (as peak broadening)
1737	ESO ester carbonyl stretch
1731	Urethane carbonyl stretch
1716	Biuret/Allophonate carbonyl stretch
1704	Isocyanurate carbonyl stretch
1531	Urethane N-H bend
1455	Isocyanurate C-N stretch
1434	Oxazolidone C-N stretch
1414	Isocyanurate ring deformation
842-823	Epoxy ring deformations (Invisible)
1240	Epoxy ring deformation (invisible)
816	Isocyanurate out of plane bending
723	Alkyl -CH rocking (Reference Peak)

The conclusion obtained from leaching test shows that the biuret and isocyanurate formation which cause crosslinking, is higher in the polymer sample than extractables. Comparison of the peaks at 1704 cm^{-1} and 1716 cm^{-1} in Figure 4.50 and 4.51 show the effect of crosslinking on extraction of polymer.

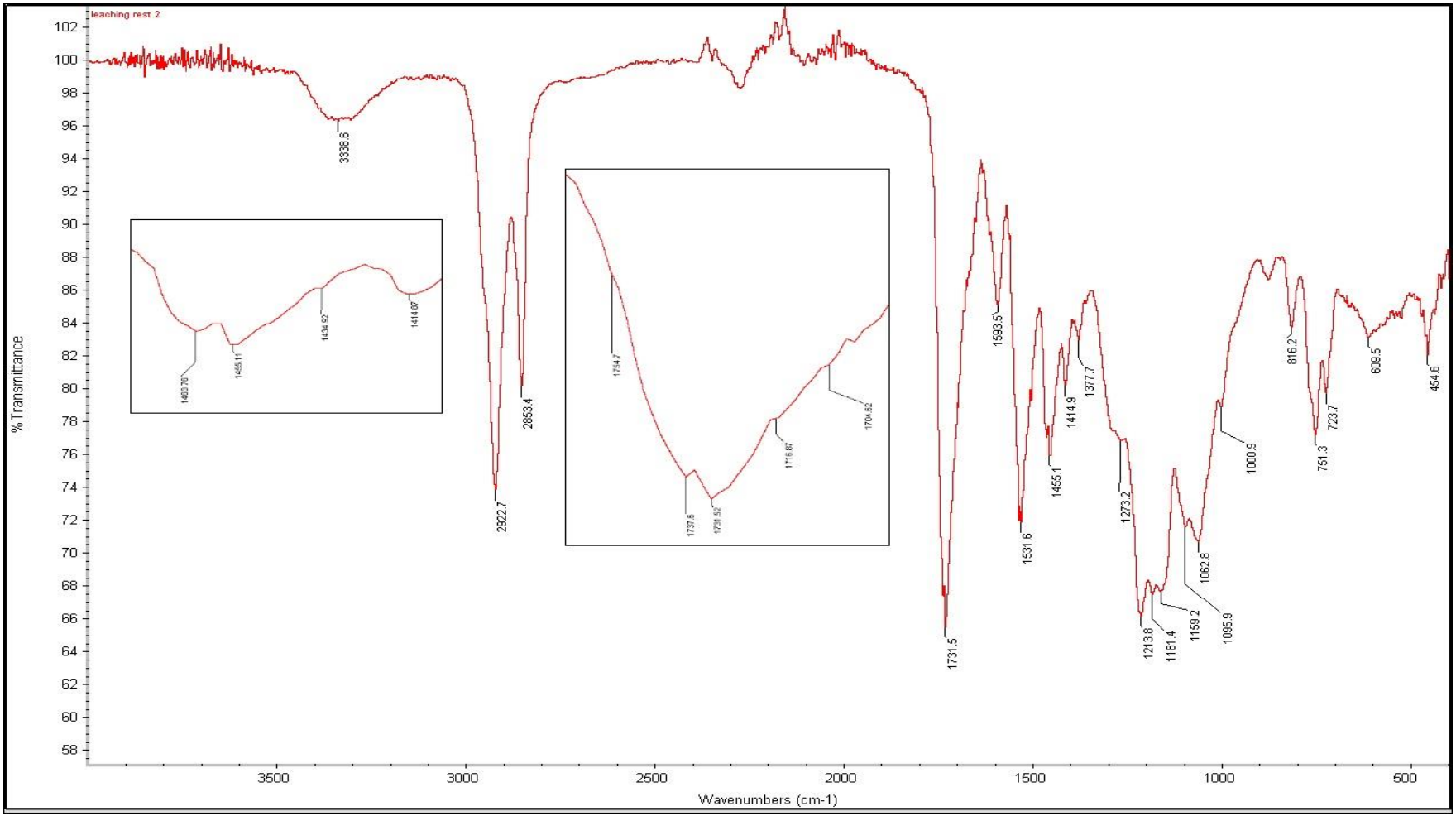

Figure 4.51. FTIR Spectrum of the polymer after leaching test.

4.6. Thermogravimetric Analysis

Thermogravimetric Analysis were done for polymers synthesized with $SbCl_3$. Figure 4.52 shows TGA of the 0.4 MDI 110 ^oC sample. There are 4 different types of degradation at 183, 220, 298, 399 ^oC. In Figure 4.53 derivative of weight according to temperature vs temperature could be seen and from the literature information, the first two peaks at 202 and 266 ^oC belongs to urea/urethane/allophonate and biuret which are indistinguishable. The second peak at 373 ^oC belongs to oxazolidone and the last peak at 466 ^oC belongs to isocyanurate.

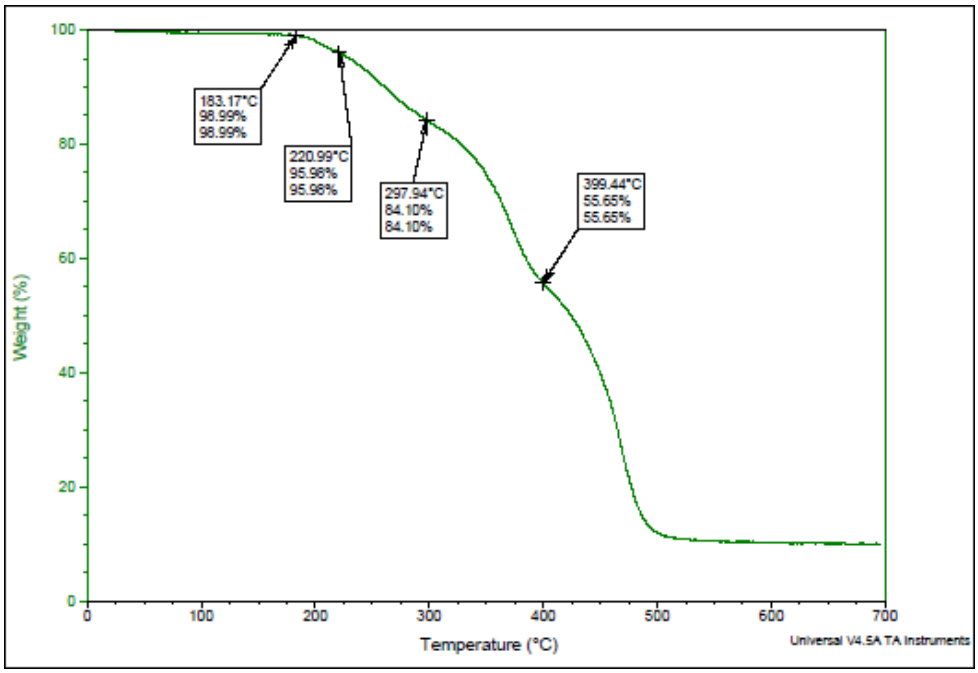

Figure 4.52. Change in weight of 0.4 MDI 110 vs. Temperature.

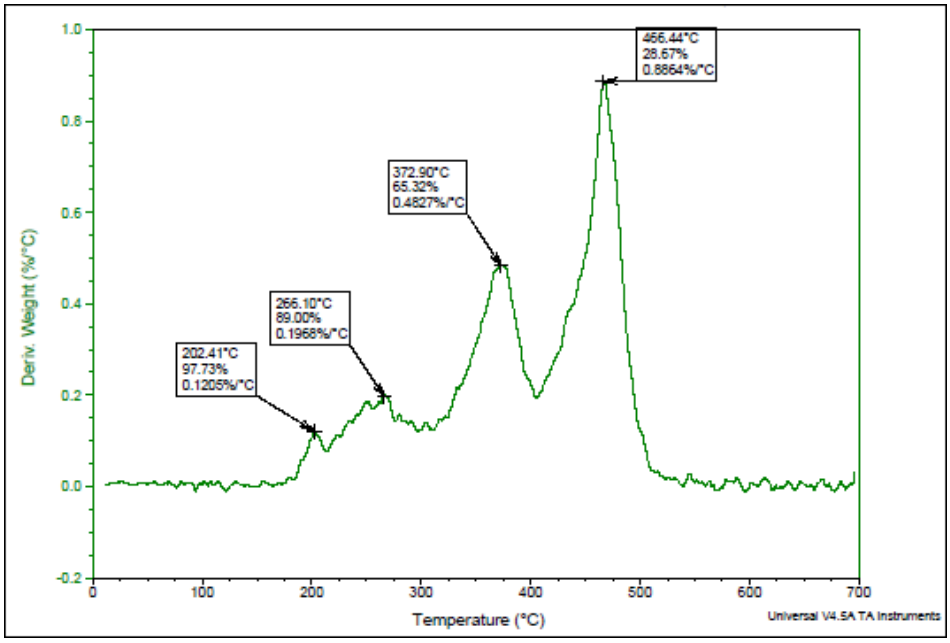

Figure 4.53. Derivative of weight change (0.4 MDI 110) according to temperature vs. temperature

The second TGA graph in Figure 4.54 belongs to 0.2 TDI 120 ^{o}C sample. There are three different types of degradation at 210, 283, 418 ^{o}C. In Figure 4.55 derivative of weight according to temperature vs temperature could be seen. The first peak at 262 ^{o}C belongs to urea/urethane/allophonate and biuret which are indistinguishable. The second peak at 399 ^{o}C belongs to oxazolidone and the last peak at 462 ^{o}C belongs to isocyanurate.

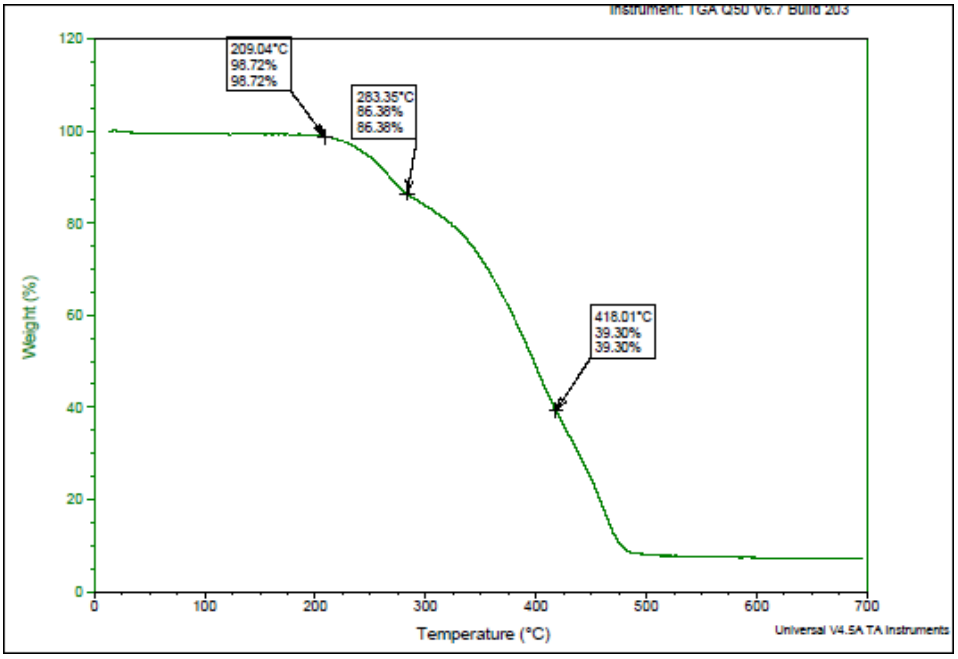

Figure 4.54. Change in weight of 0.2 TDI 120 vs. Temperature.

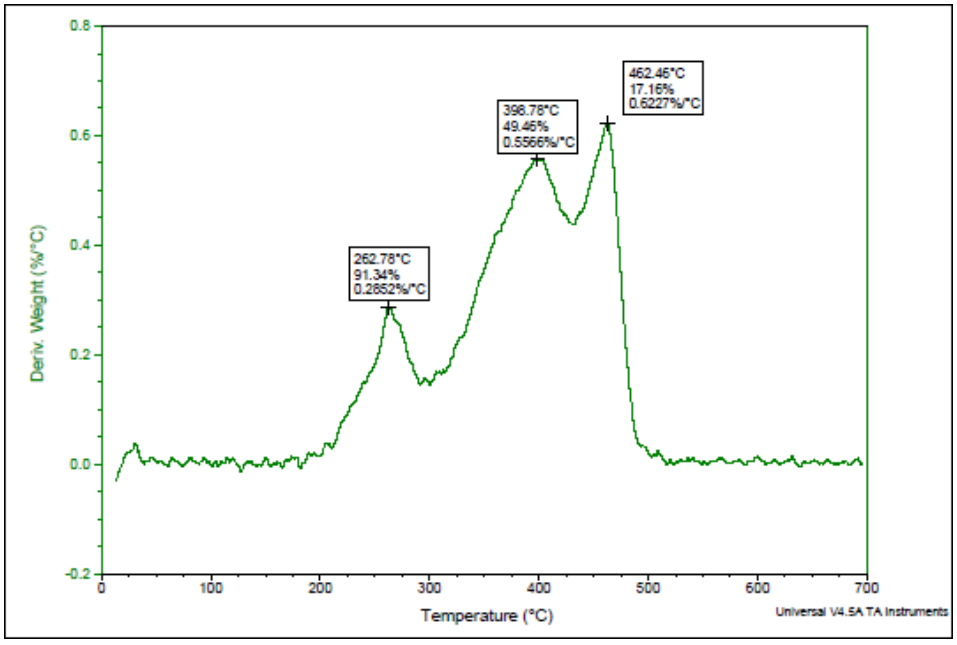

Figure 4.55. Derivative of weight change (0.2 TDI 120) according to temperature vs. Temperature.

The last Figure 4.56 shows the TGA graph of 0.5 IPDI 90 ^{o}C sample. There are two main slope changes at 205 ^{o}C, 284 ^{o}C. In Figure 4.57, derivative of weight change according to temperature vs temperature could be seen. The first peak at 266 ^{o}C belongs to urea/urethane/allophonate and biuret which are indistinguishable. The second peak at 435 ^{o}C belongs to combination of isocyanurate and oxazolidone groups. From previous graphs they gave two separate peaks due to heterogeneity. This sample is more homogeneous. From FTIR spectrum of that sample, oxazolidone and biuret/allophonate formation were proved. Both FTIR and mechanical properties shows the extra amount of crosslinking was seen for IPDI samples. Extra crosslinking is based on biuret and allophonate formation. Unfortunately, these functional groups degrade at the similar temperatures with chain-like urethanes and ureas, therefore the amount of these crosslinking groups could not be determined.

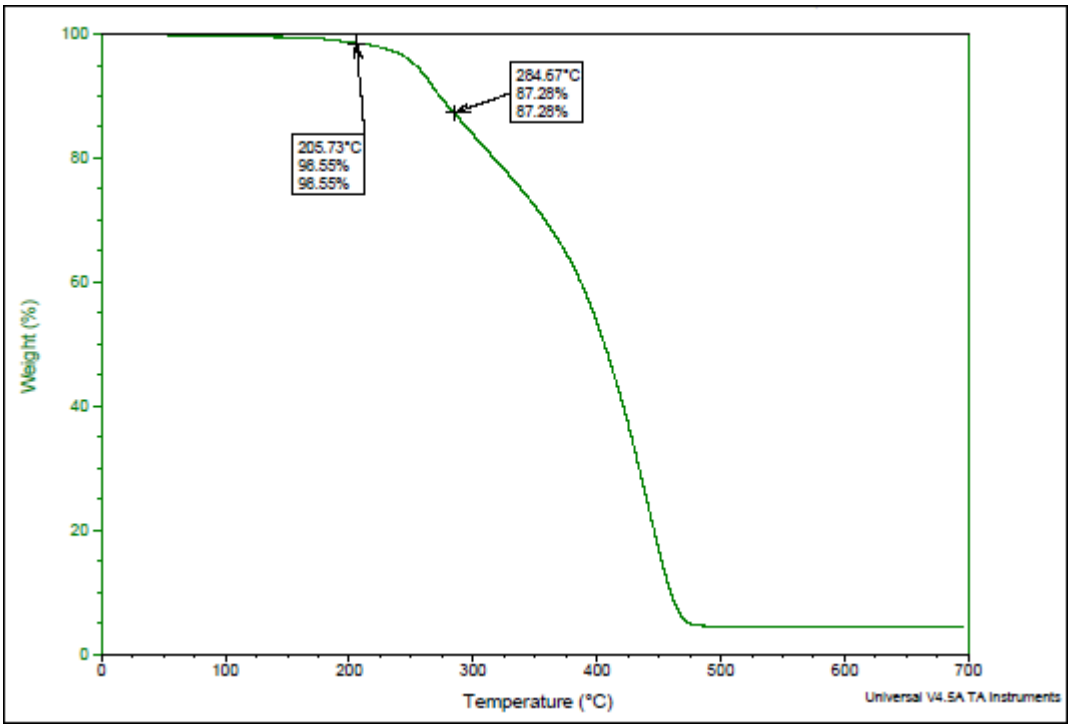

Figure 4.56. Change in weight of 0.5 IPDI 90 vs. Temperature.

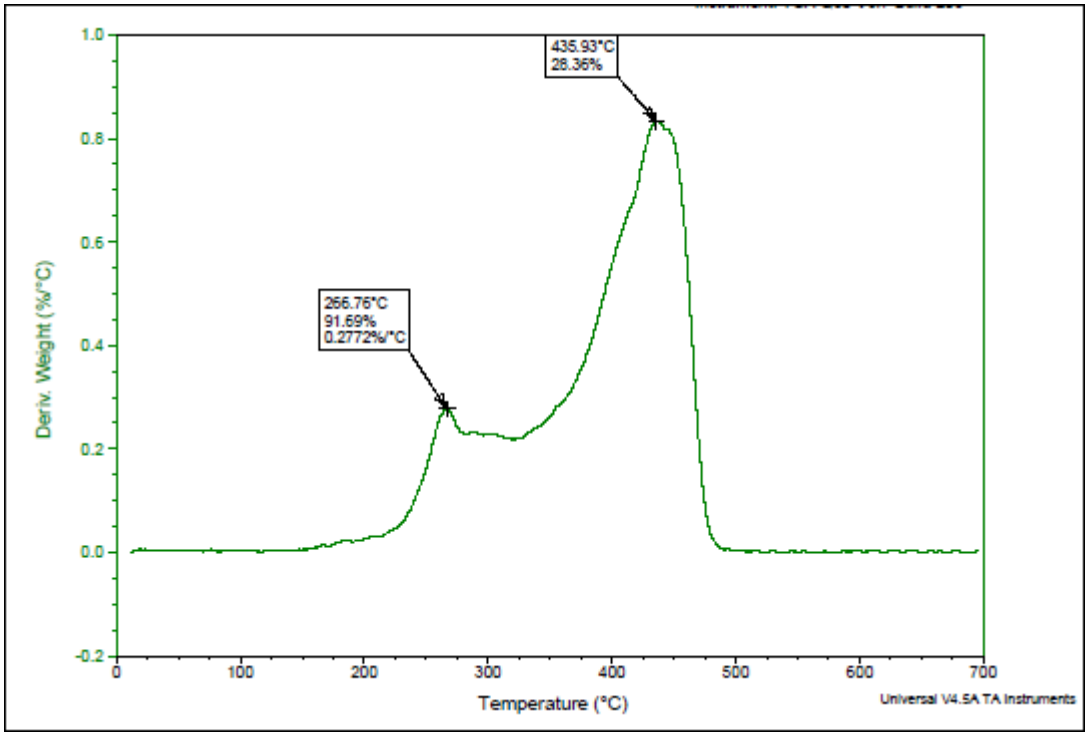

Figure 4.57. Derivative of weight change (0.5 IPDI 90) according to temperature vs. Temperature.

FTIR Characterizations of Section 4, were done [62-65] accordingly.

5. CONCLUSION

In this study, polymerization of epoxidized soybean oil was performed with using different diisocyanate monomers in the presence of either tertiary amine or Lewis Acid catalyst.

Isocyanate-epoxy reaction was known in the literature, the main product is oxazolidone but with numerous side reactions that follow the main reaction, also give isocyanurates and open chain urethanes.There is a dilemma about FTIR characterization of oxazolidone polymers. Carbonyl stretch of oxazolidones was evaluated either at 1739 cm^{-1} or 1754 cm^{-1} by different researchers.Therefore, to understand the scope of the reaction, several model compounds were synthesized with a monoisocyanate and epoxidized soybean oil with different catalysts at different temperatures. Under atmospheric conditions, above 80 ^{o}C, oxazolidone formation was observed. When the medium is not dry, primary amine (aniline), urea (1,3 diphenyl urea) and urethane side products were observed DABCO catalysis of the reaction gave isocyanurate as the dominant product. For $SbCl_3$, open chain urethane and oxazolidone is dominant over all other reactions. Under absolutely dry and under nitrogen conditions, reactions are simpler. In the literature, high reaction temperature conditions are claimed to be better for oxazolidone formation but with the Lewis Acid catalysis, epoxy homopolymerization started to occur above 70 ^{o}C which consumes the epoxide groups. Presence of ESO ester carbonyl stretch peak at 1740 cm^{-1}, interferes with the urethane carbonyl peaks. This study asserted that the oxazolidone carbonyl stretch is at 1754 cm^{-1}. Polymeric model compounds that were synthesized with epoxy silane and DGBPA which are simpler compounds than ESO due to lack of carbonyl groups, assisted in this decision.

Polymer samples were synthesized with four different diisocyanates above 80 ^{o}C with $SbCl_3$ catalyst and their swelling, compressive, thermal behaviours and surface hardness values were determined. Because they are thermoset polymers only FTIR characterization was done.

Leaching test shows that the conversion of polymerization is 97% .

Surface Hardness tests were conducted with Shore D durometer. Increasing catalyst concentration and increasing reaction temperature increased surface hardness.

Swelling experiments in hexane show that as catalyst concentration and temperature is increased, swelling ratio is decreased.

Compressive behaviour of polymers shows that for the polymers have the highest compressive strength values ever reported for ESO based polymers. The compressive strength values were close to unsaturated polyesters and phenolic epoxy resins. These polymers could be used commercially with industrial processes such as RIM.

Compressive strength values could not be correlated with reaction conditions. Compressive modulus values, however, correlate very well with catalyst concentration and temperature. Modulus increases with increasing catalyst concentration and increasing temperature.

Thermal behavious of polymers indicates that both urea/chain-like urethane, oxazolidone and isocyanurate groups present in the polymers.

As expected for all mechanical tests, MDI-based polymers gave better results than TDI and IPDI-based polymers. IPDI polymers gave the lowest mechanical properties.

6. REFERENCES

1. Lligadas, G, *Biobased Thermosets from Vegetable Oils. Synthesis, Characterization, and Properties*, Ph.D. Thesis, Universitat Rovira Virgili, 2006.

2. Islam, M. R., M. D., Beg, S., Jamari, "Development of Vegetable-Oil-Based Polymers", *Journal of Applied Polymer Science*, Vol. 131, pp. 40787-40800, 2014.

3. Mathers, R., T., "How Well Can Renewable Resources Mimic Commodity Monomers and Polymers?", *Journal of Applied Polymer Science Part A: Polymer Chemistry*, Vol. 50, pp. 1-15, 2012.

4. Espinoza, L. M., M. A. R., Meier, "Plant oils: The perfect renewable resource for polymer science?!", *European Polymer Journal*, Vol. 47, pp. 87-852, 2011.

5. Meier, M. A. R., J. O., Metzger, U. S., Schubert, "Plant Oil Renewable Resources as Green Alternatives in Polymer Science", *Chemical Society Reviews*, Vol. 36, pp. 1788-1802, 2007.

6. Cahoon, E., B., "Genetic Enhancement of Soybean Oil for Industrial Uses: Prospects and Challenges", *The Journal of Agrobiotechnology Management & Economics*, Vol. 6, pp. 11-13, 2003.

7. Hammond, E. G., L. A., Johnson, C., Su, T., Wang, P. J., White, *Bailey's Industrial Oil and Fat Products; Soybean Oil*, John Wiley & Sons Inc., 6th edition, 2005.

8. Ichhaporia, P. K., *Composites from Natural Fibers*, Pro Quest, North Carolina, 2008.

9. Dunford, N. T., *Food and Industrial Bioproducts and Bioprocessing*, Wiley-Blackwell, Oklahoma, 2012.

10. Saithai, P., J., Leconte, E., Dubreucq, V., Tanrattanakul, "Effects of Different Epoxidation Methods of Soybean Oil on the Characteristics of Acrylated Epoxizided Sotbean Oil-co-poly(methyl methacrylate) Copolymer", *Polymer Letters*, Vol. 7, pp. 910-924, 2013.

11. Boger, D. L., "Epoxidation Reactions", 2014, http://www.chemistry.uoc.gr/synaps/lectures/vassilikogiannakis/Chapter04.pdf, [Accessed January 2015].

12. Larock, R., M., Hanson, United States Patent, 6211315, 2001.

13. Khot, S. N., J., Lascala, E., Can, S., Morye, G., Williams, G., Palmese, S., Kusefoglu, P. R., Wool, "Development and Application of Triglyceride-Based Polymers and Composites", *Journal of Applied Polymer Science*, Vol. 82, pp. 703-723, 2001.

14. Wool, R., S., Kusefoglu, G., Palmese, S., Knot, R., Zhao, United States Patent, 6121398.3.

15. Crivello, J. W., United States Patent, 5318808, 1994.

16. Sharmin, E., F., Zafar, *Polyurethane; An Introduction*, In Tech, 2012.

17. Shricastava, R., "Bhopal Gas Disaster: Review on Health Effects of Methyl Isocyanate", *Research Journal of Environmental Science*, Vol. 5, pp. 150-156, 2011.

18. Jaisson, S.,C., Pietrement, P., Gillery, "Carbamylation-Derived Products: Bioactive Compounds and Potential Biomarkers in Chronic Renal Failure and Atherosclerosis", *Clinical Chemistry*, Vol. 57, pp. 1449-1505, 2011.

19. Bello, D., C. A., Herrick, T. J., Smith, S. R., Woskie, R. P., Streicher, R. M., Cullen, Y., Liu, C. A., Redlich, "Skin Exposure to Isocyanates: Reasons for Concern", *Environmental Health Perspectives*, Vol. 115, pp. 328-335, 2007.

20. Shricastava, R., "Bhopal Gas Disaster: Review on Health Effects of Methyl Isocyanate", Research Journal of Environmental Science, Vol. 5, pp. 150-156, 2011.

21. Geddie, J. E., *A Guide to Occupational Exposure to Isocyanates*, NCDOL, Raleigh, 2013.

22. Mille, J. D., "The National Institute for Occupational Safety and Health (NIOSH)", 2014, http://www.cdc.gov/niosh/docs/90-101/, [Accessed December 2014].

23. *Workplace Health and Safety; Bulletin*, Government of Alberta, 2010.

24. Koleske, J. V., *Paint and Coating Testing Manual*, ASTM International, 1995.

25. Szycher, M., *Szycher's Handbook of Polyurethanes*, CRC Press, 2nd edition, 2012.

26. *Catalysts in Polyurethane Foams: A One-day Seminar*, Rapra Technology Limited, 1997.

27. Herbstman, S., "Trimerization of Isocyanates by Trialkylantimony and Arsenic Oxides", Vol. 30, pp. 1259-1260, 1984.

28. Blank, W. J., Z. A., He, E. T., Hessell, "Catalysis of the Isocyanate-Hydroxyl Reaction by non-Tin Catalysts", *Progress in Organic Coatings*, Vol. 35, pp. 19-29, 1999.

29. Britain, J. W., P. G., Gemeinhardt, "Catalysis of the Isocyanate – Hydroxyl Reaction", *Journal of Applied Polymer Science*, Vol. 4, pp. 207-211, 1960.

30. Hatada, K., T., Kitayama, O., Vogl, *Macromolecular Design of Polymeric Materials*, CRC Press, 1997.
31. Galante, M. J., R. I. J., Williams, "Polymer Networks Based on the Diepoxide-Diisocyanate Reaction Catalyzed by Tertiary Amines", *Journal of Applied Polymer Science*, Vol. 55, pp. 89-98, 1995.
32. Kricheldorf, H. R., *Handbook of Polymer Synthesis*; *Part B*, CRC Press, 1991.
33. Hatada, K., T., Kitayama, O., Vogl, *Macromolecular Design of Polymeric Materials*, CRC Press, 1997.
34. Flores, M., X. F., Francos, J. M., Morancho, A., Serra, X., Ramis, "Ytterbium Triflate as a New Catalyst on the Curing of Epoxy-Isocyanate Based Thermosets", *Thermochimica Acta*, Vol. 543, pp. 188-196, 2012.
35. Senger, J. S., I., Yilgor, J. E., McGrath, "Isocyanate-Epoxy Reactions in Bulk and Solution", *Journal of Applied Polymer Science*, Vol. 38, pp. 7-82, 1989.
36. Yeganeh, H., S., Jamshidi, P. H., Talemi, " Synthesis, characterization and properties of novel thermally stable poly(urethane-oxazolidone) elastomers", *European Polymer Journal*, Vol. 42, pp. 1743-1754, 2006.
37. Lee, C. S., T. L., Ooi, C. H., Chuah, S., Ahmad, "Rigid Polyurethane Foam Production from Palm Oil-Based Epoxidized Diethanolamides". *Journal of the American Oil Chemists' Society*, Vol. 84, pp. 1161-1167, 2007.
38. Kordomenos, P. I., J. E., Kresta, "Thermal Stability of Isocyanate-Based Polymers.1. Kinetics of the Thermal Dissociation of Urethane, Oxazolidone and Isocyanurate Groups", *Macromolecules*, Vol. 14, pp. 1434-1437, 1981.

39. *Chemistry and Technology of Polyols for Polyurethanes*, Smithers Rapra Publishing, 2005.

40. Petrovic, Z. S., I. J., Javni, United States Patent, 6399698, 2002.2.

41. Panda, H., *The Complete Technology Book On Natural Products (Forest Based)*, National Institute of Industrial Re – Forest Products, 2004.

42. *Developments in Polymer Analysis and Characterization*, Smithers Rapra Publishing, 1999.

43. Shah, D. U., "Towards Sustainable Polymers and Plastics: NMR Spectroscopic Analysis and Characterisation of Vernonia Seed (Vernonia Galamensis) Oil and Epoxidized Soya Bean Seed (Glycine Max) Oil", *The Scitech Journal*, Vol. 1, pp. 13-29, 2014.

44. Pathak, U. G., *Studies on Novel Polyester Polyols and Their Biocomposites*, Ph.D. Thesis, Saurashtra University, 2007.

45. Shanmugam, G., D., Bhakiaraj, S., Elavarsan, T., Elavarsan, M., Gopalakrishnan, "Benign by Design Synthesis of Novel 1H-Tetrazoles; Spectral Characterization and Antibacterial Activities", *Chemical Science Transactions*, Vol. 2, pp. 1304-1311, 2013.

46. Solomon, M. R., J., Sivaguru, S., Jockusch, W., Adam, N. J., Turro, "Decoding Stereocontrol During the Photooxygenation of Oxazolidinone-Functionalized Enecarbamates", *Organic Letters*, Vol. 12, pp. 2142-2145, 2010.

47. Teichert, A. M., *Screening of Chiral Diels-Alder Catalysts by Mass Spectrometric Monitoring of the Retro Reaction*, Cuvillier Verlag, 2007.

48. Osa, Y., Y., Hikima, Y., Sato, K., Takino, Y., Ida, S., Hirono, H., Nagase, "Convenient Synthesis of Oxazolidinones by the Use of Halomethyloxirane, Primary Amine and Carbonate Salt", *Journal of Organic Chemistry*, Vol. 70, pp. 5737-5740, 2005.

49. Dodiuk, H., H. S., *Goodman, PDL Handbook Series; Handbook of Thermoset Plastics*, Elsevier, 3rd Edition, 2013.

50. Roger, M. E., T. E., Long, *Synthetic Methods in Step-Growth Polymers*, John Wiley & Sons, 2003.

51. Szycher, M., *Szycher's Handbook of Polyurethanes*, CRC Press, 2nd edition, 2013.

52. Lu, Q., T. R., Hoye, C. W., Macosko, "Reactivity of Common Functional Groups with Urethanes; Models for Reactive Compatibilization of Thermoplastic Polyurethane Blends", *Journal of Polymer Science*, Vol. 40, pp. 2310-2328, 2002.

53. Flores, M., X. F., Francos, J. M., Morancho, A., Serra, X. Ramis, "Curing and Characterization of Oxazolidone – Isocyanurate – Ether Networks", *Journal of Applied Polymer Science*, Vol. 125, pp. 2279-2789, 2012.

54. Merline, J. D., C. P. R., Nair, C., Gouri, R., Sadhana, K. N., Ninan, "Poly(urethane-oxazolidone): Synthesis, characterization and shape memory properties", *European Polymer Journal*, Vol. 43, pp. 3629-3637, 2007.

55. Galante, M. J., R. I. J., Williams, "Polymer Networks Based on the Diepoxide-Diisocyanate Reaction Catalyzed by Tertiary Amines," Journal of Applied Polymer Science, Vol. 55, pp. 89-98, 1995.

56. Mathur, R. M., K., Prajapati, A., Varshney, "Synthesis and characterization of oxazolidones with improved thermal stability", Advanced Applied Science Research, Vol. 5, pp. 2553-2560, 2012.

57. Varshney, A., R. M., Mathur, K., Prajapati, "Thermal Characteristics of Oxazolidone Modified Epoxy Anhydride Blends", *International Journal of Chemistry,* Vol. 4, pp. 113-120, 2012.

58. Reed, D., C., Lee, *Conference; UTECH 94*, Urethanes Technology Press, 1994.

59. *Cellular Polymers 2nd International Conference*, Heriot-Watt University, Edinburgh, 1993.

60. Davallo, M., H., Pashar, M., Mohseni, "Mechanical Properties of Unsaturated Polyester Resin", *International Journal of Chemical Technology Research*, Vol. 2, pp. 2113-2117, 2010.

61. Simmons, "Epoxy Resin", 2014, http://www.epoxyworktops.com/epoxy-resin/intro.html, [Accessed February 2015].

62. Neunhoeffer, H., P. F., Wiley, *The Chemistry of Heterocyclic Compounds, Chemistry of 1 2 3-Triazines and 1 2 4- Triazines, Tetrazines and Pentazine*, John Wiley & Sons, 2009.

63. Larkin, P., *Infrared and Raman Spectroscopy; Principles and Spectral Interpretation*, Elsevier, 2011.

64. Smith, B. C., *Infrared Spectral Interpretation: A Systematic Approach*, CRC Press, 2000.

65. Clift, S. M., J., Grimminger, K., Muha, *New Polyisocyanurate Catalysts for Rigid Polyurethane Foams*, Air Products and Chemicals Inc., 1994.